LAND COVER CHANGE MAPPING OF EASTERN ONTARIO, 1995 TO 2005 USING OBJECT-BASED CLASSIFICATION.

By

Laura Dingle Robertson, B.A. (Hons.)

A thesis submitted to
the Faculty of Graduate Studies and Research
in partial fulfillment of the requirements of the degree of

Master of Science

Department of Geography and Environmental Studies
Carleton University
Ottawa, Ontario
July 2007

Your file Votre référence
ISBN: 978-0-494-33696-0
Our file Notre référence
ISBN: 978-0-494-33696-0

ABSTRACT

Land use/land cover (LULC) change occurs when humans alter the landscape, and will have the greatest effect on ecological systems in the 22nd century. Many fields of study require data on and monitoring of LULC change at a variety of scales. In landscape ecology, such data are important for species, population, and habitat research. LULC change assessment is dependent upon high quality input data, most often from remote sensing derived products such as thematic maps. This thesis compares pixel and object-based classifications of Landsat Thematic Mapper (TM) data for mapping and analysis of LULC change in eastern Ontario for the period of 1995 to 2005.

Object-based segmentation and nearest neighbour classification was not found to be more accurate than maximum likelihood classification for all classes. Quantitative and visual analysis revealed that some classes were better classified with the object-based method but others were not. Limitations of the object-based classification included the absorption of small and rare classes, and linear areas into larger objects, and the incapability of spatial parameters such as object shape to contribute to class discrimination at this scale.

A 1995–2005 temporal change map developed from the two object-based thematic maps using post-classification comparison was assessed and found to depict change more accurately than a change map derived from the maximum likelihood thematic maps. Further research should be conducted to assess different data inputs (e.g. higher resolution data, digital elevation models) to refine and improve these remote sensing change analysis products.

ACKNOWLEDGEMENTS

It took a catastrophic event to awaken in me a desire to live my life consciously and to follow this new road - regardless of how long and winding it may be. This thesis is dedicated to those who lived their lives with passion and found their paths cut short that morning.

My many thanks are given to Dr. Doug King for his advice and guidance throughout this process. Doug, you've been generous with the freedoms given me during this research and I appreciate your confidence in my ability. Thank you to Dr. Lenore Fahrig for her support and direction on the landscape ecology side of things. You've helped this geographer take a look at the world from a different perspective.

My fieldwork would not have been possible without the driving skills of Jon Pasher. Jon, thank you for chauffeuring me around eastern Ontario and your advice on all things remote sensing! I also greatly appreciate the introduction to that new, unique species of southern Ontario. To the other members of the GLEL, thank you for your support and guidance on unfamiliar subjects and processes, and for putting up with my many questions and interruptions. You are great examples of the spirit found in our integrated lab. To the Geography Department, especially Hazel and Natalie, thank you for keeping me on track, and for your words of encouragement throughout this process.

To mom and dad (my biggest cheerleaders), thank you for not thinking it was crazy to stop a 13-year marketing career and for supporting us during those first years while I was an undergrad. The two of you have always followed your own unique paths and allowed us to find our own ways even if it took a long, long time. Dad, thanks very much for being a set of fresh eyes on this work. To Brenda and David, thanks for the

competition and encouragement. Our unique, shifting alliance helped me hone my critical thinking and negotiation skills! To my BFFs - Paul, Blake, Michelle and Jennifer Kuta - there have been times in the past we've followed our own paths and there will be times in the future when our roads may not cross, but know that you are always in my heart. The inspiration and encouragement you've given me throughout this period of my life and throughout our friendships have always been appreciated.

Alistair, you've given me the freedom to follow these new dreams at a time when most husbands would be looking to settle into a comfortable, stable life. Thank you for building my confidence in my own abilities; you always believe in me especially when I don't believe in myself. Thank you for putting up with more than your fair share of "grey-hair" moments. You are my greatest friend and biggest supporter and I am grateful to know you.

"But still they lead me back to the long winding road"
Lennon/McCartney

TABLE OF CONTENTS

LIST OF TABLES

LIST OF FIGURES

LIST OF APPENDICES

LIST OF TERMS

6S	Second Simulation of the Satellite Signal in the Solar Spectrum
ASTER	Advanced Spaceborne Thermal Emission and Reflection Radiometer
ATCOR	Atmospheric Correction Program
CIR	Colour infrared
DN	Digital Number
DOS	Dark Object Subtraction
EOMF	Eastern Ontario Model Forest
EROS	Earth Resources Observation Systems
ETM+	Enhanced Thematic Mapper Plus
FNEA	Fractal Net Evolution Approach
GCPs	Ground control points
GLCM	Grey level co-occurrence matrix
GLEL	Geomatics and Landscape Ecology Research Laboratory
GPS	Global Positioning System
ISODATA	Iterative Self-Organizing Data Analysis Technique
LULC	Land use/land cover
MAD	Multivariate Alteration Detection
MDDV	Modified Dense Dark Vegetation
MIR	Mid-infrared
MLC	Maximum likelihood classification
MODTRAN	Moderate Spectral Resolution Atmospheric Transmittance algorithm
MSS	Multispectral Scanner
NAD 83	North American Datum of 1983
NDVI	Normalized Difference Vegetation Index
NIR	Near infrared
PA	Producer's Accuracy
PCC	Post-classification comparison
PIFs	Pseudo-invariant features
RMSE	Root mean square error
TIR	Thermal infrared
TM	Thematic Mapper
UA	User's Accuracy
USGS	United States Geologic Society
UTM	Universal Transverse Mercator

CHAPTER ONE

1.0 Introduction

This thesis examines remote sensing methods for mapping and analysis of land use/land cover (LULC) change in eastern Ontario (Figure 1.1) for the period of 1995 to 2005 at a regional scale.

LULC change occurs when human actions directly or indirectly alter land cover or change land use from one form to another. LULC change can take place on untouched land (forest conversion to agricultural land) and on transformed lands (increased intensity of anthropogenic practices) (Foley *et al.*, 2005). By 2100 LULC change is predicted to have the greatest effect on global ecological systems, including climate change and invasive species threats (Chapin *et al.*, 2000). With increasing conversion of natural lands to human-use lands and intensification of altered lands there is increasing loss, fragmentation and spatial simplification of habitat. These transformations have impacts on the flora and fauna in the landscape. Land-use policies must consider the importance of land use practices and LULC change to human health and welfare (increased food production, higher standards of living) while minimizing environmental effects (Foley *et al.*, 2005).

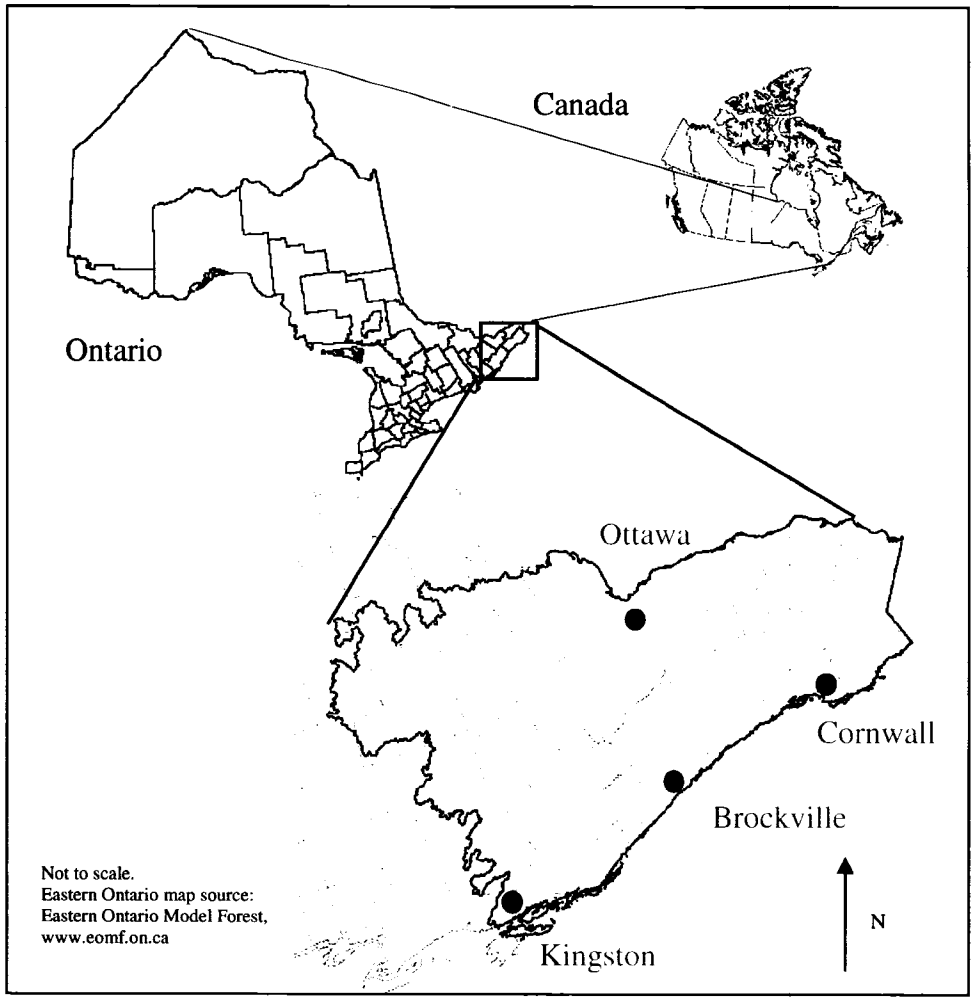

Figure 1.1 – Study region of eastern Ontario, Canada. Watermark lines represent local counties. Dark boundary line outlines the EOMF.

1.1 LULC change effects and rates

LULC change affects all vegetated environmental systems of the earth. For example, 40 to 50% of grasslands, forests and wetlands have been urbanized or converted to agricultural areas (Chapin *et al.*, 2000).

Terrestrial ecosystems have been affected through the conversion of unaltered lands to agriculture and urban areas. If trends continue, 10 trillion hectares of natural ecosystems will be transformed to agricultural lands by the year 2050. With these

changes, there has been an increase in the release of pesticides and anthropogenic nutrients such as nitrogen and phosphorous (Tilman *et al.*, 2005).

Urban areas encroach upon surrounding vegetated landscapes and fragment habitats and this can alter regional climate through the urban "heat island" effect (Voogt and Oke, 2002). Limited vegetation cover, the form and structure of the buildings and the impervious nature of the urban materials (concrete, pavement) inhibit evapotranspiration and cooling. Regional circulation is altered, causing increased precipitation downwind of major cities (Lo *et al.*, 1997). In addition to changing climate, air quality can be affected by LULC change. Air quality is reduced by increased dust sources, vehicle emissions, and added ash and smoke from biomass burning.

Changes have been made to the hydrosphere through the control and manipulation of waterways for irrigation purposes and as a result of pollutants being added to the system (Tilman *et al.*, 2001). These changes cause increased mean annual discharge from some land forms, contamination of streams and lakes, and an increased use of water resources.

The eastern Ontario region has been undergoing significant LULC change for more than a century. Eastern Ontario is a diverse and fragmented region made up of urban and suburban enclaves surrounded by agricultural lands, waterways, forests and plantations of coniferous and deciduous species, quarries and sand pits, and wetlands. The area has experienced similar terrestrial, aquatic and atmospheric changes as many other parts of the world, including wetland loss (Mitsch and Gosselink, 2000), urban

area increase (Guindon *et al.*, 2004; Zhang and Guindon, 2005) and cropland increase (2001 Agriculture Census, Statistics Canada).

There are many different methods of assessing LULC change and its effects on the environment. In the Carleton University Geomatics and Landscape Ecology Research Laboratory (GLEL) research has been initiated to study ecological response lag and effects of LULC on biodiversity in the eastern Ontario region. An essential investigative tool of such temporal analysis is the ability to map the dynamics of land cover at a variety of spatial and temporal scales to determine what scales can be used to evaluate the effects of landscape change on species. Remote sensing can provide spatial and temporal data at many different scales that can be used to analyze land cover changes over time. In this thesis, capabilities for mapping LULC change using remotely sensed data at the regional scale of eastern Ontario are evaluated.

1.2 Remote sensing of LULC change

Remote sensing land cover classification methods have been shown to provide accurate land cover maps over large regions (Foody, 2002; Cingolani *et al.*, 2004). LULC change detection and mapping has been demonstrated as being feasible in many environments and at many scales (Johnson and Kasischke, 1997). Change mapping methods using thematic maps for two or more dates have been shown to accurately provide the change direction (from/to land cover changes) (Abuelgasim *et al.*, 1999; Mas, 1999).

There have been many remote sensing-based studies on LULC change all over the world. Many are focused on vegetation change amongst forest, agriculture, urban and other land cover types (e.g. Collins and Woodcock, 1996; Pax-Lenney *et al.*, 2001;

Lu *et al.*, 2005; Janzen *et al.*, 2006; Virk and King, 2007). There have been a few comparative studies (e.g. Flanders *et al.*, 2003; Yan *et al.*, 2006; Yu *et al.*, 2006) on LULC change mapping using the two classification methods chosen for this thesis. (Pixel-based maximum likelihood classification and object-based hierarchical segmentation/classification). There have also been several remote sensing change studies using regional scale (Landsat) imagery (e.g. Mas, 1999; Pax-Lenney *et al.*, 2001; Cingolani *et al.*, 2004; Chen *et al.*, 2005; Virk and King, 2007).

In the eastern Ontario region there have been few published studies (Guindon *et al.*, 2004; Zhang and Guindon, 2005) concerned with long term LULC change, however, these focused on the urban areas of the region. Additionally, there are no published studies for the region that utilize the classification methods tested in this thesis. The size of the study area and the availability of historical regional scale satellite imagery make remote sensing practical and cost effective for land cover mapping and LULC change monitoring.

1.3 Research context and scope

This study is part of a larger research initiative within the GLEL. In this integrated laboratory, researchers in geomatics and landscape ecology attempt to advance habitat modeling and mapping, and species conservation. Currently, projects being implemented include the study of: ecological response lag of species to landscape change, effects of roads on species movement and persistence, and species specific habitat requirements. The research discussed in this paper was designed to contribute primarily to the first of these, and to future landscape ecology regional scale research in eastern Ontario. The data for this study were part of a set of Landsat data from 1975,

1984, 1995 and 2005 that were acquired for the GLEL prior to the development of this research. As one of the first studies of remote sensing-based regional LULC change mapping within the context identified above, this thesis is concerned with testing and evaluation of methods of LULC classification and of LULC change mapping. It therefore focuses on one time period from 1995 to 2005.

1.4 Research objectives

The two primary research objectives were:

1) Determine if land cover change can be accurately mapped across eastern Ontario for the period of 1995 to 2005 at a regional scale.

2) Compare a traditional pixel-based maximum likelihood LULC mapping method to a recently developed object-based hierarchical segmentation/nearest neighbour classification method and determine:

   i. which provides the most accurate maps of the area,

   ii. the relative advantages and limitations of each method

   iii. and how the accuracy of land cover classifications for each date and method affect the overall accuracy of subsequently derived change maps.

1.5 Thesis structure

This thesis is organized into five chapters. The first chapter introduces the topic of LULC change and the importance of using remote sensing to map LULC change. Chapter one also outlines the research scope, research objectives and outlines the overall organization of this thesis. The background research, as it was derived from the literature, is found in chapter two. This includes a summary of LULC change in the

context of landscape ecology, regional LULC mapping with Landsat, remote sensing classifications and temporal LULC change analysis. Chapter three presents the study area, outlines the methodology used for the selection of field sites and describes the field work. Chapter three also presents the image data, pre-processing, georectification, atmospheric correction, classification techniques and temporal analysis techniques. The results from the two classification techniques and the change detection method are presented in chapter four. Chapter five outlines the major findings of this research and links these findings to those in the literature. It also discusses the significant contributions and limitations of this research and makes recommendations for future research.

CHAPTER TWO

2.0 Background

This chapter provides a summary of LULC change in the context of landscape ecology. Contextual information is also provided on regional LULC mapping with Landsat and on remote sensing classifications and temporal LULC change analysis as derived from the literature.

2.1 LULC change: global and local changes

The impacts of LULC changes have been investigated for several years in many contexts. A broader understanding of these impacts on the global environment has only recently been achieved (Foley *et al.*, 2005). Global conversions to human-use lands have resulted in loss, fragmentation, and simplification of a variety of ecosystems.

Agricultural area has increased 70% worldwide over the last 50 years (Foley *et al.*, 2005). There has been an increase in the discharge of pesticides and anthropogenic nutrients resulting from these expansions. Humans currently release amounts of nitrogen and phosphorus to the Earth's ecosystems equal to all other sources (Carpenter *et al.*, 1998). Agricultural area enlargement has also resulted in an increased need of water for irrigation. It is estimated that irrigated area will increase 1.3 times by 2020 and 1.9 times by 2050 (Tilman *et al.*, 2005). Intensified agricultural practices cause an increase in the release of anthropogenic greenhouse gases. Clearing land for agricultural purposes also affects air quality by adding ash and smoke in areas with slash and burn practices. Forest to agricultural conversion has been shown to increase the mean annual discharge from a watershed (e.g. Costa *et al.*, 2003). Hydrosphere changes have also occurred due to increased urbanization.

Eastern Ontario (Figure 1.1) is a region that has been undergoing significant LULC change. The area's boundaries have been defined by different management and monitoring organizations for a variety of purposes. One particular entity, the Eastern Ontario Model Forest (EOMF) program, one of eleven programs in Canada's Model Forest Network (EOMF, 2006) has defined the area for forest monitoring purposes and those extents are shown on Figure 1.1.

Eastern Ontario is a diverse and fragmented region. Urban areas in the region are increasing in size. From 2001 to 2006 there has been an increase in the populations of the major urban centres of 4.9% for Ottawa, 1.6% each for Brockville and Cornwall and 3.8% for Kingston (Statistics Canada, 2006). The urban and sub-urban land uses in these areas have increased in size to accommodate these people. Zhang and Guindon (2005) revealed an increase of approximately 75 km^2 in urban land cover around the Ottawa-Gatineau region during the time period of 1966 to 2001. The average size of farms in eastern Ontario increased from 239 acres to 265 acres from 1996 to 2001. This represents an increase of 9.2% in total area (2001 Agriculture Census, Statistics Canada). Wetlands are dynamic and are affected by changes in climate, water and soil chemistry and hydrology (National Wetlands Working Group, 1997). Wetlands support many plant and animal species that are considered endangered or threatened (National Wetlands Working Group, 1997). Local changes include the estimated loss of approximately 66% of pre-European settlement wetlands near the urban area of Ottawa-Gatineau (Mitsch and Gosselink, 2000).

The noted projection of global agricultural land-use growth (see above and 1.1) reveals the importance of understanding and quantifying LULC change through time.

Past change may relate to what is currently happening in the landscape. With knowledge of past change it may be possible to reduce current change impacts on the future landscape. It is also important to understand the effects that LULC change have on species' persistence and extinction. Landscape ecology is concerned with relations between species and landscape dynamics.

2.1.1 Landscape ecology, LULC change and species' persistence

Landscape ecologists investigate the relations between spatial patterns and processes in ecological systems at different spatial and temporal scales (Turner *et al.*, 2001). Following a paradigm shift in ecology from the traditional 'balance of nature' viewpoint to the 'hierarchical patch dynamics' model (Wu and Loucks, 1995), landscape ecology studies have adhered to an understanding that landscapes are not homogenous and are ever-changing (Turner *et al.*, 2001).

The 'balance of nature' viewpoint proposed that populations and systems remain in a stable equilibrium and return to such a state after disturbance (Milne and Milne, 1960 *IN* Wu and Loucks, 1995). The ideas concerning hierarchical patch dynamics evolved when the balance of nature perspective failed to take into consideration the effects of multiple temporal and spatial scales and the inherent heterogeneity found in landscapes (Wu and Loucks, 1995). In general, hierarchical patch dynamics proposes that within a system there is a series of interconnections between different levels that are distinguished by the differences in the rates of the processes occurring at each level (Turner *et al.*, 2001).

A patch can be defined as an area in a landscape that is continuous, that provides resources for a species and is surrounded by uninhabitable land cover (the 'matrix')

isolating it from comparable patches (Turner *et al.*, 2001). Patches are dynamic over time and space, and each responds differently to disturbance processes, resulting in a heterogeneous landscape with multi-aged and multi-resource capable patches (Turner *et al.*, 2001). Some of the varying disturbances can be human-induced through LULC change practices such as land use conversion. Larger patches consist of smaller patches, and the overall dynamics of an ecological system are driven by the interactions between the patch levels (Wu, 1999). Although the exact variables that influence a process may not change with movement in the hierarchy from local to regional to global, the overall importance of the variables or the direction of the relationship may change (Turner *et al.*, 2001). Therefore, patterns and processes occurring within the hierarchy may change with scale (Wu, 1999).

Scale can be defined as the spatial or temporal elements of a pattern or process and generally has discernable levels of organization (Turner *et al.*, 2001). In landscape ecology studies and data, the spatial scale is characterised by the extent and grain. Extent refers to the size of an area of interest (the study area) and grain refers to the smallest spatial resolution in observed data (Turner *et al.*, 2001). In remote sensing, scale has traditionally referred to the relation between a linear measure (e.g. distance) in a paper map or image and the corresponding measure on the ground. In digital remote sensing, the nominal ground pixel size (often generally referred to as the spatial resolution) is essentially interchangeable with grain (Lillesand *et al.*, 2004). For example, the 30 m by 30 m pixels of a Landsat Thematic Mapper (TM) scene could be considered the grain of that image.

Considering hierarchical patch dynamics together with metapopulation theory, landscape ecologists attempt to interpret the relationships between changing patch dynamics and the persistence of species at different spatial and temporal scales. A metapopulation is defined as a group of distinct populations of the same species that are spatially separate but have the ability to interact in some form (Turner *et al.*, 2001). Metapopulation dynamics are driven by critical thresholds such as the amount of connectivity in the landscape and how the landscape transforms over time and space (Loreau *et al.*, 2003).

It is generally agreed that habitat destruction and fragmentation is one of the principal causes of species extinction (Pimm and Raven, 2000; Gu *et al.*, 2002). Determining when change occurred in the landscape (e.g. when fragmentation happened) may be the key to understanding a species' current persistence (or lack thereof). A species may be extinct or struggling to exist today because of a change that occurred 50 years in the past, and not because of a change that occurred within the current year.

Within the ecological context of this research and for many other applications, there is a need for accurate land cover classification maps, at regional extents over a long temporal period. Using these classification maps changes that have occurred between different time intervals can be assessed. This thesis is concerned with capabilities for mapping LULC change using remotely sensed data at the regional scale.

2.2 Remote sensing: An overview of data, processing, classification, and temporal change analysis methods relevant to this thesis

Remote sensing is the art and science of obtaining information about the Earth from images representing electromagnetic energy that is reflected or emitted from the land cover surface (Campbell, 2002). Remote sensing land cover classification methods have been shown to provide accurate land cover maps over large regions (Foody, 2002; Cingolani *et al.*, 2004). Remote sensing change mapping methods have also been shown to accurately provide the change direction (from/to land cover changes) over different time intervals (Abuelgasim *et al.*, 1999; Mas, 1999).

2.2.1 Regional LULC mapping: Landsat data

Landsat imagery has been found to be useful for mapping various land covers in the landscape (Jensen, 2005) and has been commonly used in similar types of classification and change mapping studies (Mas, 1999; Cingolani *et al.*, 2004; Chen *et al.*, 2005) at regional scales (Foody, 2002; Virk and King, 2007). From the studies of ecological response lag described above, it has been found that long time frames (30 to 100 years) reveal a lag response. Since 1972 a series of Landsat satellite sensors has been in continuous orbit of the earth, obtaining spectral data coverage of the world.

2.2.2 Geometric processing of image data

Most images contain positional errors due to the Earth's curvature, terrain changes and inaccuracies caused by sensor/scanner motion and perspective (Campbell, 2002) that need to be corrected. Images should also be referenced to a map projection that enables a user to find sites based upon a coordinate system. Additionally when working with several multi-temporal images, geometric registration (co-registration in some of the literature) is required. Foody (2002) states that errors due to mis-

registration have often been erroneously attributed to mis-classifications of thematic classes.

A geometric correction of the images ensures that all pixels correspond to the same horizontal position through a translation, scaling change and rotation to match the reference image or map (Jensen, 2005). Usually this is done using a polynomial mathematical model that produces the best fit to the x, y coordinates of selected ground control points (GCPs). The GCPs can be points collected in the field using a Global Positioning System (GPS) or selected on the reference image. Registrations can be image-to-map, image–to-image or some combination of the two. The GCPs are easily identifiable points on both images (and/or map) such as bridges, or road junctions. Perfect registration of multiple sets of imagery with pixels of different sizes may be difficult. It is suggested that an allowable error of ½ pixel size is appropriate (Lunetta and Elvidge, 1998). Geometric correction methods are fairly standardized in remote sensing. A similar procedure to that above is applied to geometrically align images that constitute a mosaic, using cutline pixels or GCPs in the overlap area of the referenced and unregistered image(s).

2.2.3 Atmospheric correction of image data

Atmospheric absorption and scattering affect solar radiation in its path towards the Earth's surface and then, in turn, in the path towards the recording sensor. Song *et al.* (2001) describe two categories of atmospheric correction: absolute and relative. In temporal analysis, it is generally not necessary to correct atmospheric effects if two thematic land cover maps, derived separately from imagery of two dates, are to be compared for change (Song *et al.*, 2001). However, minimization of these effects is

critical where image data from more than one date are to be compared or if one date is providing reference for some portion of the thematic map development of the other image(s). In this research, images of eastern Ontario from different dates were combined to form a mosaic, and data from a single reference date were used to classify data from an earlier date. Thus, normalization of atmospheric differences between images was critical. The following discussion provides a theoretical and methodological background to the aspects of atmospheric correction relevant to this thesis.

2.2.3.1 Absolute and relative corrections

Absolute corrections

Digital numbers (DNs) are discrete numerical values given to each pixel by the sensor during the collection phase for storage and analysis. Absolute corrections attempt to change these DNs into scaled surface reflectance (Jensen, 2005). Algorithms that use radiative transfer models (e.g. Second Simulation of the Satellite Signal in the Solar Spectrum (6S); Moderate Spectral Resolution Atmospheric Transmittance (MODTRAN)) have been developed for atmospheric corrections. Radiative transfer models are complex physical and numerical models that rely on atmospheric data that must represent the atmospheric properties at the time of image acquisition. In general, radiative transfer models model how radiation passes through the atmosphere in relation to the physical properties of clouds, aerosols, and gases present that may cause adsorption, emission and scattering of radiation from or onto the same path of the object of interest. The equations used incorporate such variables as time of year, altitude, latitude and longitude, solar zenith angle, elevation of the study area and the general type of climate. These equations are applied and the DNs are converted to scaled

surface reflectance. More details on absolute correction models can be found in Vermote *et al.* (1997); Berk *et al.* (1998); Zhao *et al.* (2000); Song *et al.* (2001); Ghulam *et al.* (2004).

One readily available algorithm is the Atmospheric Correction (ATCOR) program derived from the MODTRAN 4 radiative transfer model (Richter, 1991; revised 1996). This algorithm has the benefit of not requiring any ancillary data other than solar zenith angle and visibility at the time of acquisition. The atmospheric properties of this model are pre-defined and selectable by the user. These consider the condition of the atmosphere (tropical, mid-latitude, or US standard atmosphere along with rural, urban, desert or maritime), an adjacency parameter that represents the effects of backscattering, and the path length through an elevation parameter. The calibration files are derived from the sensor's calibration defaults.

Other absolute correction methods rely on data derived from the image (e.g. dark-object subtraction (DOS) method (Chavez, 1988)). The DOS method assumes that there is constant haze that adds brightness to all pixels and that at least a few pixels should have zero DN value (Chavez, 1988). The user selects a constant DN value. (This value is chosen from the histogram of a designated band at the point where the frequency of pixels increases significantly (Figure 2.1)).

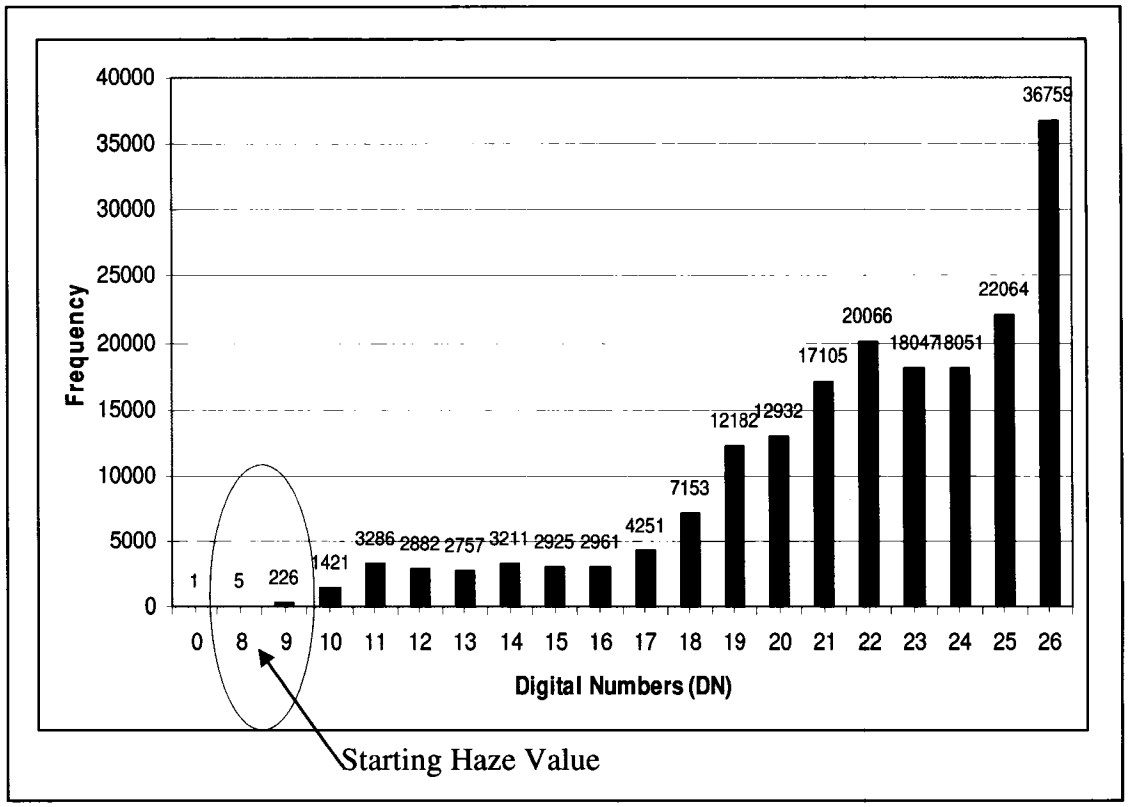

Figure 2.1 - Example of the lower portion of a band histogram. Starting haze value to denote atmospheric condition would be 8 (Chavez, 1988).

This starting haze value selected from one band denotes the atmospheric condition at the time of acquisition (e.g. very clear, clear, moderate, hazy, very hazy (Chavez, 1988)). The correction (function) value is then applied to each band. This is a set value and is determined by the atmospheric condition. Considering that some bands contribute more to scattering than others, the correction (function) value is different for each band for each atmospheric condition and is based on the relative contribution of scattering of each band (e.g. progressively smaller from band 1 through to band 7. For example, on a very clear day TM bands 1, 2, and 3 account for 93.6% of all scattering (Chavez, 1988)). The DNs are first converted to radiance at the sensor using calibration values available for the particular sensor. In this thesis radiometric calibration values

for Landsat 5 are derived from Chander and Markham (2003). The radiance at the sensor was derived using the equation:

$$L_\lambda = \left(\frac{LMAX_\lambda - LMIN_\lambda}{Qcal\max}\right)Qcal + LMIN_\lambda \quad (2.1)$$

where L_λ is the spectral radiance at the sensor in W m^{-2} sr^{-1} μm, *Qcalmax* is the maximum quantized calibrated pixel value, $LMIN_\lambda$, is the spectral radiance scaled to *Qcalmin* in W m^{-2} sr^{-1} μm and $LMAX_\lambda$, is the spectral radiance scaled to *Qcalmax* in W m^{-2} sr^{-1} μm (Chander and Markham, 2003). Once the DNs are converted to at-satellite radiance, the correction (function) values (Chavez, 1988) are applied to each band using the starting haze value derived from the histogram. Table 2.1 shows an example of a conversion of the starting haze value using the function values derived for a very clear atmosphere:

Table 2.1 - Examples of haze value calculation for each band.

Band	Correction (function) value (for very clear atmosphere)	Starting haze value (after conversion to at-satellite radiance)	Haze value (per band, LHaze)
1* (selected as atmospheric condition band)	1.00		8.000
2	0.563	* 8	4.504
3	0.292		2.336
4	0.117		0.936
5	0.075		0.600
7	0.002		0.016

The haze value is then removed from each band using equation 2.2:

$$\text{DOS haze removal} = \pi * (L_\lambda - \text{LHaze}) \quad (2.2)$$

where LHaze is the calculated haze value. One modified version of DOS uses the cosine of the solar zenith angle as a substitute for atmospheric transmittance (the fraction of incident radiant energy that passes through a particular medium (Chavez, 1996)). Another modified DOS algorithm considers atmospheric transmittance in a Rayleigh scattering atmosphere (DOS 3 in Song *et al.*, 2001). Another means of modifying the simple DOS method is with a simple shift to align the left side of the histograms so that dark objects are spectrally similar across several images (Pax-Lenney *et al.*, 2001). A similar method, the Modified Dense Dark Vegetation (MDDV) assumes that areas of dense, dark vegetation are present and are used as dark objects to modify Landsat bands 1 and 3 based upon a surface reflectance relationship with band 7 (Schroeder *et al.*, 2006).

Relative corrections

Relative corrections normalize the variations of the spectral bands across several scenes to one selected scene (Jensen, 2005). In temporal analysis, this type of correction assumes a linear relationship between image bands over time. The linear relation can be derived from measurement of the brightness of pseudo-invariant features (PIFs) that are radiometrically stable, such as a deep lake, large flat asphalt roof, a salt lake, etc (Song *et al.*, 2001). Alternatively, if the change is small in relation to the total image area, then the linear relation can be found by regressing whole images from two dates. PIFs may be selected automatically in some algorithms such as the Multivariate Alteration Detection (MAD) (Schroeder *et al.*, 2006). The choice of the particular atmospheric correction depends upon the presence of certain features in the imagery, the accuracy of

each method, the availability of atmospheric properties or particular spectral bands and the ease of the implementation.

2.2.3.2 Comparisons of relative and absolute correction studies

Pax-Lenney *et al.* (2001) assessed the results of several corrections on classification accuracy. This was of particular interest because these classifications used generalization, the extension of training sample data statistics across time and space that is implemented in this thesis (see 3.6.3). The researchers tested DOS (Chavez, 1988), modified DOS (Chavez, 1996), DOS3 (Song *et al.*, 2001), a histogram matching approach applied to DOS, and an algorithm using 6S radiative transfer model. The classes were Coniferous and Non-coniferous and the dates of the Landsat data ranged from June to October. Within a single scene, classification accuracies for a fuzzy neural network classifier were found to be highest using either DOS or modified DOS methods for midsummer imagery. Accuracies declined across a regional extent (across multiple scenes).

Schroeder *et al.* (2006) tested DOS3 (Song *et al.*, 2001), the MDDV approach, an algorithm using 6S, PIF method, the MAD technique and two combinations of absolute and relative corrections (referred to as "absolute-normalization") on multi-temporal Landsat data. They were interested in forest changes over western Oregon for the time period of 1984 to 2004 using imagery from July, August and September. The results showed using the combined "absolute-normalization" method by relatively correcting imagery using either the PIF or MAD methods to a 6S corrected "master" image resulted in the lowest root mean square error (RMSE, the square root of the sum

of squared differences between the corrected and reference reflectance divided by the number of observations.

Based on results of these and other comparative studies (Song *et al.*, 2001, Chen *et al.*, 2005) and the availability of the ATCOR2 algorithm, the DOS method, ATCOR2 algorithm, and combinations of DOS/PIF method and ATCOR2/PIF method were selected and implemented using methods described in 3.4.2.

2.2.4 Classification of remote sensing data for land cover mapping

There are several key land cover classification methods that can be employed including algorithms that are based on parametric or non-parametric statistics (Jensen, 2005). Parametric methods include maximum likelihood classification and are used if the underlying remote sensing data are normally distributed and there is some previous knowledge regarding the landscape (Jensen, 2005). Non-parametric methods can be used if the underlying remote sensing data are not normally distributed, if the data are non-ratio (e.g. categorical attribute data) or if the LULC composition and form is unknown (Jensen, 2005).

Classifications can be hard or soft. Hard classifications assign the unit of interest specifically to one class of *n*-available classes. Soft (e.g. fuzzy, used in this thesis) classifications assign a membership value that represents the degree of similarity of the pixel to each class found within the unit of interest. Membership can be assigned based upon nearest-neighbour relations whereby the Euclidean distance in *n*-dimensional space is calculated to the nearest training class (Jensen, 2005). The membership value can be ranked between zero, representing a complete uncertainty of membership and one representing complete certainty of membership for each class (Flanders *et al.*,

2003). The membership value for the top class is assigned to the unit of interest. Often second and third membership values are available for review.

These various methods can classify pixels or objects. The difference between pixel-based and object-based classification is that although pixel-based methods may consider spectral and other continuous spatial information (e.g. texture) they cannot easily take into consideration contextual information such as size, shape and topological relations between entities in the image that are aggregations of pixels. The premise behind object-based methods is that land cover entities are spatial units that are of more interest and use in ecological analysis and land management than are arbitrarily defined individual pixels. By first defining such objects within an image and then classifying them, more useful thematic maps can be produced that show landscape entities as humans perceive them. Objects are derived from pixels in a variety of ways (see 2.2.4.3) with the intent to capture levels of spatial aggregation that produce meaningful and interconnected landscape features. Through continued aggregation, larger objects can be derived from existing smaller objects, resulting in an object-hierarchy with the lowest level representing pixels and the highest level representing the entire scene as one object. Intuitively, object-based methods fit well with landscape ecology studies in terms of hierarchical patch dynamics. As noted, larger patches consist of smaller patches, and the overall dynamics of an ecological system are driven by the interactions between the patch levels (Wu, 1999). The classification of objects can consider not only the spectral and other continuous information about the object, but also the size, shape and topological relations of objects to each other in their object-level and to other objects throughout the hierarchal structure (Benz *et al.*, 2004). The following section

summarizes the theory and general methods relevant to the classification methodology of this research.

2.2.4.1 Unsupervised classification

Unsupervised classification is used when there is no prior knowledge of land cover, or for data flow automation, or to aid analysis of inherent spectral class discrimination in an image. An algorithm, such as the Iterative Self-Organizing Data Analysis Technique (ISODATA) clusters pixels into natural groupings based upon their spectral properties. After these clusters are developed, the groups are then assigned to specific classes either through ground based investigation or examination of the clusters' spectral properties (Jensen, 2005).

The ISODATA technique is a developed set of rules that is based upon a k-means clustering algorithm (Jensen, 2005). The user assigns several values to parameters such as maximum number of clusters, maximum number of iterations and maximum percentage of pixels allowed to remain unchanged between iterations (Jensen, 2005). In the first iteration, arbitrary cluster means are determined and each pixel is assigned to the closest cluster based on Euclidean distance. The cluster means are then re-calculated and pixels are re-assigned to the closest cluster in subsequent iterations. The algorithm stops when a certain proportion of the pixels no longer change clusters between iterations. Within the iterative process, clusters may be merged, split or eliminated based on certain inputs regarding the minimum allowable size of clusters and the minimum allowable distance between any two cluster means (Lira *et al.*, 1999). In this research, unsupervised classification was used to aid selection of potentially distinct

land cover classes and potential sites to be used as reference data for subsequent supervised classification.

2.2.4.2 Supervised classification

For selected classes such as agriculture, forest and water, training pixels known to be representative of the spectral and/or spatial characteristics of a given class are delineated in the image. The separability of the training data can be analyzed using multivariate inverse variance-covariance weighted measures of distance between class means, such as the Bhattacharyya Distance. This measure determines the separability between a pair of classes using the mean and variance-covariance matrices (Haralick and Fu, 1983):

$$Bhat.Dist. = \frac{1}{8}(\mu_1 - \mu_2)'\left(\frac{\sum_2 + \sum_2}{2}\right)(\mu_1 - \mu_2) + \frac{1}{2}\ln\frac{\left|\frac{\sum_1 - \sum_2}{2}\right|}{|\sum_1|^{1/2}|\sum_2|^{1/2}} \qquad (2.3)$$

where, μ_1 and μ_2 are means of the classes of interest and $\sum_1$ and $\sum_2$ are the covariances. Most algorithms scale the resulting distance measure into a smaller range that is easier to analyze. For example, in this research, the algorithm scaled the resultant distance into a range between 0 and 2, where `0' indicates complete overlap of two classes and `2' indicates a complete separation between the two classes. As Bhattacharrya Distance is non-linear, values of 1.9 and greater are often used to indicate good separabililty and values of 1.7-1.9 may indicate potential for accurate classification of a pair of classes. If there are classes that are overlapping and the separability is poor (e.g. less than 1.7), a decision concerning re-training or merging of classes should be made by the user. Following the training stage, the statistical information in the training data is used to assign each image pixel to the class to which it has the highest probability of belonging.

The maximum likelihood classifier (MLC) is a widely used algorithm for supervised or unsupervised classifications. It assumes that the pixels forming a training class are normally distributed and following this assumption, the statistical probability (the Bayesian likelihood) can be calculated that a pixel belongs to a particular land cover category. The MLC method is often used in comparative studies as a reference against which other classification methods are evaluated (see 2.2.4.4).

2.2.4.3 Object-based land cover classification

Object-based classification methods have been an alternative to pixel based methods since the 1970s (Flanders *et al.*, 2003), but until high resolution satellite imagery became available in the late 1990s, they were not widely used. As described above, objects are developed from pixels, usually in a process called 'segmentation'. They are then subsequently classified based upon the information derived from the object itself and its relations to other objects in the hierarchical structure.

Image segmentation

The main goal of image segmentation is to create objects that relate to meaningful landscape features (e.g. farm fields, forest, suburbs). The technical objective in segmentation is to define objects that have minimized within-object variability, and maximized between-object variability. The creation of objects from individual pixels is based upon neighbouring pixels' (and subsequently created objects') spectral and spatial properties (Burnett and Blaschke, 2003). Segmentation algorithms fall into two main categories: edge-based and area-based (Jensen, 2005). Edges occur where there are sharp changes in brightness values. In edge-based segmentation, the growing of objects is based upon these edges and subsequent linked edges that may

signify borders between objects. Problems can occur if edges are not present where a real border exists, or edges are present where no real border exists. Area-based (also known as region-based) segmentation compares pixels or groups of pixels (the 'seed') and merges comparable areas as long as they are homogenous. An additional method of area-based segmentation can split large heterogeneous areas into smaller homogenous units. Some segmentation algorithms use a combination of splitting and merging. Available segmentation algorithms include chessboard, quadtree, multiresolution and spectral distance segmentation. In this thesis, the multiresolution and spectral difference algorithms (both area-based) were tested in the Definiens Professional 5.0 software (formerly, and referred to in this thesis as eCognition). The following outlines the general methodology for these two segmentation algorithms.

The key parameter in multiresolution segmentation is a unitless variable of scale that is correlated to the image's pixel size and is related to the parameters of colour and shape (Laliberte *et al.*, 2004). Objects are defined and delineated based upon spectral similarity of pixels, contrast of an object with neighbouring objects and object shape characteristics. The larger the value of the scale parameter the larger the image objects will be (Benz *et al.*, 2004). As the segmentation proceeds, the pixels are first grouped to minimize within-object heterogeneity. Objects are subsequently grouped based upon spectral similarity, contrast with neighbouring objects and shape characteristics (Yan *et al.*, 2006). Objects are grown evenly and simultaneously across the entire scene. In the eCognition algorithm, colour (spectral information) and shape (smoothness and compactness) can be weighted by the user (Laliberte *et al.*, 2004). As objects are created they are merged together following the scale, shape, colour, smoothness and

compactness parameters. The process ends once the growth surpasses the values defined (Laliberte *et al.*, 2004). This creates one object level in the hierarchy. The multiresolution segmentation can be applied again with a different scale parameter to the first object level to obtain a second level of objects.

For the spectral difference segmentation, there must be a level of objects previously segmented (e.g. cannot use the spectral difference segmentation on pixels directly) which are then grown into larger objects. This algorithm merges neighbouring objects based upon a mean layer brightness value. The objects are merged if the difference in this value is below a specified maximum. This method can be useful in distinguishing classes of interest if a distinct difference is noted in one particular band between classes of interest. This algorithm can be weighted to only consider the difference(s) for that particular band.

Object Classification

Objects can be classified at any level within the developed object hierarchy and the class criteria may take into consideration the object's relations to neighbours, and the sub- and super-levels of the hierarchy to determine an object's membership value for a particular class.

A set of decision rules is developed for each class that are applied to each object to assign it a membership value(s) to particular classes. Possible classification rules can relate to the object's features including shape, and texture. For example, if a given class is comprised mostly of rectangular features (e.g., agricultural fields) the shape parameter 'rectangular fit' can be assigned to that class. The rectangular fit parameter is the ratio of the area fitting inside an equal area rectangle divided by the area of the object outside

the rectangle (Yu *et al.*, 2006). Other possible shape features in the eCognition software include a shape index, area of the object, border index, and compactness. Details on these are given at www.definiens.com. The position of an object in the segmentation hierarchy and its relationships to other classes in its level, within the hierarchy, and to the overall scene can also be used as classification rules. Additionally, all of the rules can be applied to all classes or to individual classes. At the individual level, classification features can be set with ranges of outcomes (e.g. all rectangular fit values between 0.75 and 0.85 classified as one class), with one set value, or with a specified minimum and maximum.

The eCognition software for object based segmentation and classification is very complex and requires much experimentation to evaluate the impacts of various methods and parameters on the thematic maps that are produced. Section 3.6.3 describes the experimentation that was conducted in this research, while the following section summarizes some previous studies comparing standard MLC classification with object based classification.

2.2.4.4 Previous research comparing object-based classifications to MLC methods

Flanders *et al.* (2003) used eCognition to segment Landsat 7 imagery into spectrally homogenous objects of roughly equal size. They subsequently classified the objects (forest cut blocks) using a fuzzy classifier to compare to a traditional pixel-based method. The scale parameter was set at 25 for the first level of segmentation and 200 for a larger-object second level. A spectral parameter of 0.2 and a shape variable of 0.8 emphasized cut block shape over spectral values because the shape of cut blocks was more homogenous than their reflectance. The results showed that using a simple

classification hierarchy improved the accuracy of classification over the MLC method. However, one of the drawbacks of this research was the need to create subsets of the imagery to subsequently train and classify the entire image. Different accuracies were obtained in each different subset: 70.0%, 91.0% and 87.5% for subsets 1, 2 and 3 respectively.

Yan *et al.* (2006) compared the MLC classifier and an object-based eCognition classification to map 12 land cover classes in a coal fire area of China using Advanced Spaceborne Thermal Emission and Reflection Radiometer (ASTER) data. Several values (5, 10 and 20) were tested for the scale parameter and a weight of 0.8 was given to the colour parameter with 0.2 given to the shape parameter (weighting spectral characteristics much more than object shape). The overall accuracies were 46.48% and 83.25% for the pixel-based and the object-based classifications, respectively.

Yu *et al.* (2006) compared the MLC method and an object-based method using a merging approach, the Fractal Net Evolution Approach (FNEA). The study area was Point Reyes National Seashore in California and the data were: images from a 4-band airborne digital camera with 1m pixels; elevation, slope, aspect and distance to waterways; and intensity, hue and saturation of three-band combinations. Fifty-two features per object were derived and ranked for use in the classification. Sixteen features were selected for use with the nearest neighbour classifier. Forty-eight classes with forty-three varieties of vegetation, and five singular classes of urban, non-urban, dune, beaches and water were classified. The overall object-based accuracy was 56.3%, with 13 classes of the vegetation achieving over 60% accuracy.

Based on the results of these studies, this research was designed to include an assessment of object based classification in mapping of land cover change.

2.2.5 Remote sensing change mapping

Change mapping is a method of identifying variations in a particular entity, surface area or process over time (Singh, 1989). There have been many comparative studies to assess various change mapping methods, and to determine for which landscapes they are most appropriate (Yuan and Elvidge, 1998; Mas, 1999; Coppin *et al.*, 2004; Lu *et al.*, 2004; Lu *et al.*, 2005). Change mapping analysis can be categorized as pre-classification and post-classification (Lunetta and Elvidge, 1998; Lu *et al.*, 2004). Lu *et al.* (2004) stress the importance of determining what type of change information is required, either change direction (from one land cover class to another) or simple change/no-change detection. For the ecological research context of this thesis (see 2.1.1), accurate land cover type change information is required. However, to aid selection of validation sites for the older imagery, one pre-classification method was also used. The following sections provide a summary of common change detection and mapping methods with emphasis on those used in this research.

2.2.5.1 Remote sensing change mapping: pre-classification methods

Pre-classification refers to analysis that is performed on raw or transformed (e.g. vegetation index) imagery that has not been categorized into discrete land cover classes. An example of pre-classification analysis is image differencing where one or more spectral bands from one date of imagery are subtracted from the same spectral band(s) of a second date. Large differences identified by a user-defined threshold are considered to be pixels that have changed. Thresholds can be determined by using the standard

deviation from the mean and supported using field observations. However, when all pixels are used for the change detection algorithm, histograms are not normally distributed and are affected by extreme maximum and minimum values. Another method for selecting thresholds is by user-testing on a trial and error basis. This method tests different threshold levels to determine which threshold level provides the most accurate change/no change information. Most pre-classification change methods provide an indication that there has been a change from one date to another (change/no change) however, these methods do not provide the direction of change or the nature of the before and after land cover classes.

2.2.5.2 Remote sensing change mapping: post-classification comparison

Post-classification comparison (PCC) analysis uses maps such as land cover classifications that have been developed from imagery (Lunetta and Elvidge, 1998). This approach provides the direction of the change (from/to change) for example, from wetland to urban. Change maps from satellite imagery can reveal information about LULC which can be examined and used by landscape ecologists and other resource managers. The maps from each date can also be compared on a pixel-by-pixel basis using a change detection matrix (Jensen, 2005). In this matrix, the pixels along the diagonal reflect the no-change areas; the pixels in the rows and columns represent the differences between the two maps, with the columns generally representing the later date and the rows representing the earlier date.

Initially, images to be used in a PCC are registered to each other and then classified into land cover types. The processing steps to classify individual date images are numerous and require careful execution. Errors contained within either of the

classification maps will be amplified by any subsequent PCC (Coppin *et al.*, 2004). It is imperative to choose the most accurate classification technique available. These techniques include classification methods described above, but all have limitations affecting accuracy.

2.2.5.3 Assessment of studies using PCC

Mas (1999) found that PCC provided the most accurate results for Landsat MSS-based change mapping in Mexico with classes of evergreen tropical forest, wetland and agriculture. The data were two Landsat MSS images from February 1974 and April 1992. Four main classes of landcover were classified using the ISODATA algorithm the two maps were analyzed with PCC. The accuracy ranged from 50% for changes for the 'from pasture-agriculture/to forest' class and up to 100% for no changes for the 'from urban/to urban' class. These results were compared to four 'change/no change' methods and two other 'from/to change' methods. PCC was found to have the highest global accuracy of 82.41% for 'from-to' change comparisons.

Prenzel and Treitz (2006) used PCC to compare two thematic maps derived from SPOT imagery of Indonesia in 1990 and 1999. The MLC method was used with eight classes: rainforest, mangrove forest, mixed vegetation, herbaceous, mud, bare soil, built up, and water. The overall accuracies were 87.5% for the 1990 image and 81.2% for the 1999 image. These maps were then cross-tabulated. It was found that 44.70% of the extent had some kind of change and that the overall accuracy of the PCC was 71.05%.

Virk and King (2007) used PCC as a means to analyze forest deforestation and reforestation in India during the period of 1986 to 2003 using Landsat TM and ETM+ data. The research was conducted in two phases whereby image differencing using the

normalized difference vegetation index (NDVI), was found to be better than differencing of the second principal component and the Kauth-Thomas greenness (KT-G) index. The NDVI difference was then reclassified to produce deforestation and reforestation maps. In the second phase, the two scenes from 1986 and 2003 were classified using the MLC method. The two thematic maps were subsequently cross tabulated and a change matrix for deforestation and reforestation was derived. In comparison with the deforestation and reforestation maps derived from the NDVI differenced method it was found that the PCC method provided a more accurate representation of forest change (deforestation and reforestation).

CHAPTER 3

3.0 Methodology

This chapter describes the study area, methodology used for the selection of field sites and field work. This chapter also describes the image data, pre-processing, georectification, atmospheric correction, classification techniques and temporal analysis techniques.

3.1 Study area: eastern Ontario

This study is part of a larger body of research being conducted within the GLEL. It was therefore important that the area selected encompass sites currently under investigation. These research projects require long term regional scale data to determine the impact of LULC change on species' persistence. In this context regional scale encompasses landscapes, and covers broad geographic areas. Therefore, the first step of this research was to identify an appropriate study area and time period.

The study area is eastern Ontario and a small portion of southern Quebec. The study area covered the region from Deep River, Ontario in the northwest, towards the east along the Ontario/Quebec border (Ottawa River, including Gatineau Park) and then along the Ontario/US border (St. Lawrence Seaway) in the south to just east of Port Hope, Ontario in the southwest (Figure 1.1). Considerations included the variety of land cover types in the area, the availability of data over a long time period, the accessibility to field data and the limited amount of published research on change over time in eastern Ontario.

Much of the underlying parent material of the area is sedimentary rock. There is an extension of the Canadian Shield bisecting the area east of Kingston through the St.

Lawrence Seaway. This incursion is known as the Frontenac Axis and results in distinctive land cover patterns as compared to the areas to the east or west (Baldwin *et al.*, 2000). The land cover in this area is mixed forests with irregular agricultural fields and wetlands. To the east and west, gleysols and luvisols support agriculture. The terrain was also affected by the last glacial period, resulting in the formation of moraines, eskers, and kames comprised of sand and gravel (Baldwin *et al.*, 2000).

Eastern Ontarian forests fall within the Great Lakes-St. Lawrence region (Thompson, 2000) and include dominant hardwoods such as sugar maple *(Acer saccharum)*, yellow birch *(Betula alleghaniensis)*, white birch (*Betula papyrifera),* white ash (*Fraxinus americana)*, black ash (*Fraxinus nigra)*, beech (*Fagus grandifolia)* and red oak (*Quercus rubra).* Softwoods include white pine *(Pinus strobus)* and red pine (*Pinus resinosa)* located mostly in plantations dating from the 1950s (EOMF, 2006). Other softwoods such as black and white spruce (*Picea mariana, Picea glauca*), jack pine (*Pinus banksiana*), eastern white cedar (*Thuja occidentalis*), tamarack (*Larix laricina*) and balsam fir (*Abies balsamifera*) are found in mixed stands (Thompson, 2000; EOMF, 2006). Over the past 150 years the forests of eastern Ontario have been in a state of decline due to lumber/logging, mining and agricultural uses of the land (EOMF, 2006).

Currently there are 9,333 farms in eastern Ontario. Average farm size increased from 239 acres in 1996 to 265 acres in 2001. Half of the farms in the area are cattle and dairy. Croplands (grain corn, soybean, hay, etc.) account for 526,091 hectares representing an increase of 9.2% from 1996 (2001 Agricultural Census, Statistics Canada). With an increase in the demand for ethanol, it is expected that there will be an

increase in corn production. Supporting this assumption, an ethanol plant opening in eastern Ontario in 2008 may increase the requirement for corn.

There are four major urban centres in eastern Ontario including: Ottawa, Cornwall, Brockville and Kingston. Ottawa (official municipal area) covers 2,778.13 km^2 with 812,129 people. Cornwall (census agglomeration) spans 508.98 km^2 with 58,485 people. Brockville (census agglomeration) covers 1,143.39 km^2 with 39,668 people and Kingston (census metropolitan area) spans 1,906.69 km^2 with 152,358 people. These numbers represent an increase in population of 4.9% for Ottawa, 1.6% for Brockville and Cornwall and 3.8% for Kingston from 2001 (2006 Community Profiles, Statistics Canada).

3.2 Data acquisition

Landsat imagery has been found to be useful for modeling vegetation in the landscape (Jensen, 2005) and has been commonly used in land cover classification and temporal analysis of regional areas (Mas, 1999; Cingolani *et al.*, 2004; Chen *et al.*, 2005; Virk and King, 2007). The size of a Landsat scene (185 km swath) enables coverage of eastern Ontario with a minimal number of scenes (four). The spectral resolution allows for the mapping of a variety of land covers as outlined in Table 3.1.

Table 3.1 - Landsat TM sensor characteristics.

Sensor	Band	Wavelength (μm)	Pixel Size	Details
TM	1 (Blue)	0.45 – 0.52	30 m	Penetrates water and derives supplementary characteristic information of land-use, soil and vegetation cover.
	2 (Green)	0.52 – 0.60	30 m	Green reflectance peak; Responds to the reflectance of vigorous vegetation.
	3	0.63 – 0.69	30 m	Differentiates between

	(Red)			plant species (chlorophyll adsorption band).
	4 (NIR)	0.76 – 0.90	30 m	Vegetation detection, biomass content, water body detection and soil moisture differentiation.
	5 (MIR)	1.55 – 1.75	30 m	Sensitive to the amount of water in vegetation and differentiates between clouds, snow and ice.
	6 (TIR)	10.4 – 12.5	120 m (resampled to 30 m)	Measures the amount of infrared energy that is emitted from surfaces; useful for vegetation and soil moisture classifications
	7 (MIR)	2.08 – 2.35	30 m	Useful for determining rock foundations; sensitive to moisture content

(Source: Jensen, 2005)

The maximum possible time frame using satellite imagery (30 year period from 1975 to 2005) has been selected in support of the overall ecological lag research project in the GLEL. For this thesis, the focus was on methodology evaluation so the time interval was reduced to the period of 1995 to 2005. The sixteen day repeat cycle of the Landsat satellite allows for the best choice of scenes during the summer growing period. Four scenes per year of interest (1995 and 2005) were required to obtain complete coverage of the entire region. Figure 3.1 provides a simplified representation of the position of the four scenes for each year. The full coverage of the four scenes per year is from 47.00° to 43.61° north latitude to −78.16° to −73.10° east longitude. Information regarding the exact position and the corresponding size in lines and pixels of each image from the overall research is in Table I-A1 (Appendix I-A). These four scenes represent the entire study area of interest.

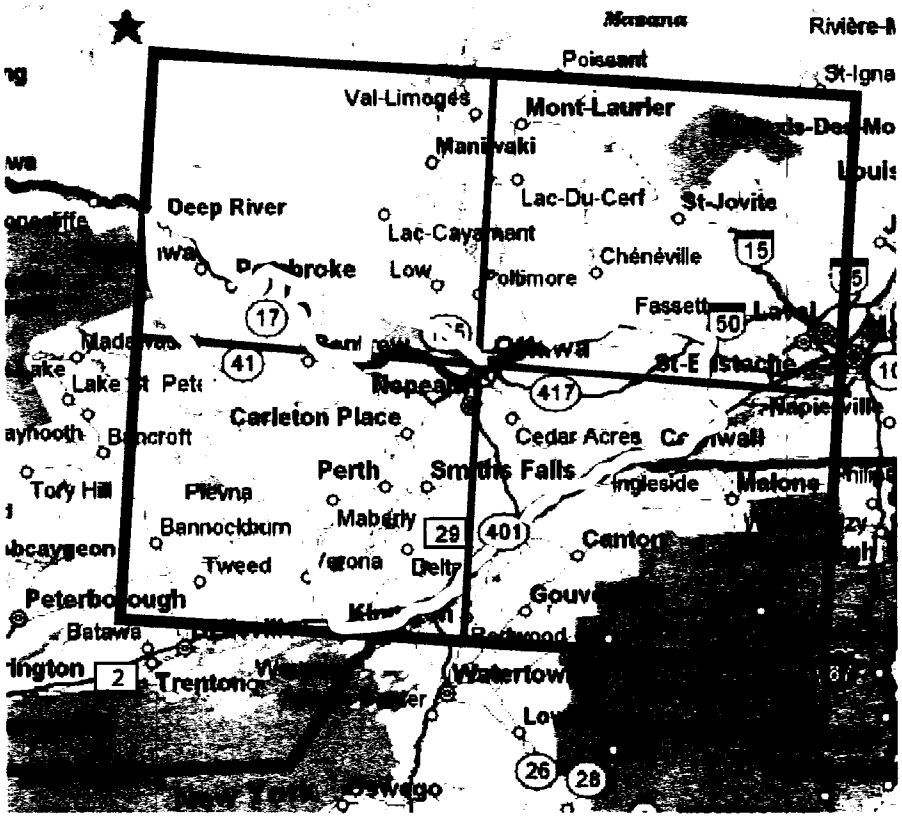

Figure 3.1 - Simplified representation of the position of the four scenes of Landsat imagery for each year (purple box). Study area borders (yellow). Not to scale.

Overall, eight Landsat 5 TM scenes were acquired from the United States Geologic Society (USGS) Earth Resources Observation Systems (EROS) Data centre. The scenes were obtained with systematic geocorrections (geometric and radiometric) in GeoTIFF (Tagged Image File Format). The residual error of these files is stated to be better than 250 meters in flat areas. Individual GeoTIFF images of each spectral band (seven for Landsat 5 TM (Table 3.1) are a greyscale of uncompressed 8-bit unsigned integers. There is one GeoTIFF file containing metadata for each scene. Although Landsat 7 Enhanced Thematic Mapper Plus (ETM+) data were available for 2005, in 2003 the satellite's scan line corrector failed resulting in reduced quality of data, especially towards scene edges. The initial need in this research to combine four scenes

into one large mosaic image made edge quality an important consideration and therefore Landsat 5 data were selected for 2005.

The key criterion for the selection of these scenes was that each scene must be cloud free (less than 10% cloud cover). The secondary criterion of the image acquisition was to ensure scenes within the same year were close to the same anniversary date (preferably June/July in the middle of the growing season). These criteria resulted in scenes spanning dates from as early as June 10th to September 13th. Table 3.2 provides the date of acquisition for each of the eight scenes, as well as the naming convention used. In particular, 2005 data were very cloudy for most of the summer, resulting in the necessity to use three scenes from September.

Table 3.2 - Landsat TM data date information.

Overall Year	Satellite & Sensor Information	Path	Row	Date of Acquisition	Name
2005		15	29	September 6, 2005	2005_1529
Landsat 5 TM (March 1, 1984 to present)		16	29	September 13, 2005	2005_1629
		15	28	September 6, 2005	2005_1528
30 m pixel Swath – 185 km		16	28	July 11, 2005	2005_1628
1995		15	29	August 10, 1995	1995_1529
Landsat 5 TM (March 1, 1984 to present)		16	29	August 1, 1995	1995_1629
		15	28	August 10, 1995	1995_1528
30 m pixel Swath – 185 km		16	28	September 2, 1995	1995_1628

Several of the scenes had cloud coverage in overlapping areas and in areas of the imagery outside the region of interest. However, in all cases these were the best possible images available for the particular years.

3.3 Pre-field work data processing

Before conducting fieldwork, the study area scenes were reviewed to determine if certain sites that appeared anomalous or rare in terms of spectral reflectance characteristics should be visited. A mosaic of all 2005 scenes for use in the field was

prepared to provide full study area coverage. Travel routes were prepared that traversed the area passing through all the major land cover types of eastern Ontario. As there was no prior knowledge of the specific land cover types, an ISODATA unsupervised classification was conducted to identify potential land cover classes that were spectrally distinct and to aid in the development of the travel routes.

3.3.1 Mosaic production and ISODATA classification

Each 2005 scene was assigned a Universal Transverse Mercator (UTM) projection (row T, zone 18) with an earth ellipsoid of North American Datum of 1983 (NAD 83). One scene was selected as a master image (2005_1628) and the other three scenes were aligned and relatively calibrated to it. Mosaics were created by orienting each scene in an overall coverage according to their spatial arrangement (Figure 3.2).

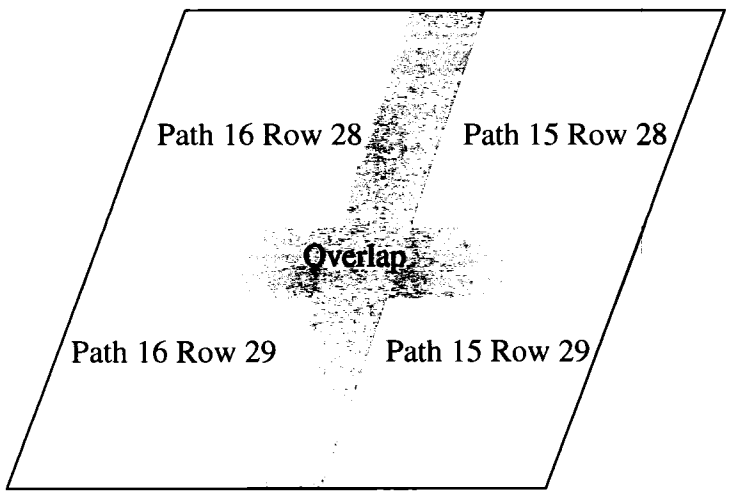

Figure 3.2 - Spatial arrangement of Landsat scenes.

Cutline pixels, representing points along which the scenes are fused, were next selected in the overlapping regions. In consideration of time (this initial mosaic was to be used only to guide fieldwork and was later to be refined for the analytical and mapping phases of this research), an automatic mosaic procedure was used. For cutline

selection there were three options available: minimum difference, minimum relative difference and edge features. The edge feature selection (a combination of the other two methods which selects cutline pixels based upon areas with a minimum difference of grey values between the scenes and considers pixels with the largest gradient (defines areas such as road edges)) was selected. This method does not provide an overall RMSE for the automatically selected cutlines. The result was one large image covering the entire area of interest (Figure I-B1a and b, Appendix I-B). Using the 2005 mosaic file, ISODATA clustering was conducted with 15 minimum clusters, 30 maximum clusters, and a maximum number of iterations of 20. A thematic map with 23 clusters was created and used as an aid in development of the travel routes (Figure I-B2a and b, Appendix I-B).

3.4 Field data acquisition

Reference data are required for supervised classifications to use in training and validation. It is important to obtain as large a representative set of data for each "class of interest" as possible. For example, a general class "Wetlands" may contain sites with dead standing trees and open water or areas with dense cattails and no open water. Additionally, over the regional scale, local differences must be accounted for and complete coverage is critical. In terms of validation sets, it is good practice to obtain a minimum number of sites. This minimum ranges from 15 to 50 validation sites per class (Jensen, 2000; Foody, 2002; Lillesand *et al.*, 2004). For this research, given the size of the study area and number of possible classes, an attempt was made to accumulate a minimum of 15 sites for each class. For rarer land cover classes (e.g. pure sand, pure bare soil) it was not possible to find 15 sample sites.

Travel routes were developed that included representations of each of the 23 clusters created by the ISODATA algorithm. Figures I-B3a and b show representations of these routes (Appendix I-B).

Fieldwork was conducted in July in the middle of the growing season. To ensure that a given site could be related back to the imagery, the land cover at the site had to have a spatial extent of at least 3 x 3 pixels (90 x 90 m). At each individual site, a laser rangefinder was used to estimate the overall size of the site. The characteristics were noted, photographs were taken and a GPS coordinate was taken for the location from which the land cover was viewed (usually the side of the road). It should be noted that these class sample sites were constrained by public road access and that only homogeneous sites were selected as representative samples, both which may cause sample bias.

All seven routes were followed; however, it was found that the majority of the 350 sites selected based on the ISODATA classification were not "good" representations of land cover classes. For example, what appeared as continuous agricultural fields (>100 x 100 m) in the ISODATA classification, were often mixed with features such as large individual trees, or ponds. Better examples of classes were found while driving the pre-determined routes. In all, 30 different land covers were noted and samples sites were visited across the entire eastern Ontario region, resulting in 600 sites overall. These 600 sites were representative of landcover across the mosaiked region of four Landsat scenes. As three scenes were subsequently dropped from analysis, this may have resulted in over- and under-sampling of certain classes in the remaining scene.

3.5 Remote sensing data pre-processing: selection of scenes

Due to the amount of processing required to mosaic and radiometrically correct eight Landsat scenes for 2 different years, and the size of each mosaic file (>1GB), the methodology development was focused on one scene per year with the intent to process the remaining data for the region once a sound methodology had been developed. The scene selected was path 15 row 29 (2005_1529, 1995_1529) (Figure 3.3). It covered a large portion of the study area (including the entire city of Ottawa, the Gatineau Park, the Frontenac Axis, etc). The portion of the scene in the United States was masked.

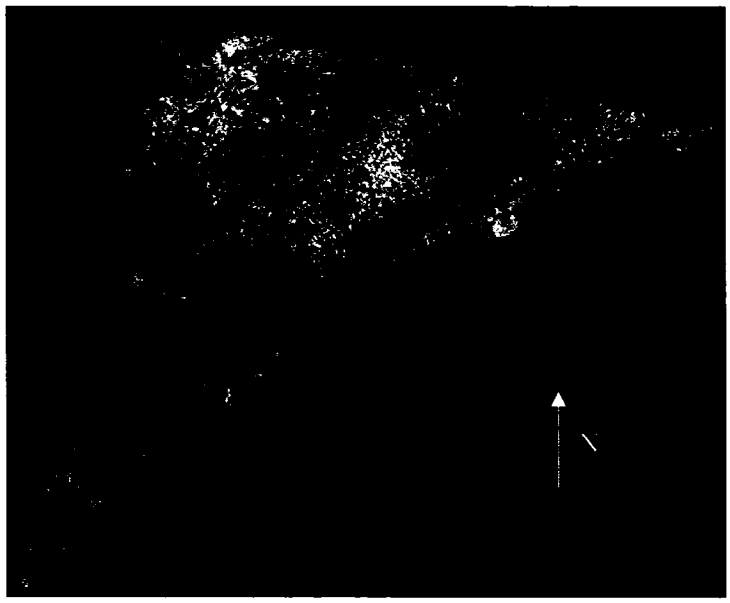

Figure 3.3 - Individual scene selected for processing (2005_1529).

3.5.1 Image registration

Image registration ensures that all pixels correspond to the same position in a selected map projection (Jensen, 2005). Error in overall thematic map accuracy can be related to the locational accuracy of the training and validation data from the field (Foody, 2002). The GPS coordinates of the training and validation sites were taken in relation to the Natural Resources Canada Ontario road vector file. To ensure that the

GPS coordinates represented 'real' site locations, 2005_1529 was registered to the road vector file. Subsequently, 1995_1529 was registered to the aligned 2005 scene.

To register the 2005 image to the road vector file, five (four required) ground control points (GCPs) and ten Check Points (CPs) were located on the images at recognizable road intersections on both the reference road file and 2005_1529. Using a first-order polynomial transformation algorithm, the 2005 scene was shifted, scaled and warped to match the reference (vector) file. Nearest neighbour resampling was used to assign the grey level from the closest pixel associated with the known coordinate in the newly aligned image. The same process was used to register the 1995 scene to the 2005 aligned scene. Table 3.3 lists the residual error results for the registrations. Tables II-C1 and II-C2, Appendix I-C list the row/line coordinates of the GCPs, CPs and individual point RMSE for the registrations. RMSE was calculated from the sample control points used in the affine transformation and not from separate validation points.

Table 3.3 - Residual RMSE (pixels) for image to vector file and image to image registrations.

Reference	Unaligned	Overall RMSE	X RMSE	Y RMSE
Natural Resources Canada Ontario road vector file	2005_1529	0.14	0.06	0.13
2005_1529	1995_1529	0.08	0.08	0.00

3.5.2 Atmospheric corrections

Two absolute atmospheric corrections and two combination methods were tested and compared (theory described 2.2.3).

They included:

1. DOS (scaled) (2005_1529 scene),
2. ATCOR2 (2005_1529),
3. DOS (scaled, per scene) and PIF method of 1995_1529 to 2005_1529,
4. ATCOR2 (per scene) and PIF method of 1995_1529 to 2005_1529.

The DOS method was selected as Pax-Lenney *et al.* (2000) found that this method worked well with generalization (see 2.2.3.2 and 3.6.3), a training method attempted in this research. Their second best result for generalization was realized using 6S, a radiative transfer model (see 2.2.3.1). ATCOR2 was selected for this research as it is a similar absolute method that is readily available and relatively uncomplicated. The combined PIF-absolute methods were selected as Schroeder *et al.* (2006) showed that relatively calibrating imagery to an absolutely corrected "master" image resulted in the lowest RMSE. To further this idea, in this research absolute correction was applied to both scenes to determine if the accuracy improved.

To determine which correction method was best for this imagery, the selected methods were applied; the resulting corrected images as well as an uncorrected image were used in a supervised classification. These classifications were subsequently assessed for overall accuracy.

3.5.2.1 Absolute corrections

DOS method

The first method implemented was the DOS. The atmospheric condition at the time of acquisition was set as 'very clear' (Chavez, 1988). The DNs were converted to at-sensor radiance using equation 2.1 (calibration values noted in Table II-A1, Appendix

II-A). Then the haze values were calculated using the starting haze and corresponding function values for each band (Table II-A2 (Appendix II-A)). The calculated haze value was applied to each band using equation 2.2 (with band 6 = π * L_λ) and these image radiance values were then essentially free of haze effects. As these files were quite large (>1GB) each band was converted back to 8-bit unsigned integers. The DOS haze removal equations were applied to 1995_1529. The calibration values to convert to at-satellite radiance for 1995 are outlined in Table II-A3 (Appendix II-A). Note that the calibration values are different for LMAX and LMIN (prior to May 4, 2003). The haze values in Table II-A4 (Appendix II-A) were then subtracted from each band using equation 2.2 and the 32-bit real numbers were converted back to 8-bit unsigned integers. These image radiance values were then essentially free of haze effects.

ATCOR2 method

ATCOR2 was applied to each of the 2005 and 1995 scenes using the parameters outlined in Table II-A5 (Appendix II-A). A haze mask and cloud mask (Figure 3.4) were next defined. Visibility over the Ottawa region for each date was obtained from the Environment Canada website. The manually delineated haze mask covered all land leaving water bodies open. The manually delineated cloud mask covered each cloud and cloud shadow apparent in the imagery. 2005_1529 did not have any clouds. 1995_1529 had minor cloud cover in the southwest. The ATCOR2 algorithm was then applied to all bands for both scenes and these image values were then free of haze effects.

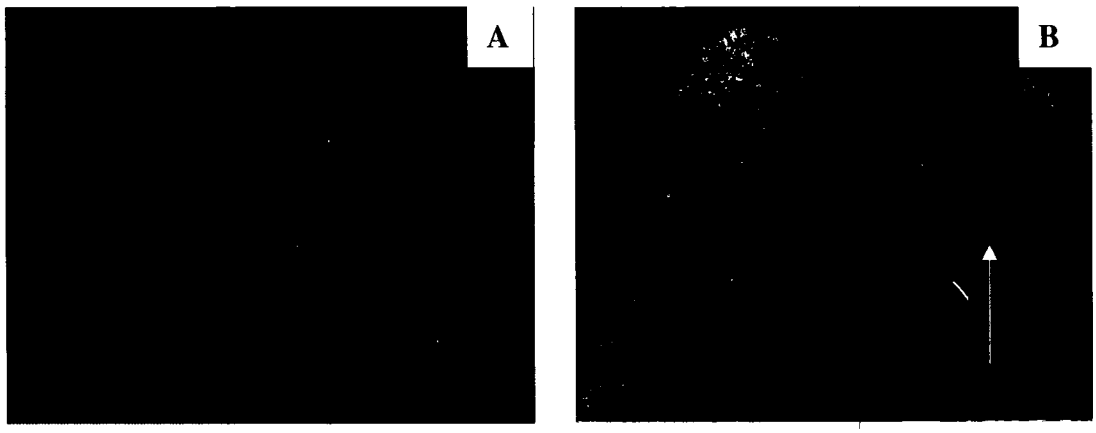

Figure 3.4 - Haze mask (a) and cloud mask (b) examples (2005_1529). Blue represents the mask that for: haze – covers all land cover; clouds – covers clouds and cloud shadows (mostly in lower left).

3.5.2.2 Relative calibration

In this research the PIF method was used. The dark and light objects selected were present in both scenes and are listed in Table II-B1 (Appendix II-B).

The average brightness values for each of these sites were derived for each band for each scene. The bands' values for 2005_1529 were set as the reference values (y values). The corresponding band values for 1995_1529 (x values) were then regressed to these. The resultant standard linear regression equations were then applied to each of the bands of scene 1995_1529. The average brightness values were derived again for the calibrated scenes and regressed once again to the 2005_1529 reference values. If there was no improvement or change to the regression equations the process was stopped. Appendix II-B contains Tables II-B2 to II-B9 listing the average brightness values for each band for each scene and Figures II-B1a-g to II-B6a-g show the regressions with equations and R^2 values for the relative calibrations performed on both the DOS and ATCOR2 corrected scenes.

The two absolute atmospheric corrections were applied to 2005_1529 and thematic maps were produced from each of these scenes (using 10 classes and the MLC

method). The results of the comparison of thematic classifications using data corrected by the algorithms are given in Tables II-C1a-c (Appendix II-C). For 2005_1529, the DOS scene had the highest accuracy (75.7%, k=0.70 (definition in 3.6.2)) followed by ATCOR2 (73.9%, k=0.67) and then the non-corrected scene (73.0%, k=0.66). It can be seen that by applying either atmospheric correction the overall accuracy of the classification improves. With further assessment of the individual class Producer's and User's Accuracies (PA and UA, definition in 3.6.2) for 2005_1529, it was found that the DOS corrected scene had the highest overall accuracy and higher kappa values.

For 1995_1529 the highest accuracy was obtained for DOS/no relative calibration (79.2%) followed by ATCOR2/PIF (77.7%), then DOS/PIF (76.1%) and finally ATCOR2/no relative calibration (73.6%) (Tables II-C2a-d, Appendix II-C).

Based on these assessments it was decided to use the DOS 2005_1529 and the DOS/no relative calibration 1995_1529 scenes for the pixel-based classification method, the object-based classifications and the temporal analysis. Testing was conducted on the other atmospherically corrected scenes from other dates but all the results presented, and further methodologies described (unless otherwise noted) are from these two particular scenes. Differences in accuracies for each method were observed for specific classes such as Wetlands, Deciduous/Mixed, Coniferous and other classes; however, further investigation into these differences was not made.

3.6 Land cover classification

The classification methods used for comparison in this research were the MLC and an object-based method using multi-resolution segmentation and classification hierarchy.

3.6.1 Maximum likelihood classification

The MLC method is often used as a base comparison for other classification methods (Flanders *et al.*, 2003) and was selected for the same purpose in this thesis. All seven bands from 2005_1529 were used as input for the 2005 classification. The 30 land cover types observed in the field were pared down to 20 potential classes (for example, classes such as Urban School and Urban Parking Lot were combined with other urban classes to create an Urban/Commercial class because, based upon separability analysis, they were spectrally very similar. Table III-A1a (Appendix III-A) lists the original 30 classes with general descriptions of these classes as observed in the field. Table III-A1b lists the 30 classes and how they were combined to the initial 20 classes used for training. Table III-A1c lists the 20 classes and shows how they were merged into the final 10 classes. Using random sampling, 1/3 of the sites for each of the 20 classes were selected to be used as training sites. The UTM location of each training site was found on the imagery and, with the aid of the field notes and photos, training polygons were delineated. This was completed for all 20 classes. Figure III-A1a-d (Appendix III-A) shows examples of training polygons for selected classes. Additional Deep Water and Bare Soil sites were added through visual interpretation of the imagery. Separability of the training data for all class pairs was determined using the Bhattacharrya Distance. The histograms of the various training classes were evaluated to determine if they were bi-modal or overlapping. Training classes were merged until ten distinct and separate classes were developed. These classes were: High Density Urban, Low Density Urban, Bare Rock, Coniferous, Deciduous/Mixed (mixed containing coniferous), Water, Wetlands, Agricultural Field 1, Agricultural Field 2 and

Bare Field. Upon completion of the development of these training classes the MLC algorithm was applied. The average separability for these ten classes was 1.93672 with the minimum separability of 1.553918 between the Bare Rock and High Density Urban classes. Table III-A2a (Appendix III-A) lists the separability between all 10 classes based on the spectral data.

3.6.1.1 Texture analysis

Texture is used in classifications to add spatial information. Unlike spectral brightness or reflectance which is obtained from each individual pixel, texture is computed from a set of connected pixels. Haralick (1979) describes the relationship of texture with the spatial distribution and spatial dependence of grey tones. Texture was selected for the pixel-based method to determine if classifications could be improved over those derived from mean spectral information alone and to be comparable to the object-based classification method, which also uses texture.

Texture measures were derived from the grey level co-occurrence matrix (GLCM), which shows the probability of each pair of possible pixel brightnesses within a defined sample window (Haralick, 1979). Within the user-specified window, the direction and distance of the pixel pairs is defined as a function of the angular relationship between the pixels as well as a function of the distance between them (Haralick, 1979). Commonly used GLCM textures in remote sensing pixel-based classifications include: Contrast, Correlation, Entropy and Homogeneity (Baraldi and Parmiggiani, 1995). These particular textures were selected as each measures different aspects of the imagery (e.g. homogeneity measures the image uniformity; contrast measures the opposite of homogeneity (or the heterogeneity)). Each of these texture

algorithms available in PCI were tested individually and in combination by comparing the separability of the 2005_1529 scene training polygon. Only when Homogeneity was applied to bands 2, 3 and 4, was there an improvement to the separability of the pairs of classes with the minimum separability including High Density Urban and Bare Rock; Low Density Urban and Wetlands; Deciduous/Mixed and Agricultural Field 1. This was applied with a window size of 3 x 3 pixels, using 256 grey levels for each band chosen. Homogeneity measures image uniformity and assumes larger values for smaller grey tone differences in pixel pairs (Baraldi and Parmiggiani, 1995).

$$\text{Homogeneity} = \sum_{i=0}^{quantk} \sum_{j=0}^{quantk} \frac{1}{1+(i-j)^2} * h_c(i,j) \qquad (3.3)$$

where quant k is the quantization level of band k. Table III-A2b (Appendix III-A) lists the improved separability between the 10 classes. Based on the results of these tests, Homogeneity texture was used with the MLC.

3.6.1.2 Generalization: signature extension

For change detection studies using multiple Landsat images it is suggested that multi-temporal reference data (derived from some other data source (e.g. archived imagery)) be obtained. These data would be used to train and validate each scene individually (Cohen and Shoshany, 2005). This requires extensive effort and is often influenced by the user in terms of ability to manually interpret archived imagery.

An alternative to using multi-reference data is the use of signature extension, or generalization, which is defined as the application of spectral (and spatial) signatures developed in one time and space to other data. Generalization requires less effort and less user –influence on reference data (Pax-Lenney *et al.*, 2001). Based on this, it was decided to extend the signatures developed for the 2005_1529 training classes to

1995_1529. The band means of each class can be found in Table III-B1a, Appendix III-B. These include the mean values for the 7 spectral bands plus values derived for the three Homogeneity bands. These signatures were used to classify the 1995_1529 scene using the MLC (with bitmap masks covering the cloudy areas).

3.6.2 Classification accuracy assessment

MLC classification accuracy was measured using error matrices and accuracy statistics. An error matrix compares reference data with the classification data and contains rows and columns representing the number of classes (Lillesand *et al.*, 2004). This matrix provides information regarding the errors of omission (exclusion of pixels from a class, or conversely the Producer's Accuracy (PA), which is 100% less the % errors of omission) and errors of commission (erroneous inclusion of pixels into a class, or conversely the User's Accuracy (UA), which is 100% less the % errors of commission (Lillesand *et al.*, 2004)). Foody (2002) recommends that a target of 85% overall accuracy and at least 70% User's and Producer's Accuracy for each class be achieved.

Another measure of accuracy is the kappa (k) coefficient of agreement which indicates the accuracy of the map beyond that which would be obtained through a random assignment of pixels to land cover classes (Jensen, 2005). Unlike overall accuracy, kappa incorporates the errors of commission and omission and can be used to compare confusion matrices. Foody (2002) recommends the presentation of the confusion matrix along with kappa coefficient as minimum measures of accuracy. In this study, the remaining two thirds of the field sites were used as reference data to derive the error matrices for classifications of the 2005_1529 scene.

3.6.2.1 Image differencing to define validation sites for accuracy assessment of pre-2005 classifications

It has been noted that when remotely sensed data are used as reference data for classification accuracy assessment, errors can occur (Foody, 2002) because the reference data themselves generally have errors. For the accuracy assessment of 1995_1529 reference data could either be derived from archived imagery (air photos) or from reference data obtained in the field. The only field data available was the 2006 data (used for 2005_1529). The question became: how to use this data but not include sites that had changed?

Image differencing is one of the most widely used image-based change detection algorithms. In several comparative studies, it was considered one of the most accurate methods to detect change (Nelson 1983 *IN* Collins and Woodcock, 1995; Mas 1999; Jensen 2005; Lu *et al.*, 2005). The algorithm subtracts one date of original or transformed imagery from a second date with the results of the difference stored as a new image (Jensen, 2005). Because unchanged pixels are usually clustered about the mean, which should be close to 0.0 DN, the changed pixels are generally found within the difference histogram distribution tails. For this research, 2005_1529 and 1995_1529 were differenced using +/- 1 standard deviation as the threshold (Yuan and Elvidge, 1998; Mas, 1999) between changed and unchanged pixels. The resultant image was then overlaid with a vector file of all 2005 reference data sites. Those sites that fell on or near (within 1 pixel) a changed site were discarded. The remainder of the sites were used as reference data for the accuracy assessment of 1995_1529.

The thematic maps derived from both of these MLCs were used in temporal analysis.

3.6.3 Object-based classification

Improvements to systems and sensors have led to a recent surge of interest in object-based classifications (Blaschke and Strobl, 2001). These methods were selected for this research because of the intuitive relationship between hierarchical patch dynamics in landscape ecology (Wu, 1999) and the segmentation of imagery into an overall hierarchy (pixels – objects – whole image). There is also the relationship to the developed classification hierarchy where land cover classes can be related to super- and sub- classes.

3.6.3.1 Image segmentation

All processing of the object-oriented classification, accuracy assessment and temporal analysis was completed using eCognition. Tests of various segmentation algorithms and input parameters were evaluated visually and the following methods were selected for further classification. The first step was segmentation of 2005_1529. For the purposes of this research, multi-resolution segmentation was first selected. Scale parameters of 5, 10 and 20 were tested. The shape and colour parameters can be set for each particular segmentation level (Laliberte *et al.*, 2004). Colour values from 0.1 to 0.9 were tested, with shape values as {1- colour}. Shape can be further developed with the parameters smoothness and compactness, but for this research these were kept at 0.5. A second segmentation at one level above this first segmentation was implemented using the spectral difference method. Larger scale parameter values produced coarser objects. It was decided that rather than combining the objects created in the first level using the multiresolution segmentation again (and thus, only creating coarse objects) after testing, the spectral difference method was selected as it refined the

objects developed in the multiresolution segmentation level without creating exceptionally large and coarse objects. The objects created by this second level visually appeared to make sense in the landscape (e.g., roads were group together into long linear objects). In this research, maximum difference parameters of 2, 3 and 5 of band 5 (MIR) were tested. This band was selected after reviewing each class histogram in each band developed from training the first segmentation level. To continue with the 'generalization' methods, 1995_1529 was segmented in the same manner.

3.6.3.2 Classification hierarchy

Using the same field data as the MLC method (Table III-A1c), classes were first developed using the mean spectral values of training objects found in the first level. Additionally, the standard deviations of the spectral values per band, as a first order texture measure, were assessed for all classes.

Shape parameters were next tested including: shape index, border index, area, compactness and 'rectangular fit' for all classes. Tests of a variety of values for each parameter and for combinations of parameters were conducted to evaluate their impacts on classification accuracy. Through this extensive testing, a classification hierarchy for the 2005 image was developed. This hierarchy was extended to 1995_1529 for classification of that scene. Table III-B1b in Appendix III-B lists the signatures derived from 2005_1529. A nearest-neighbour classifier was applied using this classification hierarchy. The thematic maps derived from these classifications were then used in temporal analysis of land cover change.

3.6.3.3 Accuracy assessment of individual land cover classifications

As with the MLC methods, classification accuracy for the object-oriented classification was measured using error matrices and accuracy statistics using the same reference data for 2005_1529, as well as those sites derived for 1995_1529 with the image differencing method. In addition, as the classification process in eCognition was fuzzy-based, a stability map was produced that shows the difference between the best and second best membership assignment for an object as a score out of 100 and provides statistical information such as the mean, minimum and maximum membership values per class (Flanders *et al.*, 2003). Stability maps were generated for both 2005_1529 and 1995_1529.

3.7 Temporal analysis of land cover change

The PCC method as described in chapter two (see 2.2.5.2) was used for temporal analysis. This method was selected as it indicates the change in land cover over time, which is important for ecological analysis. The thematic maps (2005_1529 and 1995_1529) developed from the MLC were imported to IDRISI Andes and cross tabulated on a pixel-by-pixel basis. The same process was repeated for the object-based thematic maps. Overall change maps and maps revealing specific (individual class related) changes were created as well as matrices showing the numbers of pixels in each class on each date (from/to change matrices). These were analyzed to determine and evaluate the nature of LULC changes that occurred in eastern Ontario during the ten year period from 1995 to 2005.

CHAPTER FOUR

4.0 Results

The results from the two classifications and the temporal change analyses are presented in this chapter.

4.1 Maximum likelihood classification: 2005_1529 scene

Ten classes were developed for the MLC. Examples of each land cover type (photographs) and of the corresponding thematic class are in Appendix III-C (Figures III-C1a-j). Although these are examples of individual sites, classes were composed of several varieties of the generalized land cover(s) from across the scene (e.g. Wetlands comprised of swamps, closed water marshes, treed marshes, etc). Figures III-C2a-i (Appendix III-C) present photographs of these different land covers. Tables III-A1a-c (Appendix III-A) provide descriptions of what land covers are contained in each class and how the initial field observed classes were merged into the final 10 classes of interest.

4.1.1 Overall thematic map analysis

Figure 4.1 presents the entire 2005_1529 MLC 10-class map. It can be seen that areas in the west/southwest on the Frontenac Axis have been classified as Deciduous/ Mixed forest with patches of Coniferous, irregularly shaped Agricultural Fields (both type 1 and 2) and Wetlands (red circle). Areas to the south/southeast of Ottawa have been classified as Agricultural Field 1 interspersed with Bare Fields and Agricultural Field 2 (green circle). In the same area there are some forested (Deciduous/Mixed and Coniferous) regions. High Density and Low Density Urban classified areas correspond to the urban areas of eastern Ontario (Figure 1.1).

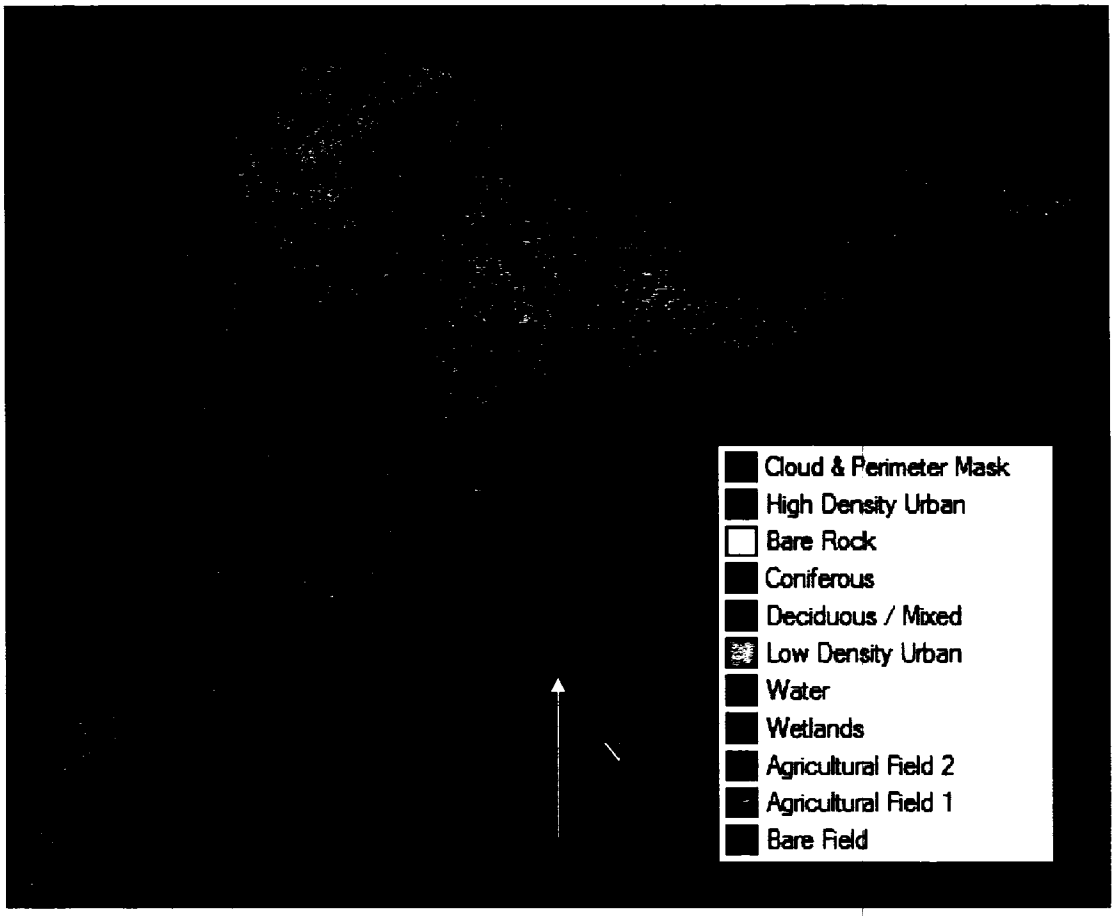

Figure 4.1 – Thematic map of eastern Ontario developed from 2005_1529 scene using the MLC and 10 classes of interest.

Table 4.1a is the error matrix for this classification from which the accuracy statistics were derived. In terms of PA, only Water was significantly confused with Wetlands. The following classes with sample sizes of at least 10 pixels were moderately confused: High Density Urban and Low Density Urban; Deciduous/Mixed and Coniferous; Deciduous/Mixed and Low Density Urban; Agricultural Field 2 and Low Density Urban; and Agricultural Field 1 with Deciduous/Mixed, Low Density Urban and Wetlands respectively. For UA the following classes were moderately confused: Low Density Urban with High Density Urban, Coniferous, Deciduous/Mixed, Water, Agricultural Field 2 and Agricultural Field 1; High Density Urban with Bare Rock, Low

Density Urban, Water and Agriculture Field 2; Coniferous with Deciduous/Mixed and Wetlands; Deciduous/Mixed with Coniferous and Agricultural Field 1; Wetlands with Water and Agricultural Field 1, Agricultural Field 1 with Deciduous/Mixed, Low Density Urban and Wetlands; and Agricultural Field 2 with Deciduous/Mixed, Low Density Urban, Wetlands and Agricultural Field 1. Classes with small pixel amounts are not discussed.

Table 4.1b (summarized with the other classifications' accuracy data in Table 4.5) lists the accuracy statistics. The overall accuracy was 75.7% with an overall kappa (k) value of 0.70. The average PA was 71.8% and the average UA was 73.9%. The Wetlands class was the poorest. Water was the best class; however the low PA reflects significant confusion with Wetlands and moderate confusion with High and Low Density Urban. For land use classes, the best class was Agricultural Field 1. In terms of meeting accuracy requirements (Foody, 2002; 3.6.2) only Agricultural Field 1 and Bare Field satisfied the requirement with High Density Urban, Bare Rock, Coniferous, and Agricultural Field 2 just below 70%. The average PA and UA were above 70%.

4.1.2 Analysis of selected sub-sites

Figures 4.2 a-f presents thematic maps of six sub-sites of interest. (These are for overall comparison between 1995 and 2005, and between the two classification methods. Figure 4.3 shows the location of these sites within the whole scene. The legend found on Figure 4.1 applies to these figures). These are sites where there has been ongoing research in the GLEL (e.g. Gatineau Park, Quebec; Wetlands, Rideau River, Ontario) or where temporal change was dominant (e.g. Barrhaven, Ontario;

Cornwall, Ontario) or well-known "natural" sites in eastern Ontario and Quebec (e.g. Mer Bleue Bog; Larose Forest; Gatineau Park).

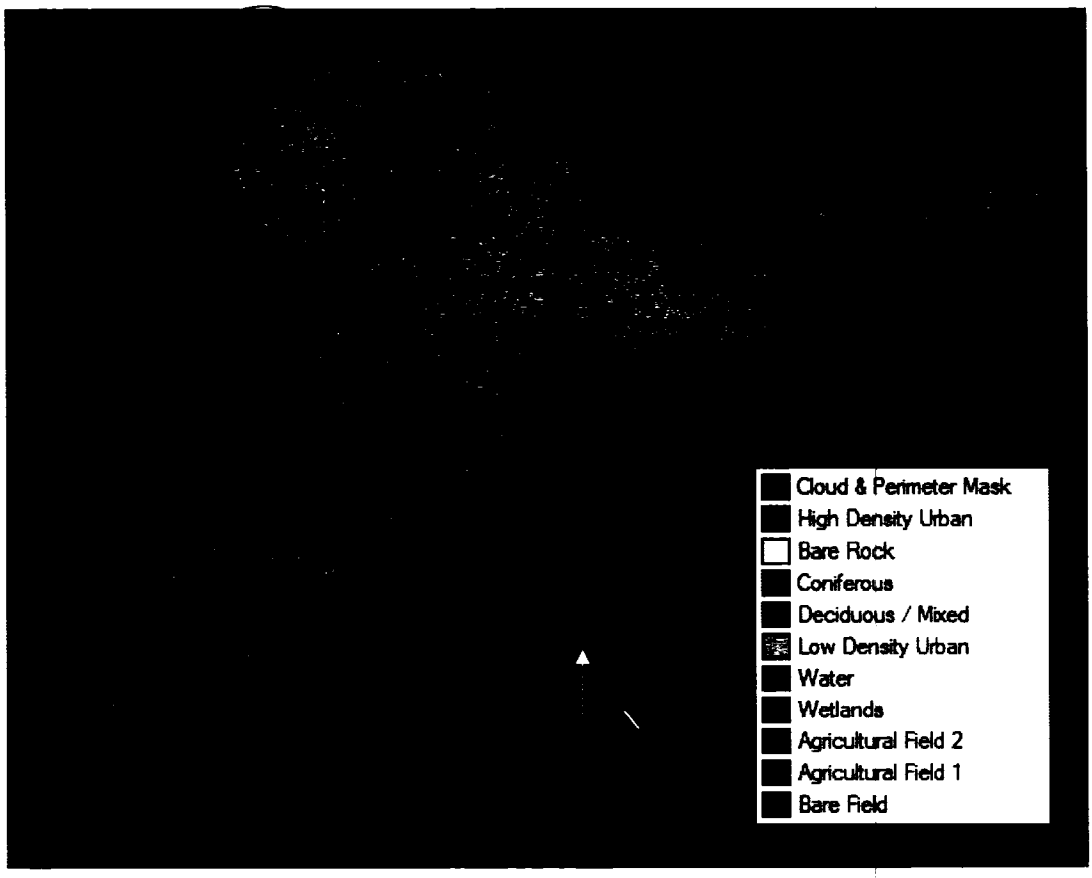

Figure 4.3 – Location of sub-sites of interest on the thematic map derived from 2005_1529 scene. Legend applies to the subsets in Figures 4.2a-f.

It is interesting to note that for 2005_1529 validation set Wetlands and Low Density Urban were not confused. In Figures 4.2a and 4.2f Low Density Urban classified pixels are located in these known wetland areas. The Agricultural Field 1 and Deciduous/Mixed classes did overlap (inclusion/exclusion) in the error matrix and Figures 4.2b and 4.2c show traditionally forested areas with Agricultural Field 1 classified pixels. It is also interesting to note that Bare Rock was confused with the High Density Urban class and Figure 4.2e reveals a large block of Bare Rock classified pixels in this urban area (Barrhaven).

Table 4.1a – Error matrix for the 2005_1529 pixel-based maximum likelihood classification (10 classes). Columns represent reference cover types. Rows represent classified cover types.

	High Density Urban	Bare Rock	Coniferous	Deciduous /Mixed	Low Density Urban	Water	Wetlands	Agricultural Field 2	Agricultural Field 1	Bare Field	Totals
High Density Urban	16	1	0	0	1	1	0	4	0	0	23
Bare Rock	0	2	0	0	0	0	0	0	0	1	3
Coniferous	0	0	8	3	0	0	1	0	0	0	12
Deciduous/ Mixed	0	0	1	18	0	0	0	0	4	0	23
Low Density Urban	5	0	1	2	20	1	0	5	3	0	37
Water	0	0	0	0	0	5	0	0	0	0	5
Wetlands	0	0	0	0	0	4	7	0	3	0	14
Agricultural Field 2	0	0	0	1	1	0	1	19	1	0	23
Agricultural Field 1	0	0	0	5	1	0	1	0	69	0	76
Bare Field	0	0	0	0	0	0	0	1	0	4	5
Unknown	0	0	0	0	0	0	0	0	1	0	1
Totals	21	3	10	29	23	11	10	29	81	5	222

= Reference pixels correctly classified.

Figure 4.2a – Mer Bleue Bog, ON (2005).

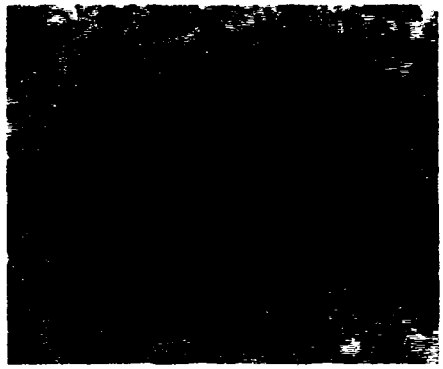

Figure 4.2b – Larose Forest, ON (2005).

Figure 4.2c – Gatineau Park, PQ (2005).

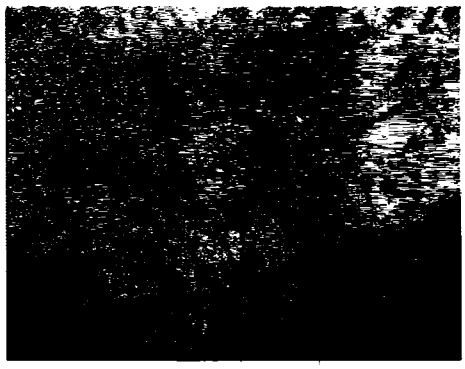

Figure 4.2d – Cornwall, ON (2005).

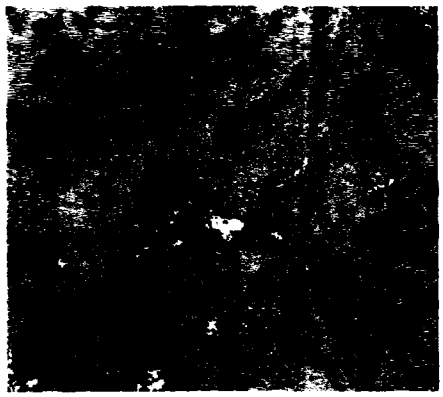

Figure 4.2e – Barrhaven, ON (2005).

Figure 4.2f – Wetlands, Rideau R., ON (2005).

Table 4.1b - Accuracy statistics for the 2005_1529 maximum likelihood classification (10 classes).

Overall Accuracy:	75.7%		
Overall Kappa Statistic:	0.70		
Class Name:	**Producer's Accuracy:**	**User's Accuracy:**	**Kappa Statistic:**
Bare Field	80.0%	80.0%	0.80
Bare Rock	66.7%	66.7%	0.66
Coniferous	80.0%	66.7%	0.65
Agricultural Field 1	85.2%	90.8%	0.86
Agricultural Field 2	65.5%	82.6%	0.80
Deciduous/ Mixed	62.1%	78.3%	0.75
High Density Urban	76.2%	69.6%	0.66
Low Density Urban	87.0%	54.1%	0.49
Water	45.5%	100.0%	1.00
Wetlands	70.0%	50.0%	0.48
Average	71.8%	73.9%	
Average w/out Bare Rock Class	72.0%	73.5%	

4.2 Maximum likelihood classification: 1995_1529 scene

The signatures (Appendix III-B, Table III-B1a) derived from the ten classes for the 2005_1529 MLC were used to classify 1995_1529. Figure 4.4 presents the 1995 thematic map. Reference sites were not collected in 1995 therefore image differencing was used to develop a change/no change map over which the reference sites (collected in 2006) were projected (Figure III-D1, Appendix III-D).

4.2.1 Overall thematic map analysis

The thematic map derived from 1995_1529 is visually similar to Figure 4.1; however Deciduous/Mixed classified areas are more apparent in the south and southeast in the 1995 thematic map (green circle).

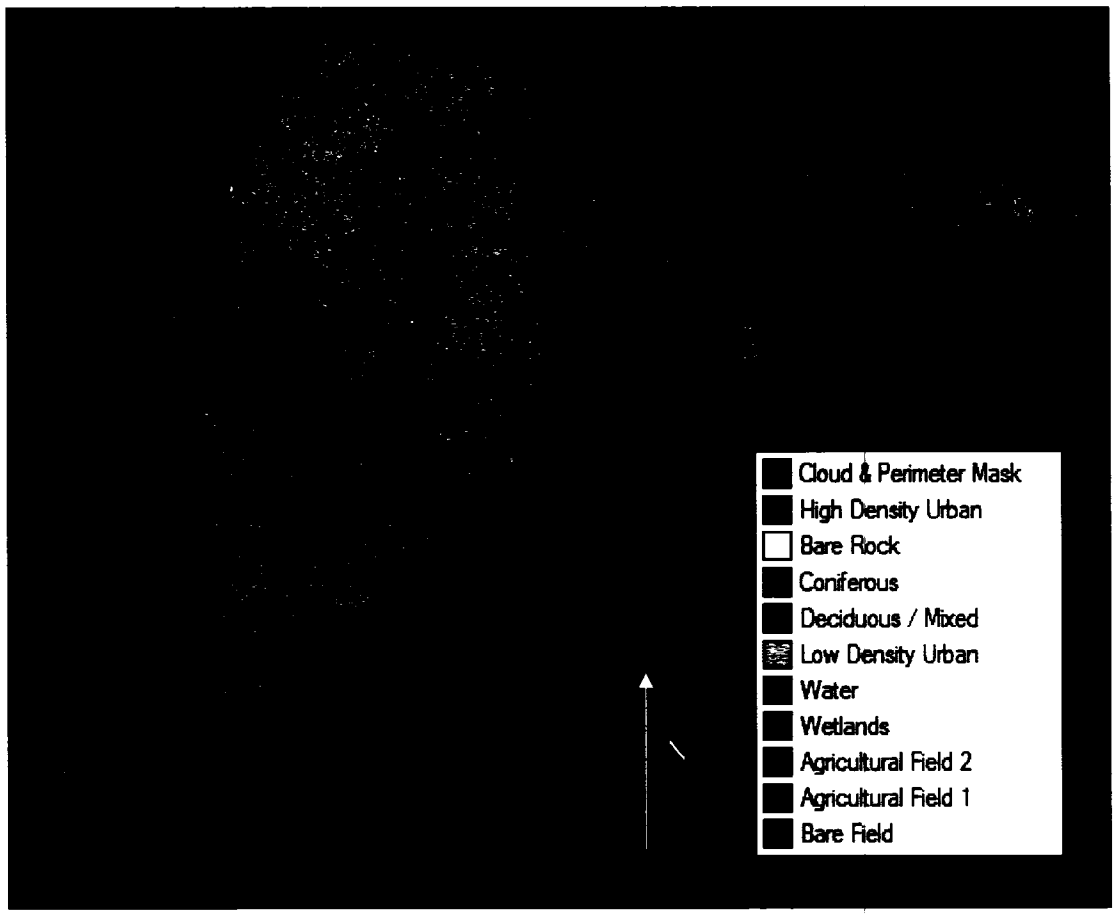

Figure 4.4 – Thematic map of eastern Ontario developed from 1995_1529 scene using the MLC and signatures of 10 classes of interest. Legend applies to the subsets in Figures 4.5a-f.

There are not as many Wetlands classified over the Frontenac Axis as in Figure 4.1; there are more Agricultural Field 1 classified areas in that region (red circle). Table 4.2a is the error matrix for this classification. In terms of PA, Agriculture Field 2 was significantly confused with Agriculture Field 1. Unlike the 2005 classification, Water was not significantly confused with Wetlands; however there was minor confusion.

Similar classes to the 2005 classification were moderately confused. Overall there was less confusion between classes for this classification than for 2005.

Table 4.2b (summarized with the other classifications' accuracy data in Table 4.5) presents the accuracy statistics for this thematic map. The overall accuracy for this classification was 79.2% with an overall kappa value of 0.73. This is interesting as these values were better than those obtained for 2005. The average PA was 70.7% and the average UA was 73.5%, which was worse than the 2005 average accuracies. The Wetlands class was again the poorest and Water was the best. The Water class PA improved over the 2005 classification. For land use classes, the best class was again Agricultural Field 1. Four classes satisfied the requirement of 70% UA and PA target, including Agricultural Field 1, High Density Urban, Bare Rock and Deciduous/Mixed, which is two more classes than the 2005 classification. Low Density Urban and Coniferous were just below 70%.

Table 4.2a – Error matrix of the 1995_1529 pixel-based maximum likelihood classification with 10 classes. Columns represent reference cover types. Rows represent classified cover types.

	High Density Urban	Bare Rock	Coniferous	Deciduous /Mixed	Low Density Urban	Water	Wetlands	Agricultural Field 2	Agricultural Field 1	Bare Field	Totals
High Density Urban	15	0	0	0	1	0	0	2	0	1	19
Bare Rock	1	3	0	0	0	0	0	0	0	0	4
Coniferous	0	0	6	1	0	0	2	0	0	0	9
Deciduous/ Mixed	0	0	2	21	0	0	1	0	4	0	28
Low Density Urban	3	0	1	0	19	0	1	1	4	1	30
Water	0	0	0	0	0	7	0	0	0	0	7
Wetlands	0	0	0	0	0	2	3	1	0	0	6
Agricultural Field 2	0	0	0	0	0	0	0	9	0	1	10
Agricultural Field 1	0	0	0	0	2	0	0	7	73	0	82
Bare Field	1	0	0	0	0	0	0	0	0	1	2
Totals	20	3	9	22	22	9	7	20	81	4	197

= Reference pixels correctly classified.

Table 4.2b - Accuracy statistics for the 1995_1529 maximum likelihood classification (10 classes).

Overall Accuracy:	79.2%		
Overall Kappa Statistic:	0.73		
Class Name:	**Producer's Accuracy:**	**User's Accuracy**	**Kappa Statistic:**
Bare Field	25.0%	50.0%	0.49
Bare Rock	100.0%	75.0%	0.75
Coniferous	66.7%	66.7%	0.65
Agricultural Field 1	87.7%	89.9%	0.83
Agricultural Field 2	50.0%	90.9%	0.90
Deciduous/Mixed	95.5%	72.4%	0.69
High Density Urban	75.0%	78.9%	0.77
Low Density Urban	86.4%	61.3%	0.56
Water	77.8%	100.0%	1.00
Wetlands	42.9%	50.0%	0.48
Average	70.7%	73.5%	
Average w/out Bare Rock	70.5%	74.8%	

4.2.2 Analysis of selected sub-sites

Figure 4.5a-f presents the same six sub-sites of interest (The legend found on Figure 4.4 applies to these figures). It is interesting to note that with the altered 1995 reference (validation) set one reference site that was erroneously excluded from Wetlands was included in Low Density Urban. Figure 4.5a and 4.5f show Low Density Urban classified pixels abundantly dispersed throughout known wetland areas. This is similar to the 2005 thematic map. Also similar to the 2005 classification, Agricultural Field 1 and Deciduous/Mixed classes overlapped (inclusion/exclusion) in the error matrix, and Figures 4.5b and 4.5c show Agricultural Field 1 classified pixels in traditionally forested areas. A visual comparison of Figures 4.2d and 4.5d shows potential LULC change. In Figure 4.5d, there are more Deciduous /Mixed forest classified pixels surrounding Cornwall, whereas in Figure 4.2d there are Agricultural Field 1 classified pixels. LULC change is apparent when comparing Figures 4.2e and

4.5e. In Figure 4.2e there are more Low and High Density Urban classified areas whereas in Figure 4.5e, Agricultural Field 1 and Deciduous/Mixed classified pixels are more apparent. Additionally, there are more High Density Urban classified pixels in the later figures (Figures 4.2d-e). The Bare Rock classified area is not apparent in Figure 4.5e as it was in Figure 4.2e, revealing a potential mis-classification between the High Density Urban class and the Bare Rock class on the 2005 thematic map. Finally, oddly classified pixels of High and Low Density Urban appear in the centre of the lakes located in Figure 4.5f. These classified areas are not apparent in the later image of Figure 4.2f.

Figure 4.5a – Mer Bleue Bog, ON (1995).

Figure 4.5b - Larose Forest, ON (1995).

Figure 4.5c - Gatineau Park, PQ (1995).

Figure 4.5d – Cornwall, ON (1995).

Figure 4.5e – Barrhaven, ON (1995).

Figure 4.5f – Wetlands, Rideau R., ON (1995).

4.3 Object-based segmentation and classification: 2005_1529 scene

Multi-resolution segmentation was used to segment 2005_1529 and through testing, a scale parameter of 10 with a colour parameter of 0.6 and a shape parameter of

0.4 was selected and implemented. Figure 4.6 shows the Ottawa region and the objects grown using these parameters. This is the 10_6_4 layer in the segmentation hierarchy.

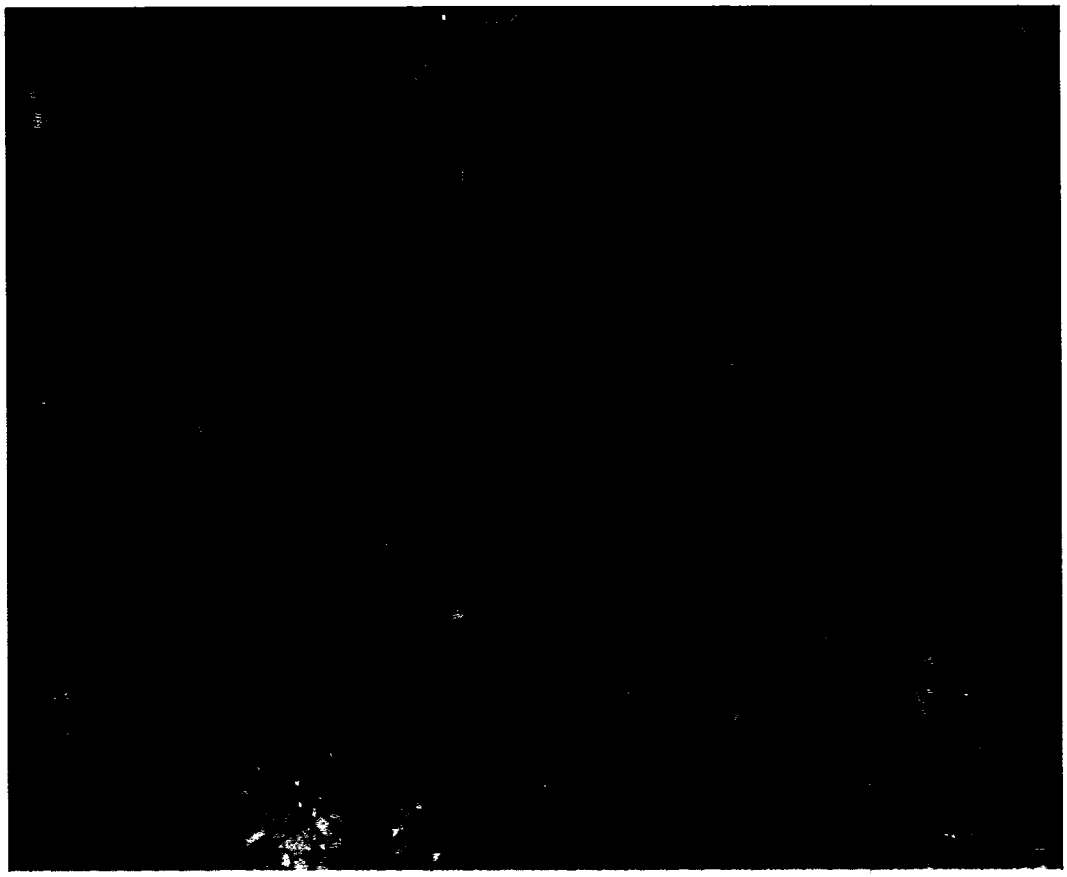

Figure 4.6 – Objects derived using the segmentation parameters in layer 10_6_4 (CIR composite).

A coarser segmentation was applied in the hierarchy above this layer and through testing the segmentation parameter for this layer was selected as a mean spectral difference of two for Band 5 (MIR). Figure 4.7 shows the Ottawa region and the objects derived using these parameters. This is the SD_2_5 layer in the segmentation hierarchy.

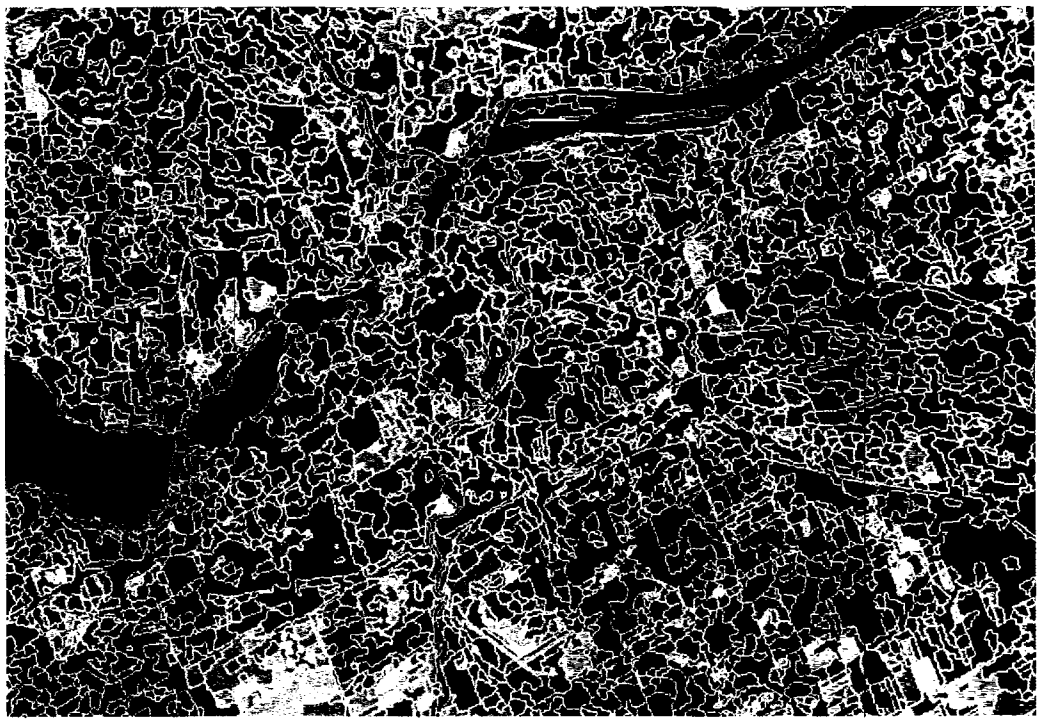

Figure 4.7 – Objects derived from the segmentation parameters in layer SD_2_5 (CIR composite).

The ten classes used for the MLC were used to develop the spectral-based hierarchy for the object-based classification. Several shape parameter values were tested to see if they improved the overall classification accuracy. These parameters were: Area, Shape Index, Border Index, Compactness and Rectangular Fit. In all cases these parameters did not improve the overall classification accuracy. In some cases individual class accuracies improved but when these parameters were applied on a class by class basis, the improvement did not occur. The spectral classification hierarchy was applied to SD_2_5; however the overall accuracy was significantly worse. It was therefore decided to continue with the object-based classification using only the spectrally-derived classification hierarchy on layer 10_6_4.

4.3.1 Overall thematic map analysis

Figure 4.8 presents the 2005_1529 object-based thematic map. Overall, the maps developed from the pixel-based classification method are abrupt with more discretely classified areas, whereas the object-based map is smoother with larger, more continuous classified areas. It can be seen that areas in the southwest on the Frontenac Axis are generally classified as Deciduous/Mixed forest with patches of Coniferous and interspersed with irregularly shaped Agricultural Fields (both type 1 and 2) and Wetlands (red circle).

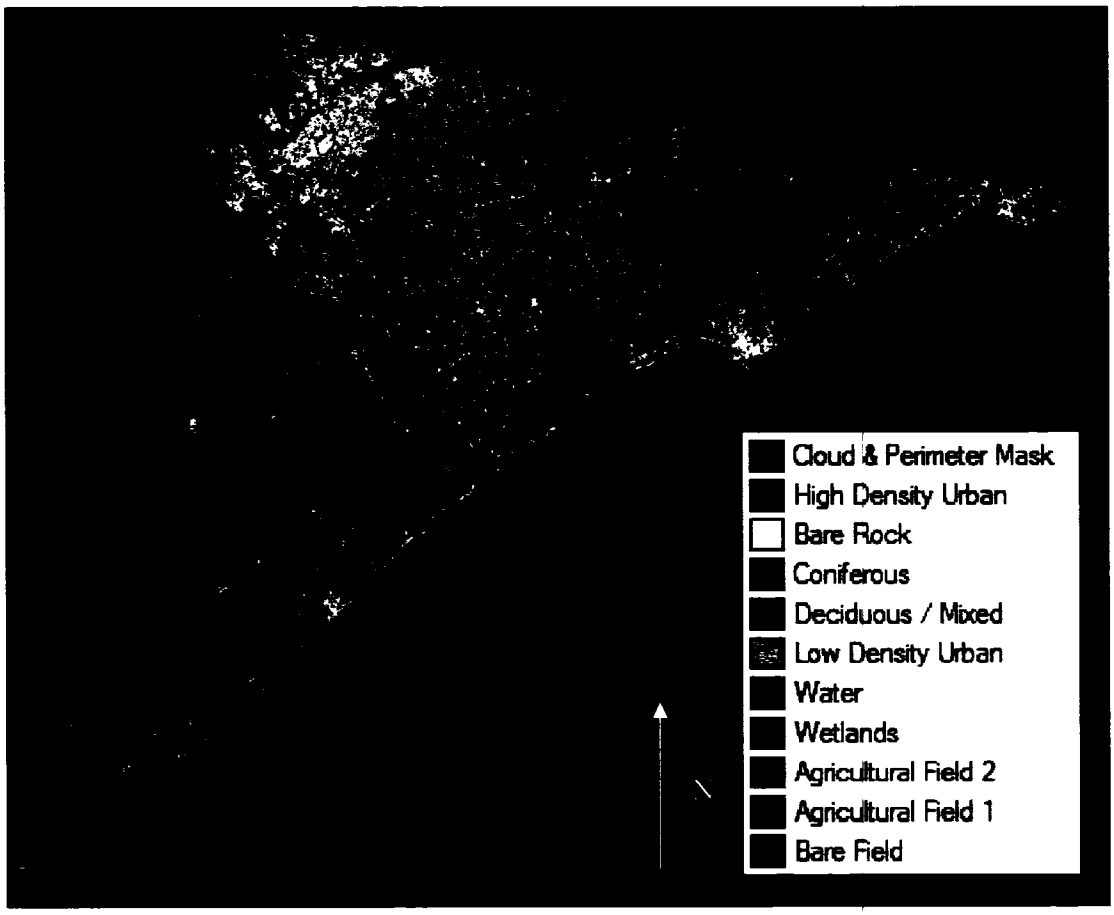

Figure 4.8 - Thematic map of eastern Ontario developed from 2005_1529 scene using the object-based method and the 10 classes of interest. Legend applies to the subsets in Figures 4.9a-f.

In comparison with Figure 4.1, Agricultural Field 2 and Wetland classified objects are more apparent in this area. Areas to the south/southeast of Ottawa have been classified as Agricultural Field 1, but with a significant difference to the pixel-based MLC method (Figure 4.1): there is an addition of a large centralized region classed as Agricultural Field 2 (green circle). In this same area there are forested (Deciduous/Mixed and Coniferous) regions, however they are larger than those located in the same region on Figure 4.1. High and Low Density Urban objects are also visually more apparent than the corresponding areas in Figure 4.1.

Table 4.3a is the error matrix for this classification. In terms of PA, Bare Rock was significantly confused with High Density Urban. Additionally, Coniferous was significantly confused with Deciduous/Mixed. Other classes that were moderately confused were: Agricultural Field 1 with Agricultural Field 2; Agricultural Field 2 with Agricultural Field 1, Coniferous, Agricultural Field 2 and Low Density Urban with Wetlands; Deciduous/Mixed with Low Density Urban and Wetlands; Low Density Urban with Agricultural Field 2. In comparison with the 2005 pixel-based classification's PA, more (and different) classes were significantly confused. In terms of UA, Deciduous/Mixed was significantly confused with Coniferous. Moderate confusion was seen between Agricultural Field 2 and Agricultural Field 1, and Low Density Urban; and between Low Density Urban and Agricultural Field 2, and High Density Urban.

Table 4.3b (summarized with the other classifications' accuracy data in Table 4.5) presents the accuracy statistics. The overall accuracy was 75.6% with an overall kappa of 0.70. These values were similar to the MLC method using the same image

data. The average PA was 65.2% and the average UA was 66.6%. These values were lower than the MLC method, however if the Bare Rock class is not considered (in both cases) these values are minimally higher for the object-based classification: 72.4% (72.0% MLC 2005) and 74.0% (73.5% MLC 2005). Bare Rock was the poorest class. (It was decided to keep this class to have an equivalent number of classes for each method; a next step would be to combine this class with High Density Urban to make an "Impervious Surface" class for both methods).

Table 4.3a - Error matrix of the 2005_1529 object-based classification with 10 classes (plus unclassified). Columns represent reference cover types. Rows represent classified cover types.

	Bare Field	Bare Rock	Coniferous	Agricultural Field 1	Agricultural Field 2	Deciduous /Mixed	High Density Urban	Low Density Urban	Water	Wetlands	Totals
Bare Field	5	0	0	0	1	0	0	0	0	0	6
Bare Rock	0	0	0	0	0	0	0	0	0	0	0
Coniferous	0	0	3	0	0	0	0	0	3	1	7
Agricultural Field 1	0	0	0	19	2	1	0	0	0	0	22
Agricultural Field 2	0	1	1	4	68	0	1	5	0	2	82
Deciduous/ Mixed	0	0	6	0	0	25	0	1	0	0	32
High Density Urban	0	4	0	1	0	0	16	0	0	0	21
Low Density Urban	0	1	0	0	7	2	4	16	0	1	31
Water	0	0	0	0	0	0	0	0	6	0	6
Wetlands	0	0	0	1	0	2	0	1	1	9	14
unclassified	0	0	0	0	0	0	0	0	0	0	0
Totals	5	6	10	25	78	30	21	23	10	13	221

= Reference pixels correctly classified.

Table 4.3b - Accuracy statistics of the 2005_1529 object-based classification.

Overall Accuracy:	75.6%		
Overall Kappa Statistic:	0.70		
Class Name:	**Producer's Accuracy:**	**User's Accuracy**	**Kappa Statistic:**
Bare Field	100.00%	83.3%	0.83
Bare Rock	0.0%	0.0%	0.00
Coniferous	30.0%	42.9%	0.40
Agriculture Field 1	76.0%	86.4%	0.77
Agriculture Field 2	87.2%	82.9%	0.70
Deciduous/Mixed	83.3%	78.1%	0.75
High Density Urban	76.2%	76.2%	0.74
Low Density Urban	69.6%	51.6%	0.46
Water	60.0%	100.0%	1.00
Wetlands	69.23%	64.3%	0.62
Average	65.2%	66.6%	
Average (without Bare Rock)	72.4%	74.0%	

The Coniferous class was the second poorest class. This class' values were worse than the 2005 pixel-based classification. Bare Field was the best class. This was different from the pixel-based classification. The Water class was the second best class and had improved PA over the MLC. For land use classes, the best class was Agricultural Field 2. The class had a better PA and UA (but worse k's). In terms of meeting accuracy requirements Agricultural Field 1, High Density Urban, Deciduous/Mixed, Agricultural Field 2, Water and Bare Field all satisfied the requirement. This is an improvement of one class than for the pixel-based MLC method. Overall, more classes developed from the object-based method have higher UAs and PAs. However unlike the 2005 pixel-based classification the average PA and UA were below 70%. Additionally, the Wetlands class was better classified than the

pixel-based method overall. The average PA and UA not including the Bare Rock class was higher.

4.3.2 Analysis of selected sub-sites

Figures 4.9a-f present the same six sub-sites presented for the MLC classification (legend is located on Figure 4.8). Visually reviewing Figures 4.9a and 4.9f, the erroneous Low Density Urban pixels that were seen in Figures 4.2a, f (and Figures 4.5a, f) are not apparent in these areas, even though there is confusion between Wetland and Low Density Urban classes. Agricultural Field 1 and Deciduous/Mixed again overlapped (inclusion/exclusion) in the error matrix and Figure 4.9c reveals some Agricultural Field 1 areas are classified in this forested region. However, in Figure 4.9b, the erroneous Agricultural Field 1 classified areas are not apparent. In Figure 4.9d there appears to be more Agricultural Field 2 and Wetlands classified areas surrounding Cornwall as compared to Figure 4.2d which had mostly Agricultural Field 1 with some Wetlands. Additionally, there is the presence of Coniferous forest (Figure 4.9d) which was not apparent in Figure 4.2d or even Figure 4.5d. When comparing Figure 4.2e and 4.9e (Barrhaven) these two figures are visually similar in terms of the land cover present. The differences in the areas are in the type of agriculture surrounding the urban areas. Additionally the erroneous Bare Rock pixels of the MLC (Figure 4.2e) are not apparent in Figure 4.9e.

Figure 4.9a – Mer Bleue Bog, ON (2005).

Figure 4.9b - Larose Forest, ON (2005).

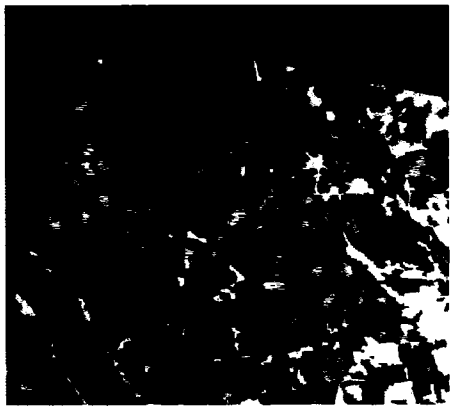

Figure 4.9c - Gatineau Park, PQ (2005).

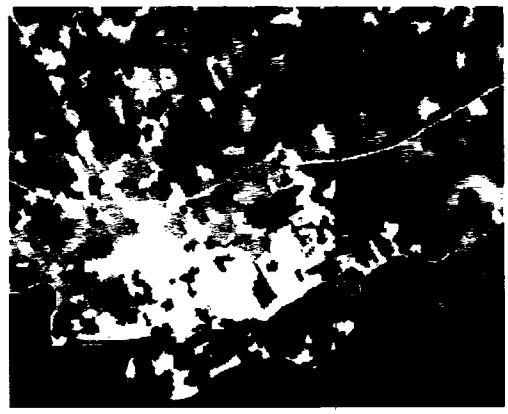

Figure 4.9d – Cornwall, ON (2005).

Figure 4.9e – Barrhaven, ON (2005).

Figure 4.9f – Wetlands, Rideau R., ON (2005).

4.3.3 Analysis of classification stability: overall thematic map

Figure 4.10 is the stability map developed for this classification. Areas in green are seen as stable (large difference between first and second best membership assignment). Areas in red are unstable (small difference between first and second best membership assignment). The stability is lower if the membership values are similar whether they are high or low (e.g. if Deciduous/Mixed = 0.94; Wetlands = 0.96 -- unstable; if Deciduous/Mixed = 0.35; Wetlands =0.36 -- unstable). These objects may be mixed land covers or they may be a single land cover of spectral and textural properties that are approximately equally similar to those for two different classes. Membership values were obtained by selecting the individual objects in the image and are not presented here. The area of the Frontenac Axis has large continuous areas of instability as does the area north of the Cornwall region (blue circles). Stable areas are apparent in water, and in urban centres, as well as through the central portion of the scene (pink circles). In general, highly accurate classes are located in the stable areas (Water, and High Density Urban) and less accurate classes are located in the unstable areas. Instability occurs more often between those classes that are confused (e.g. Deciduous/Mixed and Coniferous; High Density Urban and Low Density Urban).

4.3.3.1 Classification stability: selected sub-site analysis

Figures 4.11a-f presents the six sub-sites areas as stability maps (Legend is located on Figure 4.10). The unstable areas in Figure 4.11a have high membership values for Wetlands, Coniferous and Deciduous/Mixed. Low Density Urban did not show a high membership value for this area. In Figure 4.11b the unstable areas (red,

orange, yellow) are objects that have been given high membership values for both Coniferous and Deciduous/Mixed.

Figure 4.10 – Stability map of the 2005 object-based classification.

It is interesting to note that for this area Agricultural Field 1 does not have a high membership value. However, the unstable areas of Gatineau Park do have high membership values for both Deciduous/Mixed and Agricultural Field 1 (Figure 4.11c). Around Cornwall (Figure 4.11d) the highly unstable areas (red/orange) are where high membership values have been assigned to the vegetated classes (Deciduous/Mixed, Coniferous, Wetlands, Agricultural Field 1 and Agricultural Field 2). The yellow areas which are more stable have similar membership values between the vegetated classes (as above) and Low Density Urban. The orange area in water has similarly high

membership values for Water and Coniferous. In Figure 4.11e the unstable red area in centre has high membership values for Agricultural Field 2, Deciduous/Mixed and Wetlands. Around the wetlands in the Rideau River, the areas of instability have high membership values between both Agricultural Field classes and Wetlands.

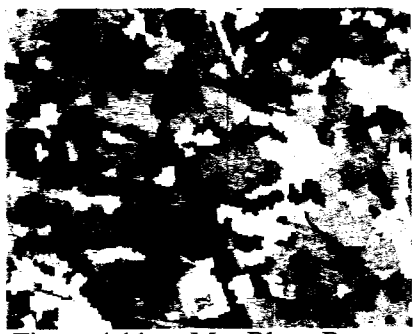

Figure 4.11a – Mer Bleue Bog, ON (2005 Stability Map).

Figure 4.11b – Larose Forest, ON (2005 Stability Map).

Figure 4.11c – Gatineau Forest, PQ (2005 Stability Map).

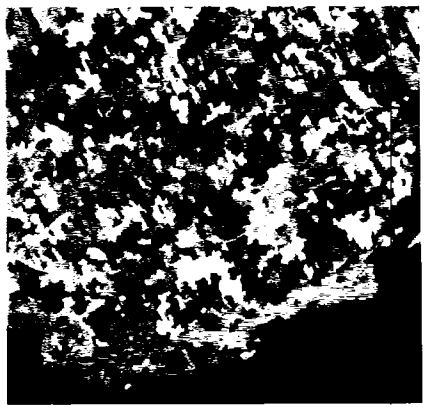

Figure 4.11d – Cornwall, ON (2005 Stability Map).

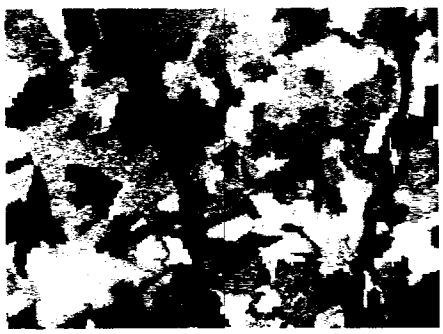

Figure 4.11e – Barrhaven, ON (2005 Stability Map).

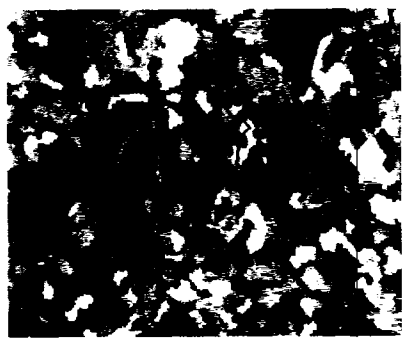

Figure 4.11f – Wetlands, Rideau R., ON (2005 Stability Map).

4.4 Object-based segmentation and classification: 1995_1529 scene

The segmentation parameters used for the 2005 segmentation (layer 10_6_4) were implemented. The 2005 object-based spectral signatures (Table III-B1b, Appendix III-B) were extended to classify 1995_1529. The subset of reference sites used for the 1995 MLC accuracy assessment was used for this classification. The overall segmentation maps and accuracies were similar in many ways to the 2005 object-based results so only differences from the 2005 object-based results will be discussed.

4.4.1 Overall thematic map analysis

Figure 4.12 presents the 1995 object-based thematic map. In comparison with Figure 4.8 Agricultural Field 2 classified areas are not as apparent over the Frontenac Axis and there are less Wetland classified areas (red circle). The centralized region in the southeast that was classified as Agricultural Field 2 (Figure 4.8) is not apparent on this figure (green circle). There is also less Coniferous located around the Cornwall area and in the Larose Forest region.

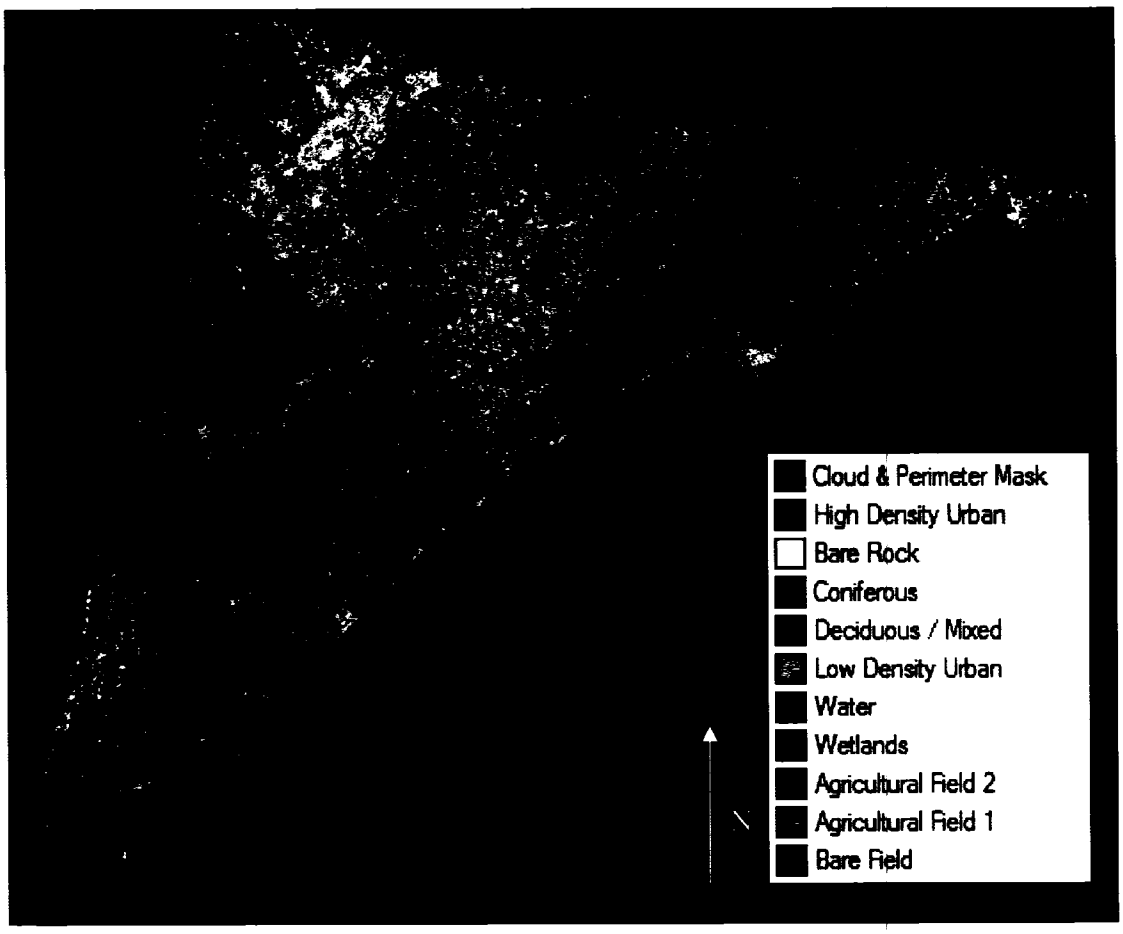

Figure 4.12 - Thematic map of eastern Ontario developed from 1995_1529 scene using the object-based method and the signatures of the 10 classes of interest. Legend applies to the subsets in Figures 4.13a-f.

Table 4.4a is the error matrix for this classification. In terms of PA (and different from 2005), Bare Field was confused with Agricultural Field 2, and High Density Urban. Wetlands were significantly confused with the Water class which was also different from the 2005 object-based classification. It is interesting to note that this classification in general has less confusion than the 2005 object-based classification and the least confusion of the four classifications overall.

Table 4.4b (summarized with the other classifications' accuracy data in Table 4.5) presents the accuracy statistics for this classification. The overall accuracy was 75.2% with an overall kappa value of 0.71. The overall accuracy is similar to both the 2005 object-based accuracy, and is lower than the MLC using the same image data. The average PA was 65.1% and the average UA was 72.0%. The PA value was similar to the 2005 object-based; however the UA value was higher. If the Bare Rock class is not considered these values are: 71.6% (72.4% object-based 2005) and 79.2% (74.0% object-based 2005). Unlike 2005, Agricultural Field 1 was the second poorest class. The best land cover class was Deciduous/Mixed. For land use classes, the best class was Low Density Urban. In terms of meeting accuracy requirements eight classes, Coniferous, Deciduous/Mixed, Low Density Urban, High Density Urban, Bare Field, Agricultural Field 2, Wetlands and Water satisfied the 70% requirement. .

Table 4.4b - Accuracy statistics of the 1995_1529 object-based classification.

Overall Accuracy:	75.2%		
Overall Kappa Statistic:	0.71		
Class Name:	**Producer's Accuracy:**	**User's Accuracy**	**Kappa Statistic:**
Bare Field	60.0%	100.0%	1.00
Bare Rock	0.00%	0.00%	0.00
Coniferous	55.6%	83.3%	0.82
Agricultural Field 1	83.3%	60.0%	0.55
Agricultural Field 2	70.5%	79.5%	0.72
Deciduous/Mixed	92.3%	82.8%	0.80
High Density Urban	70.6%	80.0%	0.78
Low Density Urban	95.2%	80.0%	0.77
Water	57.1%	100.0%	1.00
Wetlands	66.7%	54.6%	1.00
Average	65.1%	72.0%	
Average (without Bare Rock)	71.6%	79.2%	

Table 4.4a - Error matrix of the 1995_1529 object-based classification with 10 classes (plus unclassified). Columns represent reference cover types. Rows represent classified cover types.

	Bare Field	Bare Rock	Coniferous	Agricultural Class 1	Agricultural Class 2	Deciduous /Mixed	High Density Urban	Low Density Urban	Water	Wetlands	Totals
Bare Field	3	0	0	0	0	0	0	0	0	0	3
Bare Rock	0	0	0	0	0	0	1	0	0	0	1
Coniferous	0	0	5	0	0	1	0	0	0	0	6
Agricultural Class 1	0	0	0	15	10	0	0	0	0	0	25
Agricultural Class 2	1	0	0	3	31	1	0	1	0	2	39
Deciduous/ Mixed	0	0	4	0	0	24	0	0	0	1	29
High Density Urban	1	2	0	0	0	0	12	0	0	0	15
Low Density Urban	0	0	0	0	3	0	2	20	0	0	25
Water	0	0	0	0	0	0	0	0	8	0	8
Wetlands	0	0	0	0	0	0	0	0	5	6	11
unclassified	0	0	0	0	0	0	2	0	1	0	3
Totals	5	2	9	18	44	26	17	21	14	9	165

= Reference pixels correctly classified.

Table 4.5 – Summarized accuracy statistics of the four classifications (from tables 4.1b – 4.4b).

	2005 MLC	2005 Object-based	1995 MLC	1995 Object-based
Overall Accuracy	75.7%	75.6%	79.2%	75.1%
Average PA(no Bare Rock class)	72.4%	72.4%	70.5%	71.6%
Average UA (no Bare Rock class)	74.7%	74.0%	74.8%	79.2%
Overall kappa	0.70	0.70	0.73	0.71

Overall, the similarity and small differences between these values presented in Table 4.5 reveals that these differences are probably not statistically significant.

4.4.2 Analysis of selected sub-sites

Figures 4.13a-f present the same six sub-sites of interest (Legend for these figures is located on Figure 4.12). In general the classifications are similar to 2005, however Figure 4.13c shows large Agricultural Field 1 classified objects in the Gatineau Park that were not present in Figure 4.9c. In Figure 4.13d there are more Deciduous/Mixed classified areas surrounding Cornwall as compared to Figure 4.9d. There are some Coniferous classified areas in Figure 4.13d, but not as much as Figure 4.9d. The differences between 4.9e and 4.13e are in the type of agriculture surrounding the urban areas. In Figure 4.13f objects in the Rideau River are classified as Wetlands which is not apparent in Figure 4.9f. This could represent a LULC change from floating vegetation coverage in 1995 to clearer water in 2005.

Figure 4.13a – Mer Bleue Bog, ON (1995).

Figure 4.13b - Larose Forest, ON (1995).

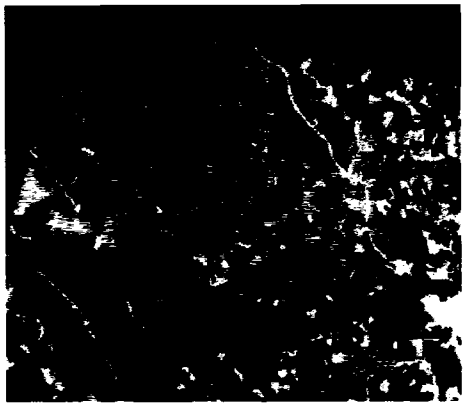

Figure 4.13c - Gatineau Park, PQ (1995).

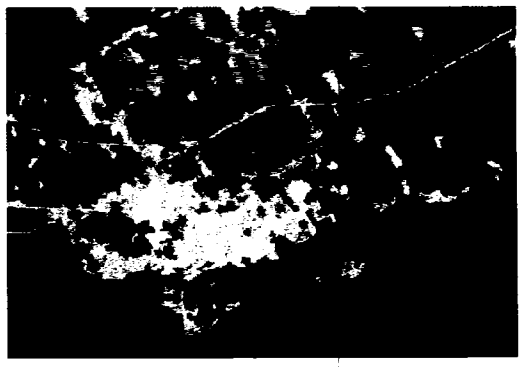

Figure 4.13d – Cornwall, ON (1995).

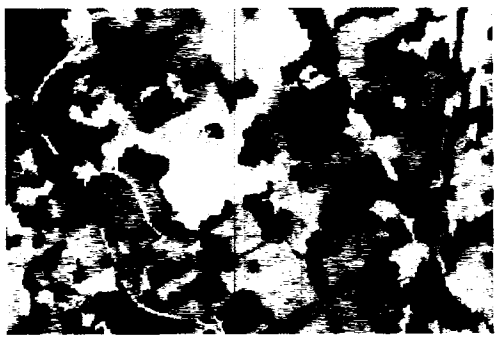

Figure 4.13e –Barrhaven, ON (1995).

Figure 4.13f – Wetlands, Rideau R., ON (1995).

4.4.3 Analysis of classification stability: overall thematic map

Figure 4.14 is the stability map developed for this classification.

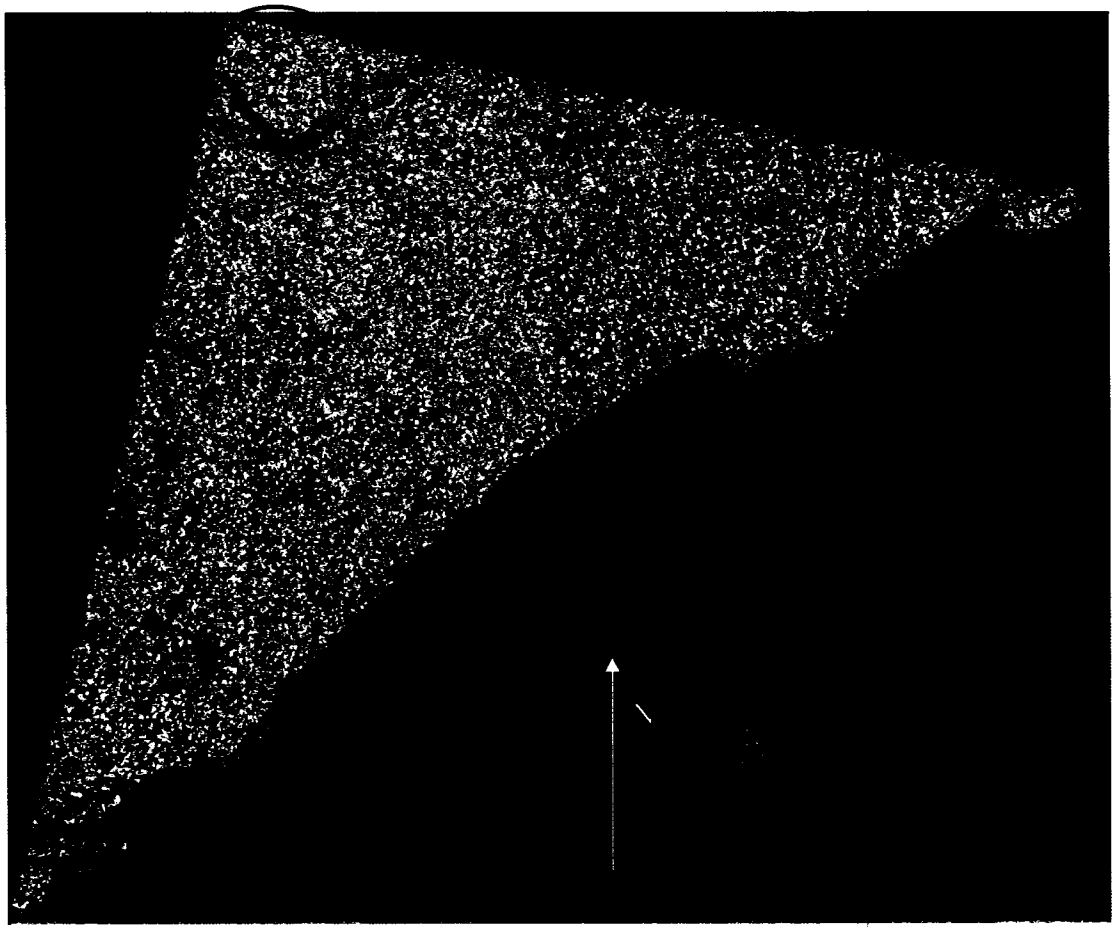

Figure 4.14 – Stability map of the 1995 object-based classification.

Overall only Gatineau Park (blue circle) has a different stability pattern (more instability) as compared to Figure 4.10. As it was the only area where the stability was different it is the only sub-site that was analyzed (Figure 4.15, (legend is located on Figure 4.14)). Similar to the 2005 stability map, the unstable areas of Gatineau Park are areas that have high membership values for Deciduous/Mixed and Agricultural Field 1. However, there are also some objects that have high membership values for both Deciduous/Mixed and Coniferous.

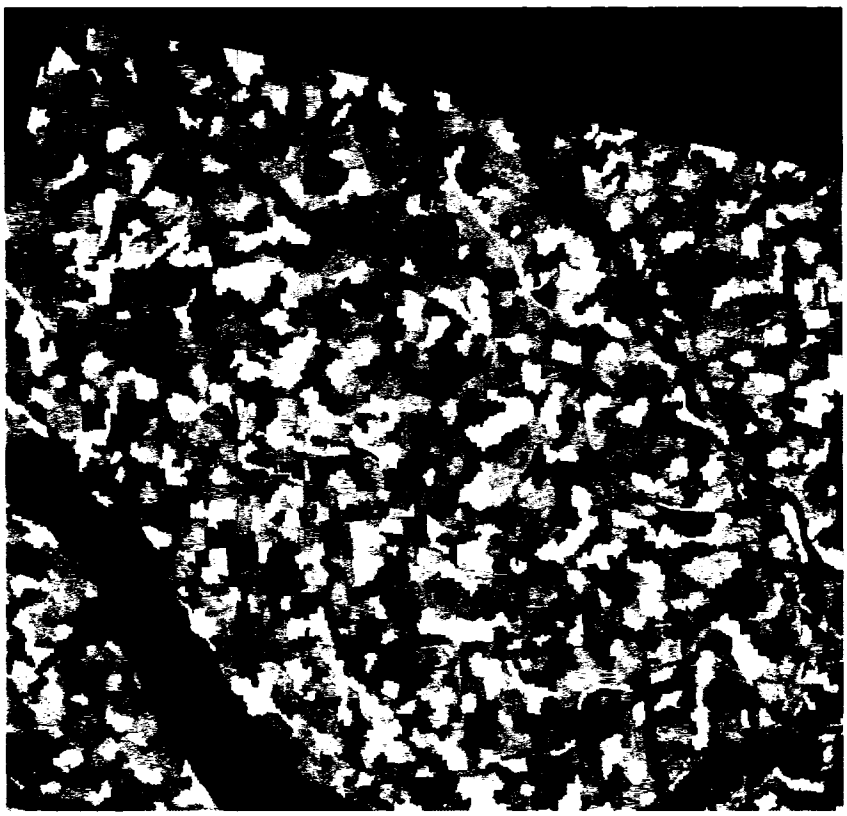

Figure 4.15 – Gatineau Park, PQ (1995 Stability Map).

4.5 Temporal analysis: pixel-based PCC

The MLC thematic maps were cross-tabulated to determine LULC changes over the ten year period. Figure 4.16 is the change map with white representing areas of change and black representing areas of no change.

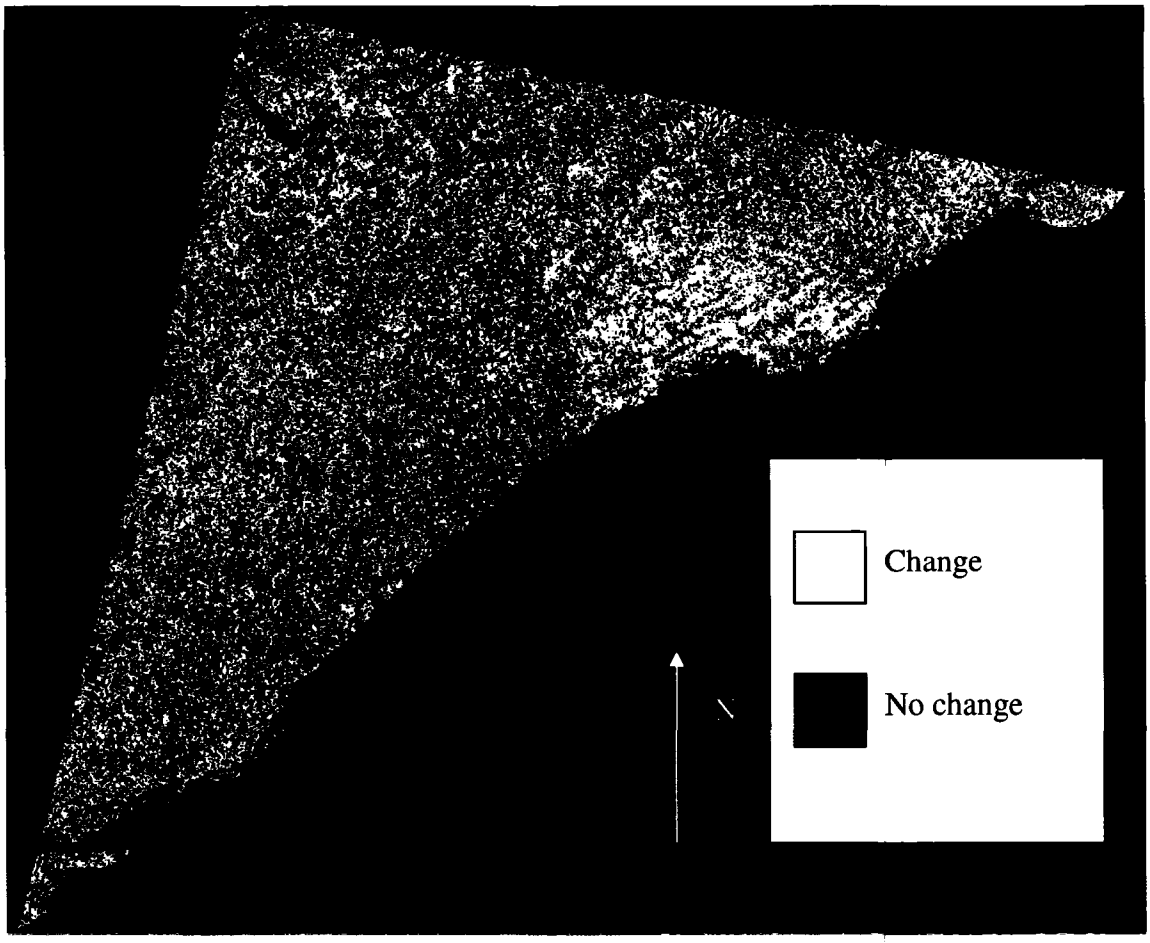

Figure 4.16 – PCC map derived from a cross-tabulation of thematic maps from the pixel-based MLC (2005_1529 and 1995_1529 scenes).

4.5.1 Overall change analysis: pixel-based PCC

In general, large areas of change in Figure 4.16 are found in the south/south east around the Cornwall region, with other dominant areas around the Ottawa region. Table 4.5a lists the areas of change per class (hectares). Table 4.5b provides a summary of this table. Based on these data, 44.4% of the land cover in eastern Ontario changed from 1995 to 2005. The class with the least change was Water (-0.2%) and the class with the most change was Bare Field (+147.0%). The class with the second largest change is Wetlands (136.0%). The increases to this class were mostly from Agricultural Field 1 (20,559ha), Deciduous/Mixed (16,320ha) and Low Density Urban (14,160ha).

The class with the largest loss was Deciduous/Mixed (-25.77%) with the losses mostly attributed to Agricultural Field 1 (47,389 hectares) and Low Density Urban (7,524 ha). The class with the second largest loss was Low Density Urban (-18.29%). These losses were mostly attributed to Agricultural Field 1 (21,789 ha) and Deciduous/Mixed (6,821 ha). The losses and gains among these three classes (Low Density Urban, Agricultural Field 1 and Deciduous/Mixed) may indicate a similarity of spectral and textural information. These changes may not be real, but indicative of errors in the original maps or confusion among these classes.

4.6 Temporal analysis: object-based PCC

The object-based thematic maps were cross-tabulated to determine LULC changes over the ten year period. Figure 4.17 is the change map with white representing areas of change and black showing areas of no-change. An unclassified class (pink) has been added that is comprised of objects that could not be assigned membership to any of the ten classes for either of the two years. This resulted in 3,441 ha unclassifed in 1995 and 3,708 ha unclassified in 2005. As these unclassified regions did not correspond over the two years, a change for any class that was attributed to, or from, unclassified pixels was subtracted from the total amount of land cover for that class (for both years).

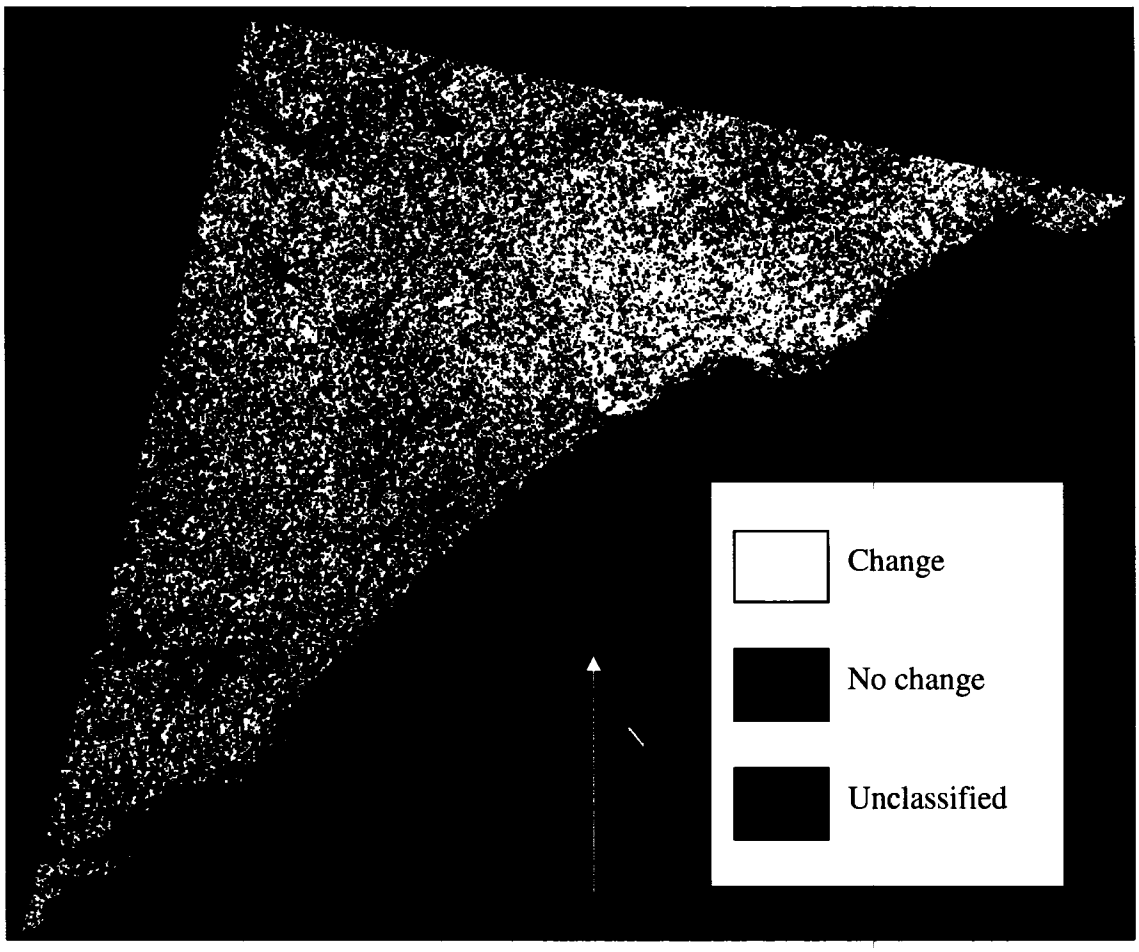

Figure 4.17 – PCC map derived from a cross-tabulation of thematic maps from the nearest neighbour object-based classification (2005_1529 and 1995_1529 scenes).

4.6.1 Overall change analysis: object-based PCC

In general, similar to the pixel-based PCC, change was found in the south/southeast around the Cornwall region, with dominant areas around Ottawa. Unlike the pixel-based PCC, this figure reveals larger, continuous areas of change/no change rather than smaller discrete areas. This pattern corresponds to the segmented objects from both 1995 and 2005 object-based classifications. Table 4.8a lists the changes per class (hectares). Table 4.8b provides a summary of this table. Based upon these data 49.2% of the landcover in eastern Ontario changed from 1995 to 2005. This is quite similar in magnitude to the amount of change estimated using the pixel-based

PCC. The class with the lowest amount of change was Water (+1.4%). This is the same as the pixel-based PCC. The class with the most change is Coniferous (+199.9%). The pixel-based comparison showed an increase of only +22% for this class. The largest contributor to this class was Deciduous/Mixed (60,492 ha). The class with the second largest amount of change was Bare Field (+107.8%). This class showed large increases contributed from Agricultural Field 1 (7,349 ha). The class with the largest loss in landcover was Bare Rock (-94.0%). The class with the largest increase in landcover from this class was Low Density Urban (21.96 ha), with the second largest amount being attributed to High Density Urban (18.27 ha). The class with the second largest loss in total landcover was Agricultural Field 1 (-46.2%). The largest increase in landcover from this class was attributed to Agricultural Field 2 (28,442 ha) with the second largest contribution to Deciduous/Mixed (23,818 ha). The class with the third largest loss in total landcover is Deciduous/Mixed class (-22.51%). This loss mirrors the pixel-based comparison.

Table 4.6a - Change detection matrix (in hectares) comparing the pixel-based thematic maps derived from 1995 (rows) to 2005 (columns).

Unchanged	High Density Urban	Bare Rock	Coniferous	Deciduous /Mixed	Low Density Urban	Water	Wetlands	Agricultural Field 2	Agricultural Field 1	Bare Field	Total
High Density Urban	9,213.48	398.16	201.24	264.15	6,797.79	1,288.53	1,660.05	1,584.54	2,754.36	53.55	24,215.85
Bare Rock	739.35	235.89	0.99	2.97	217.35	6.21	32.49	271.53	218.97	13.50	1,739.25
Coniferous	468.36	32.13	35,426.70	19,497.15	3,680.37	87.03	9,098.91	985.05	6,973.02	26.28	76,275.00
Deciduous/ Mixed	2,851.92	124.29	42,605.46	180,728.64	6,821.82	33.21	16,320.15	9,740.07	90,747.90	555.57	350,529.03
Low Density Urban	7,306.11	170.28	6,066.54	7,524.54	45,485.10	764.82	14,160.69	6,854.04	23,200.65	89.91	111,622.68
Water	685.71	0.09	222.84	29.07	551.16	65,690.91	1,323.18	14.76	22.95	0.27	68,540.94
Wetlands	719.64	21.15	3,028.50	3,888.90	2,826.00	512.37	11,821.32	2,356.02	7,442.01	30.78	32,646.69
Agricultural Field 2	1,957.86	147.15	168.12	872.10	2,994.21	15.48	2,034.99	7,725.33	20,585.70	319.41	36,820.35
Agricultural Field 1	8,802.09	582.39	5,371.02	47,389.41	21,789.99	18.45	20,559.42	51,864.39	277,494.12	2,649.42	436,520.70
Bare Field	54.18	6.21	0.27	11.52	44.46	0.09	32.94	355.50	979.83	48.15	1,533.15
Total	32,798.70	1,717.74	93,091.68	260,208.45	91,208.25	68,417.10	77,044.14	81,751.23	430,419.51	3,786.84	1,140,443.82

Table 4.7a - Change detection matrix (in hectares) comparing the object-based thematic maps derived from 1995 (rows) to 2005 (columns).

Unchanged	Bare Field	Bare Rock	Coniferous	Agricultural Field 1	Agricultura l Field 2	Deciduous /Mixed	High Density Urban	Low Density Urban	Water	Wetlands	Total
Bare Field	713.07	0.00	13.23	1,856.43	3,642.84	291.60	253.62	378.99	4.59	294.48	7,448.85
Bare Rock	23.31	15.30	1.26	0.00	16.83	0.00	664.83	300.33	0.27	0.54	1,022.67
Coniferous	20.70	0.00	15,552.45	140.13	778.14	8,218.98	51.03	297.36	467.37	3,263.49	28,789.65
Agricultural Field 1	7,349.85	1.08	1,219.05	62,820.00	109,612.71	27,014.76	992.52	5,294.61	9.81	12,524.13	226,838.52
Agricultural Field 2	3,658.23	4.05	1,506.78	28,442.07	128,014.47	31,755.87	2,269.53	11,549.25	67.05	17,216.91	224,484.21
Deciduous/ Mixed	2,445.30	0.27	60,492.69	23,818.32	52,969.23	245,136.33	929.52	8,199.63	490.23	39,055.32	433,536.84
High Density Urban	455.04	18.27	77.40	315.54	2,758.41	434.61	5,268.60	5,872.95	61.02	299.88	15,561.72
Low Density Urban	718.74	21.96	1,076.13	3,396.69	22,024.35	10,315.26	3,620.70	32,952.96	344.07	3,436.74	77,907.60
Water	0.00	0.00	670.05	12.51	71.46	438.66	5.58	280.17	67,012.74	1,050.75	69,541.92
Wetlands	96.93	0.00	5,720.13	1,206.09	4,730.58	12,361.86	165.60	1,218.51	2,076.48	19,729.26	47,305.44
Total	15,481.17	60.93	86,329.17	122,007.78	324,619.02	335,967.93	14,221.53	66,344.76	70,533.63	96,871.50	1,136,145.96

Table 4.6b - Summary of change statistics derived from the pixel-based post classification change matrix (Tables 4.6a). All absolute cell values are in hectares

	Total	Unchanged	Changed	Percent Change
Total	1,140,444	633,870	506,574	44.4%
	Total 1995	**Total 2005**	**Changed**	**Percent Change**
High Density Urban	24,215	32,798	8,583	35.4%
Low Density Urban	111,623	91,208	-20,414	-18.3%
Bare Rock	1,739	1,717	-22	-1.2%
Coniferous	76,275	93,091	16,817	22.1%
Deciduous/ Mixed	350,529	260,208	-90,321	-25.8%
Agricultural Field 1	436,521	430,419	-6,101	-1.4%
Agricultural Field 2	36,820	81,751	44,931	122.0%
Bare Field	1,533	3,786	2,254	147.0%
Water	68,541	68,417	-124	-0.2%
Wetlands	32,647	77,044	44,397	136.0%

Table 4.7b - Summary of change statistics derived from the object-based post classification change matrix (Table 4.7a). All absolute cell values are in hectares.

	Total	Unchanged	Changed	Percent Change
Total	1,136,146	577,215	558,931	49.2%
	Total 1995	**Total 2005**	**Changed**	**Percent Change**
High Density Urban	15,562	14,222	-1,340	-8.6%
Low Density Urban	77,908	66,345	-11,563	-14.8%
Bare Rock	1,023	61	-962	-94.0%
Coniferous	28,790	86,329	57,540	199.9%
Deciduous / Mixed	433,537	335,968	-97,569	-22.5%
Agricultural Field 1	226,838	122,008	-104,831	-46.2%
Agricultural Field 2	224,484	324,619	100,135	44.6%
Bare Field	7,449	15,481	8,032	107.8%
Water	69,542	70,534	992	1.4%
Wetlands	47,305	93,872	46,566	98.4%

4.7 Comparative temporal analysis: General summary of real change versus error

Real change (that is logical and expected given the nature of development and land use change in the region during this period) is found in areas that were converted from vegetation (Deciduous/Mixed, Coniferous, Wetlands, Agricultural classes) to urban (Low and High Density). In general, change from natural vegetation (Deciduous/Mixed, Coniferous, Wetlands classes) to Agricultural Fields (type 1 and 2, Bare Field) may also be real. The 2005 object-based classification classified 422,297 ha as forest (both types) representing 37% of the total land cover and an overall loss from 1995 of 40,000 ha (approximately 9.5%). The 2005 MLC pixel-based classified 353,300 ha as forest representing 31% of the total land cover and an overall loss of 73,504 ha (approximately 21%) from 1995. The EOMF states in 2004 there were 550,000 ha of forest in a slightly larger area (Figure 1.1 - total EOMF area represented by dark boundary) corresponding to approximately 34% of total land cover (EOMF, 2006). Although both classification methods come similarly close to estimating the total percent of forest of the whole landscape, the object-based comes closer to estimating the current total amount of forest cover.

Other changes that are expected to be real are changes from Agricultural Field 1 or 2 to Bare Field, and changes between Agricultural Fields 1 and 2. The Landsat scene 2005_1529 was acquired in September and 1995_1529 was acquired in August. It would be expected that more agricultural fields in September 2005 would be tilled/harvested (bare) as opposed to August 1995. Also crop rotation results in varying crop types or fallow conditions over time. Changes between agricultural field types (Tables III-A1a-c, Appendix III-A provide details on land covers in Agricultural Field 1

and 2) would also be expected. The object-based classification showed 462,000 ha as agriculture in 2005 (Agriculture Fields 1 and 2, Bare field) an increase from 1995 to 2005 of 3,336 ha (0.7%). The pixel-based MLC method classified 475,000 ha as agriculture in 2005, an increase from 1995 to 2005 of 8.6%. According to the agriculture census in 2001, there were 526,000 ha of croplands in eastern Ontario representing an increase from 1996 of 9.2% (2001 Agricultural Census, Statistics Canada). The pixel-based classification comparison comes closest to capturing this change.

In general, LULC change that is not logical and probably in error are the increases to the Wetlands class from other classes. Wetlands losses were expected over the time period (National Wetlands Working Group, 1997; Mitsch and Gosselink, 2000). It might be expected that if 2005 was wetter than 1995 areas classified as Wetlands may have been larger in extent than in 1995. Alternatively, if 1995 was an excessively dry year classified Wetlands areas may have been smaller in extent or mis-classified as another class. Figure 4.18 shows the amount of precipitation received over the Ottawa region for the months prior to the image acquisition dates. In 2005, 623.7mm of precipitation fell over the region as compared to 592.8mm prior to the acquisition of 1995 scene. There is a small overall difference between the two years and a very wet April in 2005, but it is not expected that these differences would account for the very large increase to the Wetland classified areas in 2005. Instead, the increases are probably a result of poor accuracy of the Wetlands class in both 2005 and 1995 MLC maps (kappa values = 0.48 each).

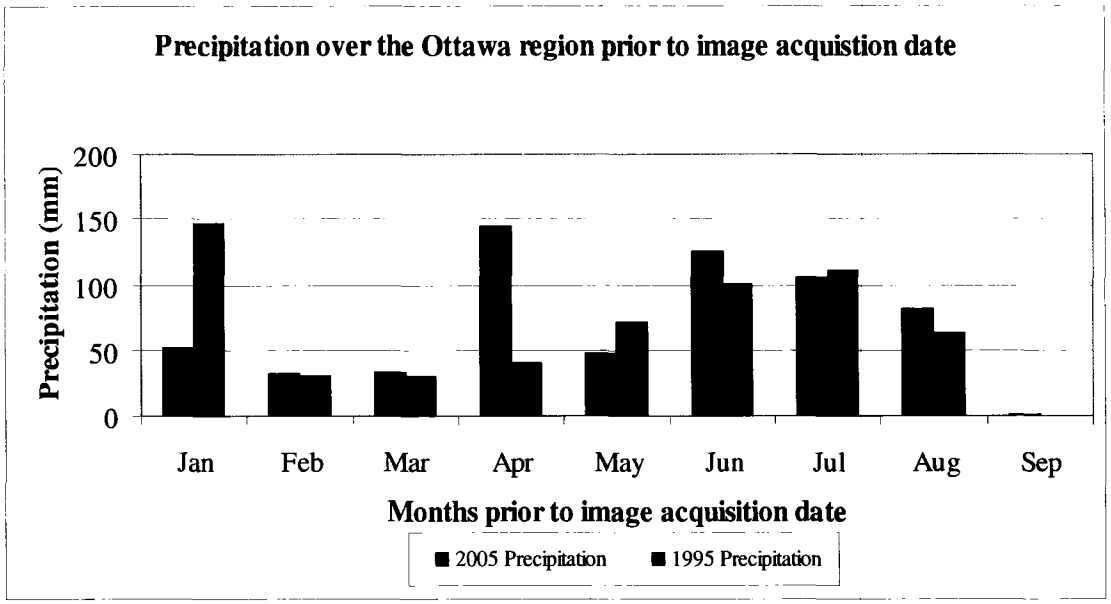

Figure 4.18 – Precipitation (mm) by month over the Ottawa region from January to image acquisition dates (September 6, 2005 and August 10, 1995). (Source: http://www.climate.weatheroffice.ec.gc.ca/climateData/dailydata_e.html).

According to the EOMF (2006) there are approximately 100,000 ha of wetlands in the eastern Ontario region. The 2005 object-based classification classified 93,871 ha as Wetlands as opposed to 77, 044 ha for the pixel-based classification. The object-based classification came closer to estimating the total area of wetlands in the region and in general both object-based classifications' Wetlands class accuracies were higher than the corresponding pixel-based accuracies. There is still the question concerning the increase of wetlands from 1995 to 2005 for both classifications. Overall, the poor classification accuracies appear to affect the PCCs and possibly resulted in erroneously tabulated change.

It is not expected that urban classified areas would revert back to natural vegetation (Wetlands, Deciduous/Mixed, and Coniferous) or agricultural areas (Agricultural Fields 1 and 2, and Bare Field). However, for both the pixel-based classification and the object-based classification total urban area decreased from 1995 to

2005. In the case of the pixel-based classification the decrease was 11,831 ha (8.7%) and for the object-based it was 12,903 ha (13.8%, High and Low Density Urban combined). It is possible that some of the increases to Deciduous/Mixed or agricultural classes might be due to suburban vegetation maturation.

Based upon visual assessment and relating these changes to other data sources (e.g. EOMF data), overall the object-based method comes closest to assessing change in the area. However basing this decision upon the statistics derived from the error matrices is difficult as the differences between the accuracies are probably not statistically significant. Further assessment is warranted.

4.7.1 Comparative temporal analysis: Examples of real change and errors

The following figures show the sub-sites of interest in true colour (red, green, blue) 1995 and 2005 images, the MLC thematic maps for each year, the object-based thematic maps for each year and overall PCC change maps with change in red. The areas circled in yellow highlight real change on all maps. The areas circled in blue highlight potential differences, classification errors on one or more of the thematic maps and areas where change was inappropriately detected. Legends for these thematic and change maps can be found on previously presented corresponding thematic and change maps (Figures 4.1-4.18).

Mer Bleue Bog, Ontario

Figures 4.19 a-h show the Mer Bleue Bog. The yellow circles highlight real change. In Figure 4.19a this area contains forest and some agriculture. In Figure 4.19b the area is now very bright white denoting bare field or an urban site. All four classifications capture these land cover classes. Both 1995 classifications (4.19c, 4.19e) show Deciduous/Mixed and Agriculture Fields (type 1 for 4.19c, and both types for

4.19e). The 2005 classifications (4.19d, f) show Bare Field interspersed with urban classes. Both PCC maps show red in the area correctly indicating the change from 1995 to 2005. Blue circles show classification errors and change detection errors. Figures 4.19a, b reveal that this area is some form of vegetation. Knowledge of the area allows the assumption that this is most likely Wetlands interspersed with some other vegetation (trees, grasses, etc). Figures 4.19c, d reveal the classification error, with areas of this known wetland classified as Low Density Urban. Figures 4.19e, f do not have Low Density Urban classified objects in this region. Further, there are also some Agricultural Field 1 classified areas in Figures 4.19c,d. It could be assumed that these are present (grasses, etc), however they are not apparent in Figures 4.19e, f. Figure 4.19g shows red pixels scattered throughout the Wetland area (blue circle) whereas Figure 4.19h shows unchanged Wetlands. It is expected that in this protected zone the vegetation type would not change (especially to urban), and therefore the object-based PCC would be correct while the MLC PCC is incorrect.

Larose Forest, Ontario

Figures 4.20 a-h show Larose Forest. The yellow circled areas show real change. In 1995 this area is forest/vegetation and in 2005 it is a cutout field (Figures 4.20a, b). The 1995 MLC and object-based classifications (4.20c, e) show this area as Deciduous/Mixed. The 2005 pixel-based classification shows this area as Bare Field surrounded by Deciduous/Mixed. The 2005 object-based classification shows this area as Bare Field surrounded by Deciduous/Mixed and Coniferous (4.20f). Both PCC change maps (4.20g, h) have red squares in the areas where the cutout is located. It is interesting to note with further review of the area (Figure 4.20b) that there are distinct

visual differences in the forested region that may have been correctly captured by the 2005 object-based classification as Coniferous. In-field investigation would be required to confirm this.

The area circled in blue shows falsely detected change. Both 1995 classifications correctly classified the area as forest and in particular Deciduous/Mixed, which can be confirmed in Figure 4.20a. In the 2005 pixel-based classification, (Figure 4.20d) the area has been erroneously classified as Agriculture Field 1. For the 2005 object-based classification (Figure 4.20f) the area has been classified as partially Coniferous and partially Agriculture Field 1. It is interesting to note that even after the atmospheric corrections were applied haze is apparent over this region (Figure 4.20b). The 2005 pixel-based classification misclassified the area in its entirety and the 2005 object-based classification misclassified a portion of the area. The 2005 object-based classification captured some of the forested portion (regardless of type), however both methods had problems in this hazy area, which were subsequently propagated into the PCCs.

Gatineau Park, Quebec

Gatineau Park (Figures 4.21a-h) is a protected part of Canada's capital region. South of the park, within the the yellow circle, is an area of real change. In Figure 4.21a, this area is vegetated with agriculture and in Figure 4.21b the same area is bare. Both 1995 classifications (4.21c, e) show this area classified as Agriculture Field 1. The 2005 MLC classification shows this region as Bare Field and the 2005 object-based classification has the area classified as Agricultural Field 1 and 2. The change from 1995 is apparent on both PCC thematic maps (4.21g, h – yellow circle).

Gatineau Park is a forested area consisting mostly of Deciduous/Mixed stands but there are areas classified as Agricultural Field 1 in all classifications. These could be erroneous, or represention of the clearings for the parkways that run through the area. All four classifications show Agricultural Field 1 areas located in the blue circle. Both object-based classifications show large patches of Agricultural Field 1 throughout the Gatineau Park, however the 1995 object-based classification mis-classifies a larger proportion of the area. As the area is known not to contain agriculture in 1995 the large changes noted in red on Figure 4.21h are incorrect. This shows the amplification of the misclassification in 1995 in the object-based PCC. The agricultural (parkways) areas on the pixel-based classifications and PCC would have to be confirmed to determine whether or not the change is correct. It can be stated, though, based upon the misclassification in 1995, that the object-based PCC would be contain more errors for this area than the pixel-based.

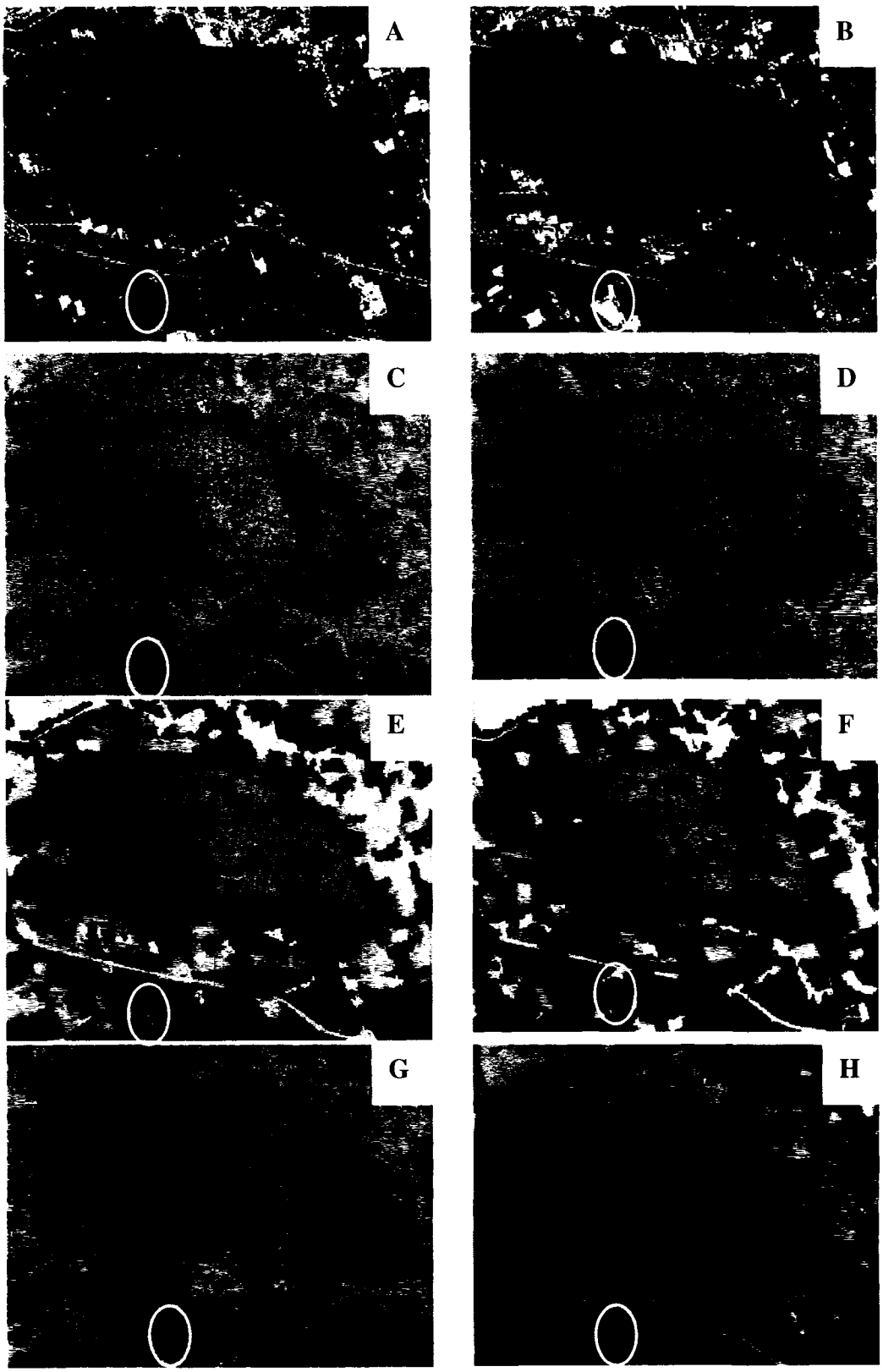

Figure 4.19 - Mer Bleue Bog a)1995 true colour; b)2005 true colour; c)1995 MLC; d)2005 MLC; e)1995 object-based; f)2005 object-based; g) MLC PCC; h)object-based PCC.

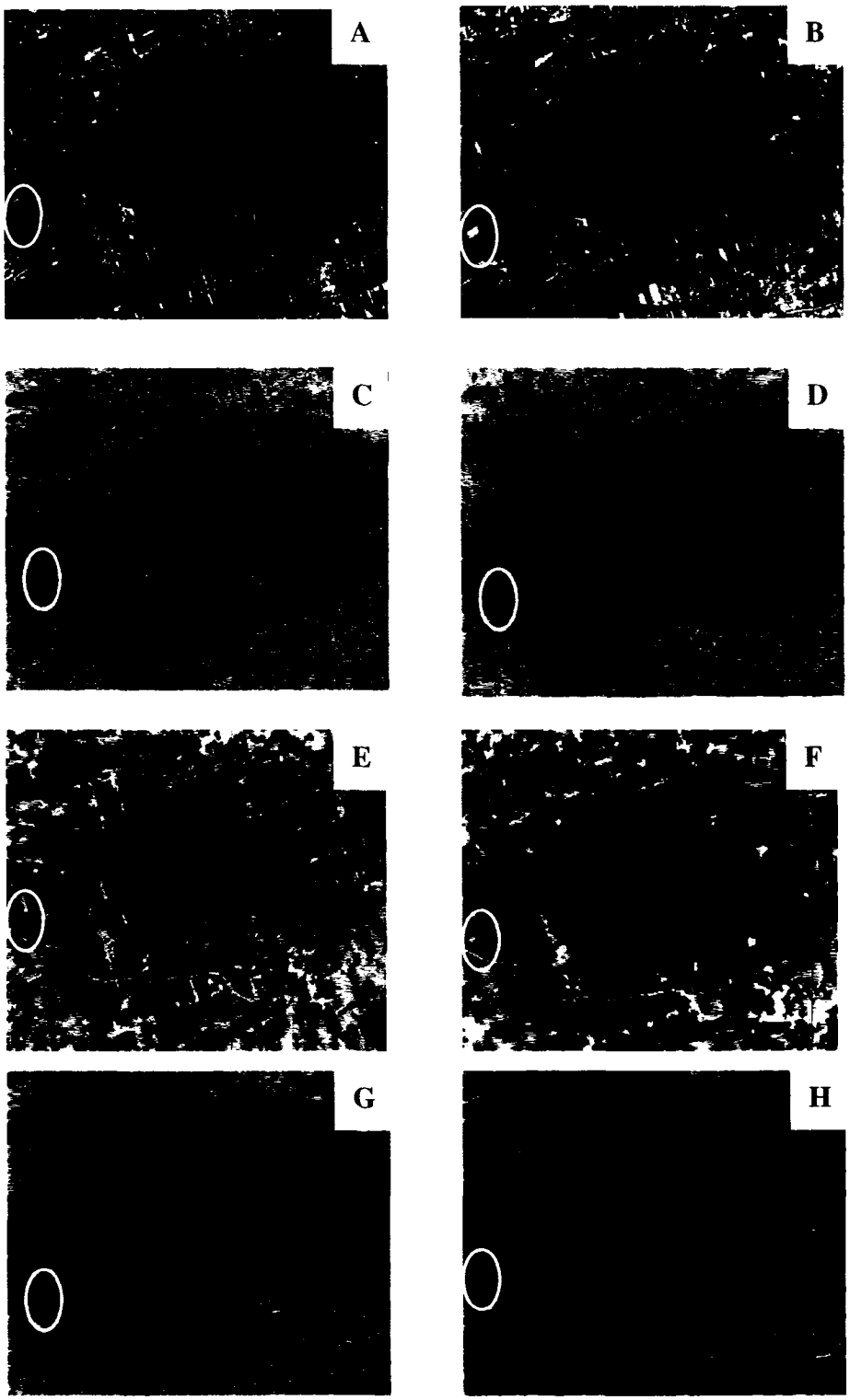

Figure 4.20 - Larose Forest a)1995 true colour; b)2005 true colour; c)1995 MLC; d)2005 MLC; e)1995 object-based; f) 2005 object-based; g)MLC PCC; h)object-based PCC.

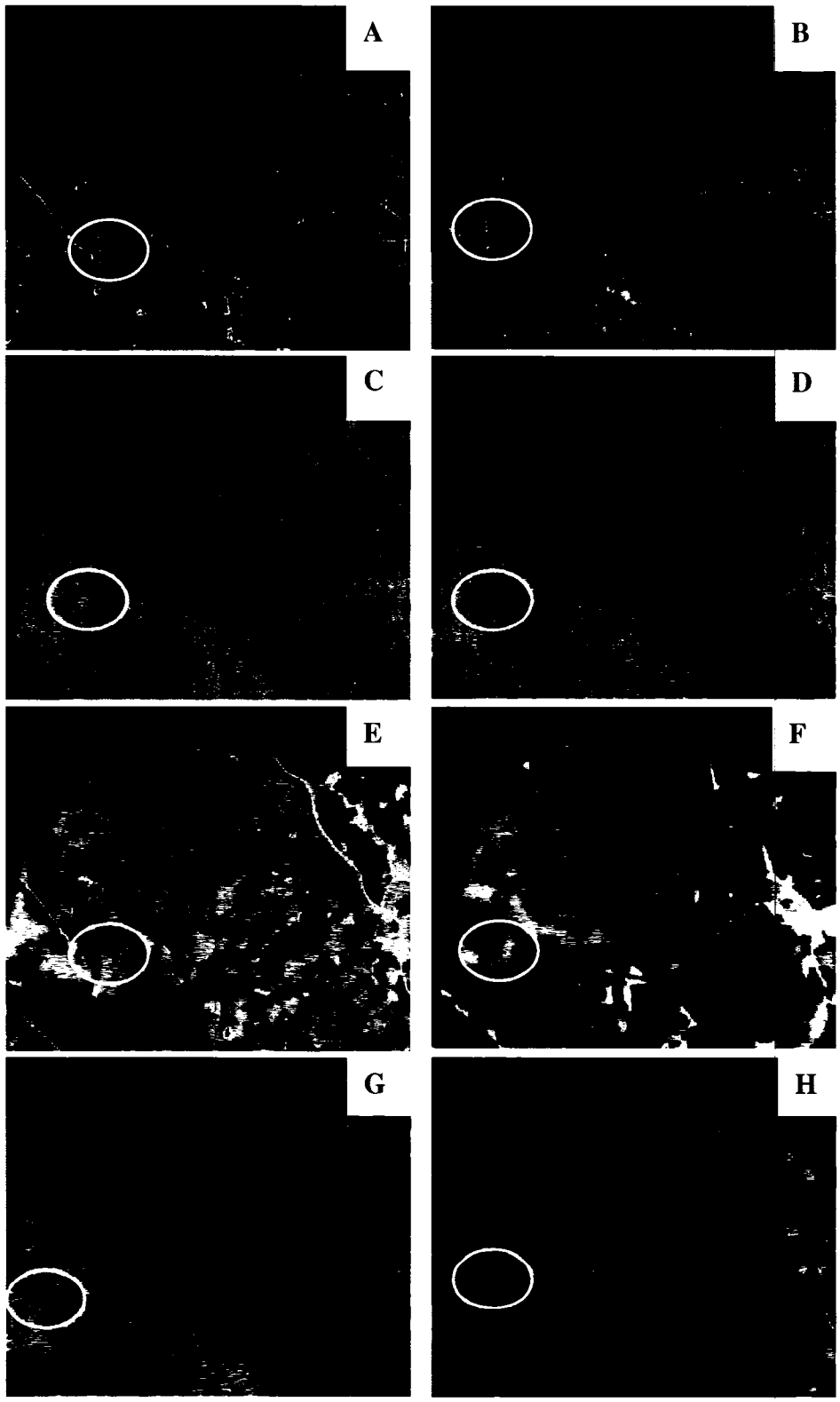

Figure 4.21 – Gatineau Park a)1995 true colour; b)2005 true colour; c)1995 MLC; d)2005 MLC; e)1995 object-based; f)2005 object-based; g)MLC PCC; h)object-based PCC.

Cornwall, Ontario

Overall, the general areas of change that were observed in Figures 4.16 and 4.17 were found to be around the Cornwall region (Figures 4.22a-h). Figure 4.22b shows that this region in 2005 was covered in a haze, and in 1995 the region was clear. An area of real change is found within the yellow circle. In 1995 this area was forested with some agriculture surrounding it. In 2005 the area was bright indicating either bare soil or some kind of urban land cover. Both 1995 classifications show this area classified as Deciduous/Mixed and Agriculture Field 1. The 2005 pixel-based classification shows this area classified as Bare field with High Density Urban pixels surrounding it (Figure 4.22d). The 2005 object-based classification does not classify this area (although it appears to be Wetlands it is actually "unclassified"; Figure 4.22f). Both PCC thematic maps show the area as changed (red, Figures 4.22g) or no classification (pink Figure 4.22h).

The area circled in blue is an area that was forested in both the 1995 and 2005 scenes (Figures 4.22a, b) and in 1995 was classified as as Deciduous/Mixed by both classifiers. The 2005 MLC map shows the area classified as Agricultural Field 1 which is incorrect based upon the visual assessment of Figure 4.22b. The 2005 object-based map shows the area classified as a mix of Coniferous and Wetlands which is different from the 1995 object-based map, but closer than the 2005 MLC to the expected class. Although haze was problematic in the Cornwall area overall, the object-based PCC performed better than the MLC PCC for change analysis in this area (although forest type would have to be confirmed in the future).

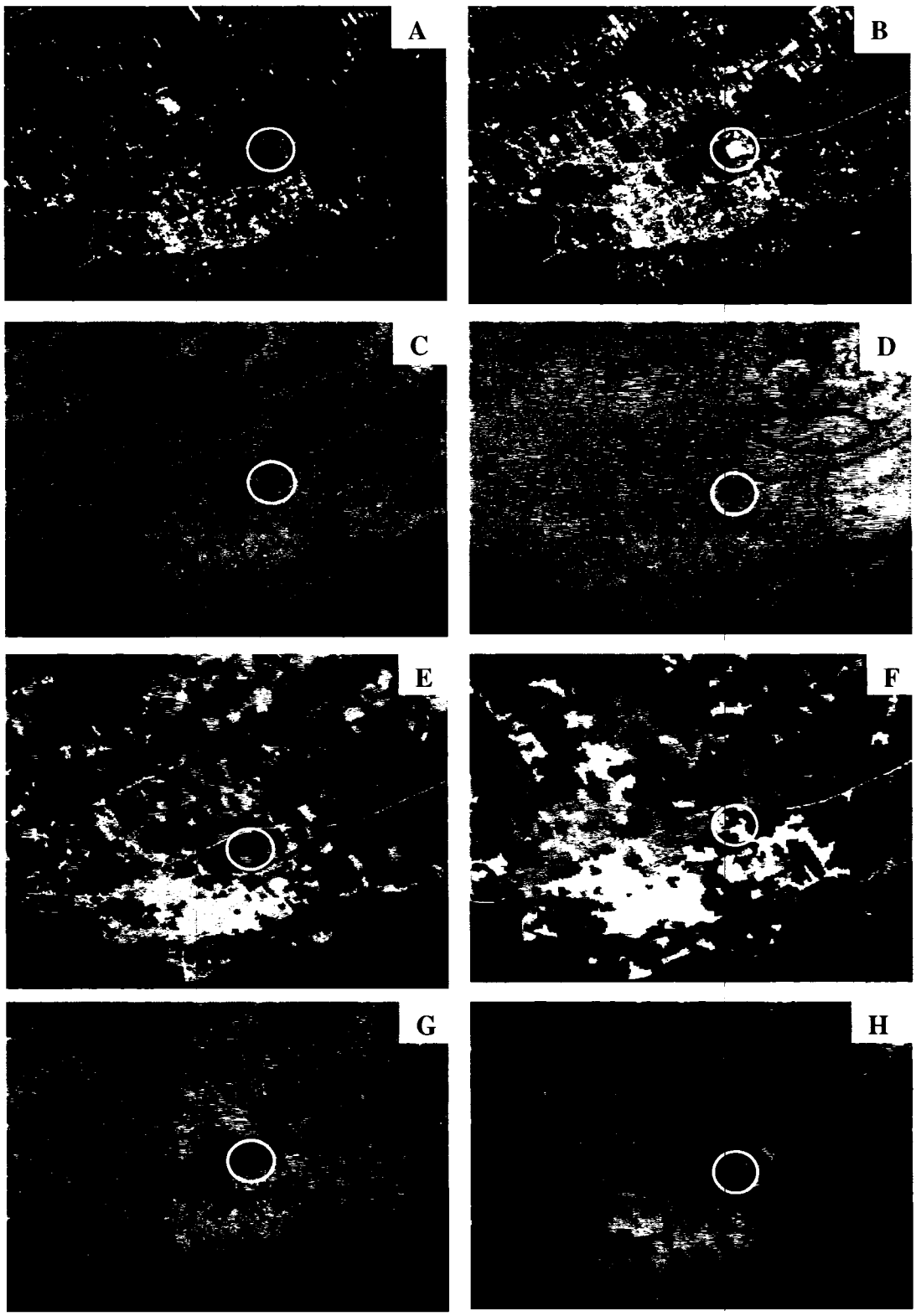

Figure 4.22 - Cornwall a)1995 true colour; b)2005 true colour; c)1995 MLC; d)2005 MLC; e)1995 object-based; f)2005 object-based; g)MLC PCC; h)object-based PCC.

Barrhaven, Ontario

Over the ten year period Barrhaven (Figures 4.23a-h) has expanded to accommodate the growing population of the region. On both PCC change maps, large areas of the region are in red reflecting changes from agriculture and natural vegetation to urban sites. Additionally, there is change between the urban classes from Low Density Urban to High Density Urban. The yellow circle on all of the figures is a site of real change from agriculture to urban.

The blue circle highlights a mis-classification on the 2005 pixel-based thematic map and a difference between the two methods. In Figure 4.23b the area in the blue circle is white and bright; the MLC classified this area as Bare Rock and the object-based classification classified this area as High Density Urban. Although this area could have been a bare field area in preparation for construction, a site visit revealed it to be an established shopping mall with a large parking lot in the centre. The object-based classification correctly identified this land cover and although, in both cases there is still a change, the change from agriculture to Bare Rock (pixel-based PCC) is incorrect, while the object-based PCC from agriculture to urban is correct.

Wetlands, Rideau River, Ontario

Figures 4.24a-h present the wetlands area in the Rideau River. The yellow circle highlights a visually apparent change from 1995 to 2005. That change of agriculture type is captured by PCC using both classification types. For areas in the pixel-based classifications (Figures 4.24c, d) that are classified as Low Density Urban (blue circle and within the river itself) the object-based method classified these areas as Wetlands. It would be expected (especially within the middle of the river) that the areas would be

Wetlands and therefore the object-based classification (and subsequent PCC) would be correct. The pixel-based classifications have confused Wetlands with the urban classes and subsequently this confusion has produced erroneous PCCs.

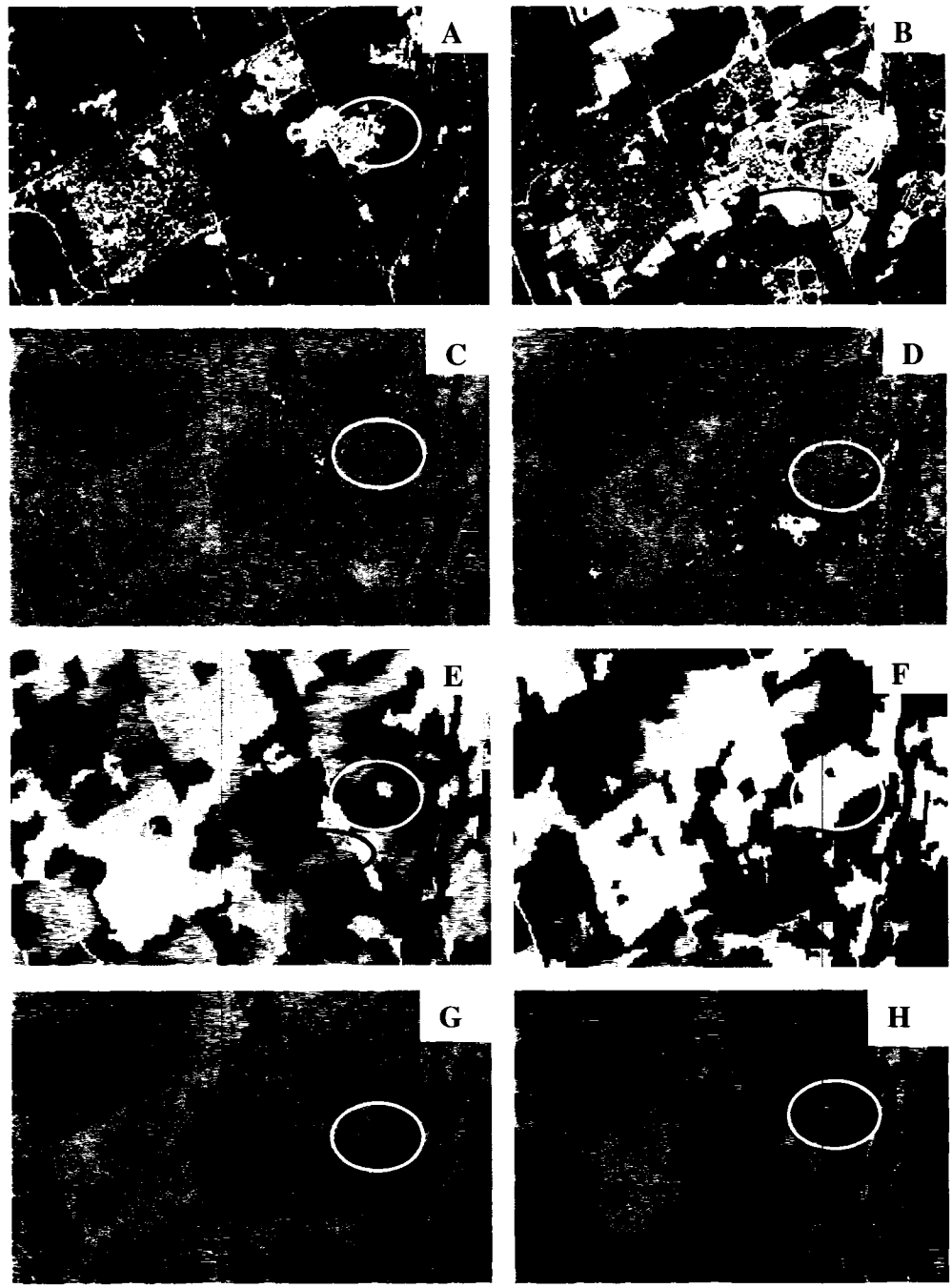

Figure 4.23 – Barrhaven a)1995 true colour; b)2005 true colour; c)1995 MLC; d)2005 MLC; e)1995 object-based; f)2005 object-based; g)MLC PCC; h)object-based PCC.

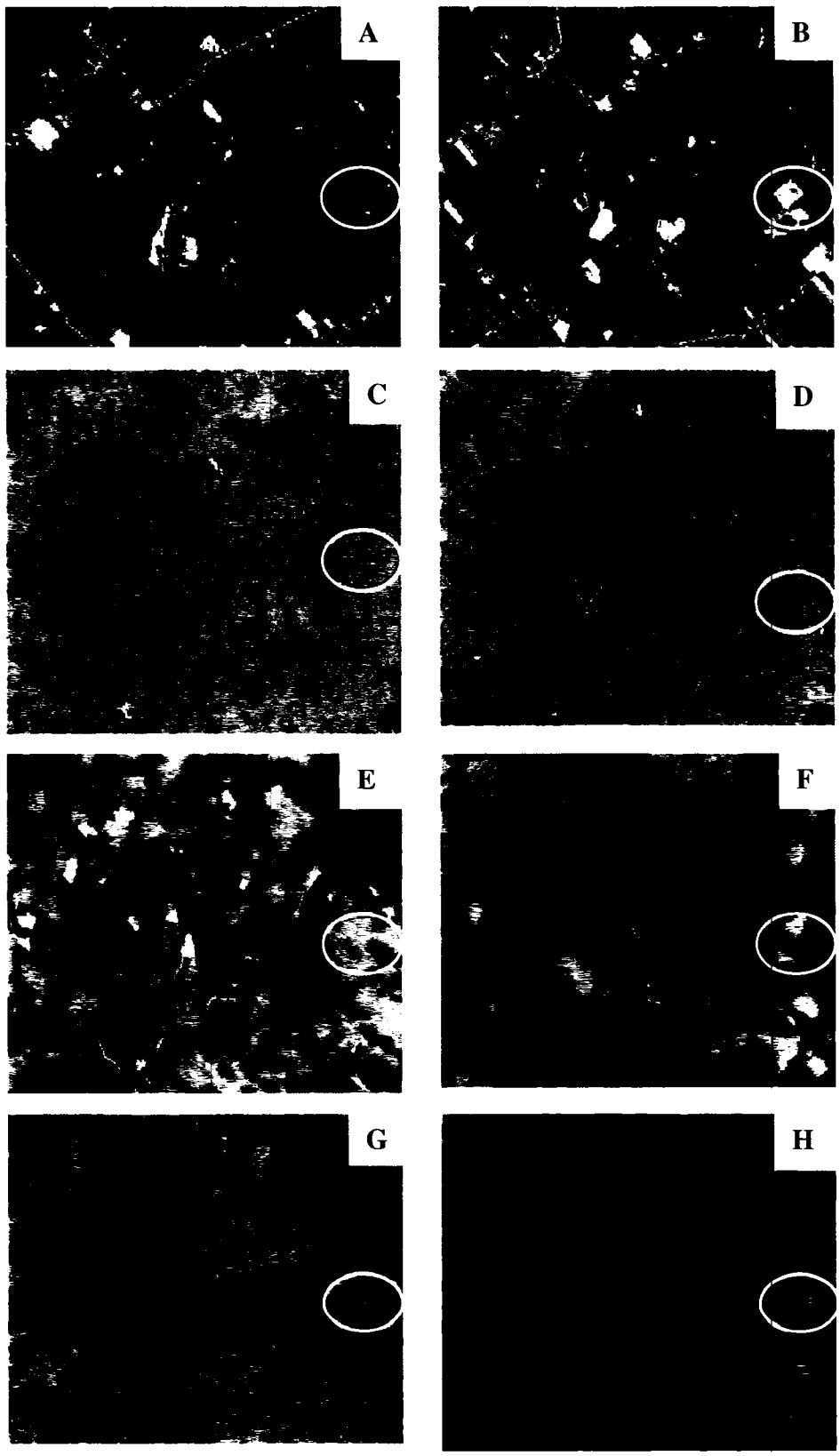

Figure 4.24 – Wetlands, Rideau River. a)1995 true colour; b)2005 true colour; c)1995 MLC; d)2005 MLC; e)1995 object-based; f)2005 object-based; g)MLC PCC; h)object-based PCC.

CHAPTER 5

5.0 Discussion and Conclusions

Chapter five summarizes the findings of this research and discusses the research outcomes in relation to the literature. The findings are presented in two sections: classifications and temporal analysis. This chapter also summarizes the significant contributions and limitations of the research, and makes recommendations for future work. The conclusions from this research are presented at the end of this chapter.

5.1 Classifications

For the research objective to compare the maximum likelihood and object-based classification methods, several significant results were produced with respect to the mapping accuracy, atmospheric correction, training signature extension and the classifiers themselves. These are described in the following sections.

5.1.1 Mapping eastern Ontario

Using Landsat TM imagery and the object-based classification method, land cover mapping of eastern Ontario met standardized accuracy requirements (PA and UA $\geq$ 70% (Foody, 2002)) for six of 10 land cover classes tested (2005) and eight of 10 classes (1995). Using the pixel-based classification only five of 10 classes met the requirements (both 2005 and 1995).

In general, these classification results are comparable to a mapping study of the Ottawa region (Guindon *et al.*, 2004) where land cover thematic maps were derived from Landsat TM imagery for five classes in an urban environment. PAs were: water (96.7%), residential (77.8%), commercial/industrial (73.1%), forest (91.9%) and herbaceous (86.3%). In this research, the best classification result (2005 object-based

nearest neighbour classification) had similar PAs for the classes: Water (92.6%), Low Density Urban (70.0%), High Density Urban (76.2%), forest (Deciduous/Mixed) (83.3%) and Agricultural Fields (type 1, 76.0% and/or type 2, 87.2%). The remaining four classes had mixed results of Bare Field (100%), Bare Rock (0.0%), Wetlands (69.2%) and Coniferous (30.0%).

It was found that mapping wetlands using the pixel-based method was not as successful as the object-based method. Wetlands are a significant and important land cover in the eastern Ontario region (>100,000 ha). The reason for the poor classification results was not related to the relative wetness of the year(s). The mixture of spectral sources (water, vegetation (live or dead, floating), etc.) in the variety of wetlands (e.g. bog, swamp, marsh, fen) across the area may have resulted in these areas being spectrally confused with other classes. Using a variety of wetland types as one broad class could result in large class variance and overlap with data for other classes. Some considerations for mapping this land cover type in the future would include mapping these areas at a higher spatial resolution, capturing a wider variety of wetland types and extending/fusing that classification to the coarser regional scale. Additionally, the choice of atmospheric correction method may also play a part in the accuracy of this specific class (see 5.1.2). For the object-based classification method further testing could be done with shape and contextual information to determine if these parameters (or combinations thereof) could improve the accuracy of this, and other poor classes.

5.1.2 Atmospheric corrections

Atmospheric correction testing was conducted only using a MLC. The most accurate 2005 MLC was obtained using DOS atmospherically-corrected imagery. This is similar to what other researchers have found (Pax-Lenney *et al.*, 2001; Song *et al.*, 2001). However, with testing on the second most accurate maps (ATCOR2 correction applied), it was found that some classes had higher UA and PA, while the overall accuracy was lower (e.g. for 2005_1529, Wetlands: PA=60%, UA=75%, k=0.74). This could be important if the thematic map was needed for specific land cover analysis. These corrections were not tested on the object-based classification method so it is not known if accuracies would have improved for wetlands or other poor classes (e.g. Bare Rock) for that method. Overall, for temporal analyses (in particular PCC), the literature (Mas 1999; Coppin *et al.*, 2004; Lu *et al.*, 2004) highlights the need for highly accurate contributory thematic maps to ensure the accuracy of the subsequent change maps. In this research, based on the MLC results, the choice was made to continue with the DOS-corrected 2005 scene for the object-based classification. However, if a classification or temporal analysis is to be used to map a specific land cover class(es), then atmospheric correction methods should be compared.

It was found that both the pixel-based and object-based methods had difficulty classifying areas in the 2005 scene where haze was present (Figures 4.20 d, f and Figures 4.22 d, f). When reviewing the pixel-based classification of the ATCOR2 corrected scene (example Figure 5.1a, b, c), it can be seen that, although the haze is visually not apparent, the areas are still mis-classified. Further examination of other atmospheric correction methods was beyond the scope of this research; however a future

consideration would be the investigation of other methods that mitigate haze effects. Alternatively, obtaining data that are haze free (versus the cloud free, the criteria typically used when ordering imagery from suppliers) may be an alternative choice for improving the classification(s).

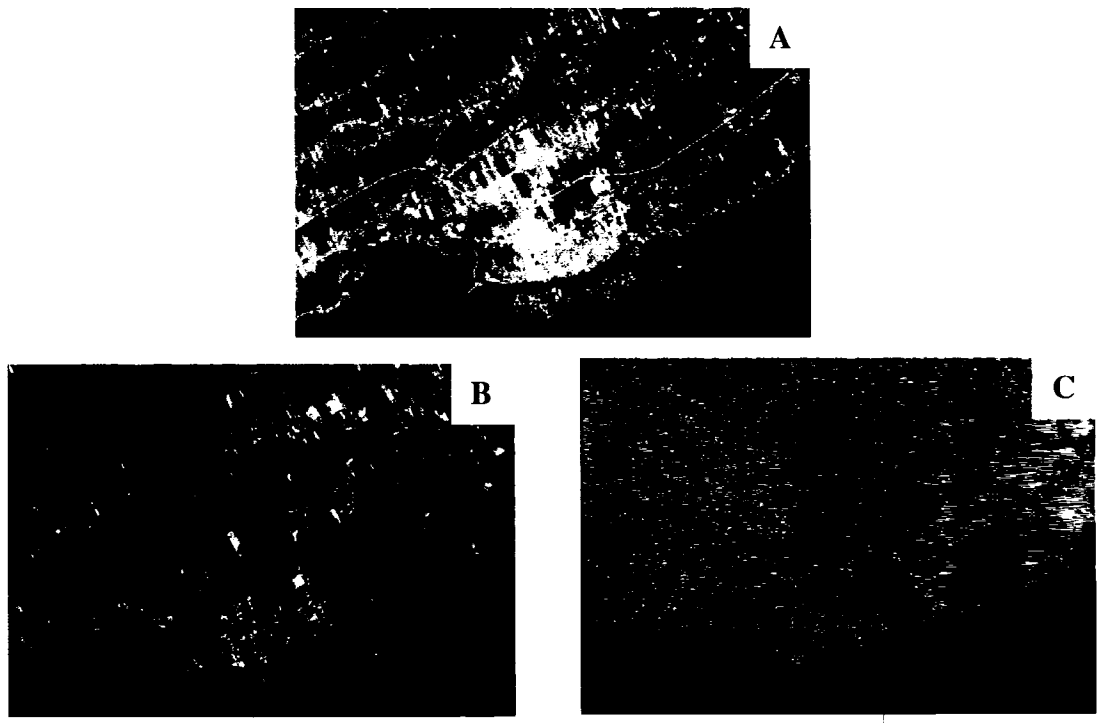

Figure 5.1 – Cornwall a)true colour composite (uncorrected 2005 scene)
b)true colour composite (ATCOR2 corrected 2005 scene)
c)thematic classification of the same scene. Areas circled in blue are mis-classified.

Schroeder *et al.* (2006) found that using a combined "absolute-normalization" method by relatively correcting imagery using either the PIF or MAD methods to a 6S corrected "master" image resulted in the lowest RMSE. This exact method was not attempted in this research although a similar method of absolute-absolute-relative normalization was attempted with mixed results. As seen in Appendix II-C, the accuracy improved when the ATCOR2 corrected 1995 scene was relatively corrected to the ATCOR2 corrected 2005 scene; the same cannot be said for the DOS 1995 corrected

scene. The accuracy declined from 79.2% for the DOS-only corrected 1995 scene to 76.1% for the DOS/PIF corrected 1995 scene. In particular, UA and PA declined for: High Density Urban, Bare Rock, Deciduous/Mixed, Low Density Urban, Agricultural Field 1 and Agricultural Field 2. This was not expected as the class signatures were extended from 2005 and therefore it would be assumed that any differences left between the two (2005/1995) would be minimized with the relative correction, resulting in an improvement in the 1995 classification. Further investigation into this is required. As noted in section 3.5.21 the DOS-corrected data was scaled from 32-bit to 8-bit. This was done for technical processing purposes only. The scaling algorithm used a simple linear equation and should not have affected the at-satellite radiance values however, further investigation would be needed to determine if there was an affect.

5.1.3 Signature extension

Signature extension was tested indirectly through assessment of classification accuracy of the 1995 scene using signatures generated from the 2005 scene. It was found that such signature extension can be used for object-based classifications through the use of identical segmentation parameters, and an extension of a spectral-based classification hierarchy. It was also found that extension of class signatures developed from the 2005 pixel-based classification was feasible and resulted in an accurate classification of the 1995 scene. These results are in general similar to Pax-Lenney *et al.* (2001). For this research, the classification methods employed were different, and there were more classes for which training data were temporally extended, although the same sensor was used (Landsat TM) and the same atmospheric correction algorithm was applied.

As noted in section 3.5.2.2, atmospheric correction testing was completed on other available data. Using these data (1984 scene) the need for seasonally similar scenes was substantiated. Using ATCOR2 corrected scenes, the signatures derived in 2005 were subsequently extended to 1984 ATCOR2-relative corrected (second best atmospheric correction results as problems with scaling the 1984 image data from 32-bit to 8-bit prohibited the use of the DOS method.) and the accuracy was assessed using a subset of the overall reference/validation set (derived using the image differencing method). From Table 5.1 it can be seen that signatures can be extended for classes that are not significantly affected by seasonality (Water, High Density Urban, and Coniferous). For other classes, the difference in the growing season between the different acquisition dates (July 10, 1984 and September 10, 2005) can account for a portion of the lower PA and UA. Because of the small sample size, there were not any validation/reference sites for the rarer Bare Rock class resulting in the 0.00% accuracies.

Table 5.1 – Thematic map accuracy statistics for the 1984_1529 (ATCOR2) corrected scene (10 classes).

Overall Accuracy: 51.80%
Overall Kappa Statistic: 0.43

	Producer's Accuracy	**User's Accuracy**	**Kappa**
High Density Urban	71.43%	62.50%	0.58
Bare Rock*	0.00%	0.00%	0.00
Coniferous	66.67%	100.00%	1.00
Deciduous/Mixed	5.56%	100.00%	1.00
Low Density Urban	77.78%	43.75%	0.35
Water	100.00%	100.00%	1.00
Wetlands	100.00%	16.67%	0.15
Agricultural field 2	52.17%	66.67%	0.60
Agricultural field 1	44.44%	51.28%	0.28
Bare Field	0.00%	0.00%	-0.03

*No remaining reference sites for this class.

Further investigations need to be made as to the size of the window of seasonality where signatures can be extended in the region. For example, could classifications be made with imagery from mid-growing season and the training data extended both backwards and forwards a certain number of days, or weeks? Moving forward, current scene signatures could also be used to classify future scenes, thus ensuring consistency throughout time of the classes of interest and enabling a continuous program of land cover classification and change analysis in the region.

A secondary future consideration would be to successfully use shape and contextual parameters in the object-based classification hierarchy and assess if these parameters can be extended to older imagery in addition to spectral information. Other segmentation methods (e.g. quadtree) should also be assessed in signature extension. Other general investigations of signature extension are warranted, in particular in using signatures derived at higher resolutions for specific classes (e.g. Wetlands) to classify coarser spatial imagery.

A third consideration should be made as to the addition of ancillary data for the object-based method. This could include digital elevation models to provide information such as drainage patterns and slope that may help further define poorer classes (e.g. Wetlands class). Other ancillary data could include higher resolution data to help define smaller and rare classes, and linear features.

5.1.4 Comparison

Many studies use MLC as a benchmark to assess new, untested classification methods. For example, Flanders *et al.* (2003), Yan *et al.* (2006) and Yu *et al.* (2006) assessed object-based methods against the MLC method and all found that overall

accuracy improved (see 2.2.4.4). The 2005 object-based classification overall accuracy was 75.6% compared to the MLC overall accuracy of 75.7%. The 1995 MLC overall accuracy of 79.2% and the 1995 object-based classification overall accuracy was 75.2%. These differences between these results are probably not statistically significant. However, overall and in general there was less confusion reveal in the error matrices between classes for the object-based classification. Additionally, through the qualitative assessment of the sub-sets of all the thematic and change maps, the object-based methods were assessed as depicting land covers, and the corresponding change more accurately.

In general (excluding Bare Rock) the PAs and UAs were higher for the object-based classification. It seems that the rareness (and in turn the small sample size of reference points) of the Bare Rock class led to poor accuracies for the object-based classifications. This could be related to the region growing segmentation process and the potential for small areas (and reference sites) of rare land cover types to be merged into the surrounding common land cover classes. Additionally it appeared that linear features were lost through the segmentation process the object-based method. In future work, the scale parameter for segmentation could be used to define the size of objects that would not absorb such small areas, linear features, or rare cover types. Alternatively, more reference/validation sites and larger sample areas for these rare classes could be used if they exist. Finally, the merging of all impervious classes (Bare Rock, and both urban classes) may also improve classification results.

A limitation (and possibly a significant finding) of this research was that the shape parameters attempted in the object-based classification hierarchy could not be

successfully implemented using Landsat TM data alone. Other object-based studies successfully implemented some of these parameters using higher resolution data (Laliberte *et al.*, 2004; Yu *et al.*, 2006) or with multi-source data (e.g., DEM, aerial imagery) combined with Landsat TM data (Burnett and Blaschke, 2003). Further testing on these parameters is warranted. Some individual class accuracies improved when some of these parameters were used for all classes at a global level, but the overall accuracy decreased (e.g. with the addition of these parameters other class accuracies declined significantly, thus reducing the overall accuracy). When the parameter was applied to the class(es) that improved on a class by class basis, the same increases in accuracy for those classes were not achieved. Testing a combination of the parameters, or applying the parameters individually to other classes is warranted. Additionally, in consideration of time, there were many parameters (texture, other shape, contextual) available in the eCognition software that were not tested that should be assessed with Landsat TM data. Discovering the issues with the shape parameters and Landsat TM data raises the question of the overall benefit of the object-based method which is complex and time-consuming. Further testing is warranted because of the general improvement in classification accuracies over the traditional pixel-based method, and in light of the possible insight into to landscape ecology and hierarchical patch dynamics.

The utilization of the image differencing method to derive a reference set for older imagery was a unique aspect of this research. This method worked well in providing a set of reference sites for older imagery (both 1995 and 1984) as opposed to using visual interpretation of aerial imagery to derive reference data. One limitation of this method was the number of rare sites obtained in the field. If only four reference

sites are obtained for a class and these are all found to have changed through time, then that class does not have reference sites for the older year. In future research, the selection and quantity of reference sites must consider potential losses of sites through the image differencing method. Compensation for these losses must be made and adequate numbers of sites of all classes must be collected in the field in the present. The threshold limit (number of standard deviations) used should be assessed to determine if that parameter had any affect on the overall numbers of validation sites for the older imagery.

5.2 Temporal analysis

For the research objective to determine how the accuracy of land cover classifications for each date and method affect overall accuracy of change maps, the accuracy of the change maps was not quantitatively assessed. Instead, a visual review of real and not real changes (see 4.6.1) provided evidence of which method and classification maps provided the most accurate change maps. Based upon this review, the object-based change map was the most accurate.

As a limitation, the object-based segmentation process may have assigned rare, small areas (e.g. Bare Rock) as part of larger objects of more common classes. These incorrectly segmented areas could then be erroneously projected as change, or alternatively erroneously not detected as change. Because there were very few examples of these rare classes this aspect was difficult to assess.

The object-based classification was more accurate in hazy areas for the 2005 image than the pixel-based method. This possibly ensured that changes in those areas were more correctly depicted; however both methods had difficulty classifying these

hazy areas and therefore the massive change noted (e.g. around Cornwall) would be questionable. This should be reassessed using haze-free imagery.

One limitation of this research was the lack of quantitative assessment of the change maps derived. Because there weren't any field data from 1995, assessment of change would have depended upon using either reference sites derived from the image differencing method or through visual assessment of aerial imagery. Moving forward, data collected in the field in 2006 can now be archived and used to assess change between now and any future assessments.

5.3 Conclusions

This research found that object-based nearest neighbour segmentation and classification was more accurate than traditional maximum likelihood classification methods for regional scale thematic mapping at 30m resolution using Landsat TM data and seven land cover classes. A limitation of this method was the absorption of small and rare class areas into larger objects of more common classes.

The 1995 and 2005 object-based thematic maps produced a more accurate PCC change map than the traditional pixel-based thematic maps. Two areas of concern were the Gatineau Park region and wetlands areas. Investigation into improvements for these areas/classes is needed. Signature extension was successful for multiple classes and the pixel-based maximum likelihood classification. More significantly, signature extension was successful with the object-based segmentation and classification method. If shape and contextual parameters are found to be of use in the future, further investigation into extension of those 'signatures' is needed. The unique method of image differencing to derive validation sets was found to be successful for assessment of older imagery for

both classification methods; future investigations into thresholds and validation set sizes are warranted to improve this method.

As part of the larger initiative within the GLEL, this research can now be used in conjunction with species data to determine the effects of land cover change on species populations. This research will contribute to current projects including ecological response lag of species to landscape change, effects of roads on species movement and persistence and species specific habitat requirements and to future landscape ecology regional scale research in eastern Ontario.

REFERENCES

2006 Community Profiles: 2006 Census. Adapted from Statistics Canada. Date last modified: March 13, 2007. http://www12.statcan.ca/english/census06/data/profiles/community/Index.cfm?Lang=E. Date of extraction: March-June 2007.

2001 Agricultural Census: Regional Profile of Ontario Agriculture: Eastern Ontario. Statistics Canada. Date last modified: December 2, 2003. http://www.statcan.ca/english/agcensus2001/first/regions/farmon.htm#11. Date of extraction: March 2007.

2001 Community Profiles: 2001 Census. Adapted from Statistics Canada. Date last modified: April 4, 2007. http://www12.statcan.ca/english/Profil01/CP01/Index.cfm?Lang=E. Date of extraction: March-June 2007.

Abuelgasim, A.A., W.D. Ross, S. Gopal and C.E. Woodcock. 1999. Change detection using adaptive fuzzy neural networks: Environmental damage assessment after the Gulf War. Remote Sensing of Environment 70: 208-223.

Baldwin, D.J.B., J.R. Desloges and L.E. Band. 2000. Physical Geography of Ontario. *IN* A.H Perera, D.L. Euler and I.D. Thompson (eds). Ecology of a Managed Terrestrial Landscape: Patterns and Process of Forest Landscapes in Ontario. Vancouver; British Columbia: University of British Columbia Press. (13-29) 336 p.

Baraldi, A and F. Parmiggiani. 1995. An investigation of the textural characteristics associated with grey level coocurrence matrix statistical parameters. IEEE Transactions on Geoscience and Remote Sensing 33: 293-304.

Benz, U.C., P. Hofmann, G. Willhauck, I. Lingenfelder and M. Heynen. 2004. Multi-resolution, object-oriented fuzzy analysis of remote sensing data for GIS-ready information. ISPRS Journal of Photogrammetry & Remote Sensing 58: 239-258.

Berk, A., L.S. Bernstein, G.P. Anderson, P.K. Acharya, D.C. Robertson, J.H. Chetwynd and S.M. Adler-Golden. 1998. MODTRAN cloud and multiple scattering upgrades with application to AVIRIS. Remote Sensing of Environment 65: 367-375.

Blaschke, T. and J. Strobl. 2001. What's wrong with pixels? Some recent developments interfacing remote sensing and GIS. Interfacing Remote Sensing and GIS GIS 6/01.

Burnett, C. and T. Blaschke. 2003. A multi-scale segmentation/object relationship modelling methodology for landscape analysis. Ecological Modelling 168: 233-249.

Campbell, J.B. 2002. Introduction to Remote Sensing. New York: The Guilford Press. 621 p.

Carpenter, S. R., N.F. Caraco, D.L. Correll, R.W. Howarth, A.N. Sharpley and V.H. Smith. 1998. Nonpoint pollution of surface waters with phosphorus and nitrogen. Ecological Applications 8: 559-568.

Chander, G. and B. Markham. 2003. Revised Landsat-5 TM Radiometric calibration procedures and post calibration dynamic ranges. IEEE Transactions on Geoscience and Remote Sensing 41: 2674-2677.

Chapin III, F. S., E.S. Zavaleta, V.T. Eviner, R.L. Naylor, P.M. Vitousek, H.L. Reynolds, D.U. Hooper, S. Lavorel, O.E. Sala, S.E. Hobbie, M.C. Mack and S. Díaz. 2000. Consequences of changing biodiversity. Nature 405: 234-242.

Chavez Jr., P. 1996. Image-based atmospheric corrections – revisited and improved. Photogrammetric Engineering & Remote Sensing 62: 1025-1036.

Chavez, P. 1988. An improved dark-object subtraction technique for atmospheric scattering correction of multispectral data. Remote Sensing of Environment 24: 459-479.

Chen, X., L. Vierling and D. Deering. 2005. A simple and effective radiometric correction method to improve landscape change detection across sensors and across time. Remote Sensing of Environment 98: 63-79.

Cingolani, A.M., D. Renison, M.R. Zak and M. R. Cabido. 2004. Mapping vegetation in a heterogeneous mountain rangeland using Landsat data: an alternative method to define and classify land-cover units. Remote Sensing of Environment 92: 84-97.

Cohen, Y. and M. Shoshany. 2005. Analysis of convergent evidence in an evidential reasoning knowledge-based classification. Remote Sensing of Environment 96: 518-528.

Collins, J.B. and C.E. Woodcock. 1996. An assessment of several linear change detection techniques for mapping forest mortality using multitemporal Landsat TM data. Remote Sensing of Environment 56: 66-77.

Coppin P., I. Jonckheere, K. Nackaerts, B. Muys and E. Lambin. 2004. Digital change detection methods in ecosystem monitoring: a review. International Journal of Remote Sensing 25: 1565-1596.

Costa, M., H. A. Botta and J.A. Cardille. 2003. Effects of large-scale changes in land cover on the discharge of the Tocantins River, Southeastern Amazonia. Journal of Hydrology 283: 206-217.

Eastern Ontario Model Forest (EOMF). 2006. "Ontario's Living Legacy". "Forest Coverage by Age", State of Eastern Ontario's Forests. National Resources Canada. Date last modified: 2004-2006. http://sof.eomf.on.ca/index_e.htm. Date of extraction: March-June 2007.

Eastern Ontario Model Forest (EOMF). 2006 "Forest Coverage by Age". State of Eastern Ontario's Forests. National Resources Canada. Date last modified: 2004-2006. http://sof.eomf.on.ca/index_e.htm. Date of extraction: March-June 2007.

Environment Canada. 2006. "Climate Data Online". Date last modified: April 6, 2005. http://www.climate.weatheroffice.ec.gc.ca/Welcome_e.html. Date of extraction: March-June 2007.

Findlay, C.S. and J. Bourdages. 2000. Response time of wetland biodiversity to road construction on adjacent lands. Conservation Biology 14: 86-94.

Flanders, D. M., M. Hall-Beyer and J. Pereverzoff. 2003. Preliminary evaluation of eCognition object-based software for cut block delineation and feature extraction. Canadian Journal of Remote Sensing 29: 441-452.

Foley, J.A., R. DeFries, G.P. Asner, C. Barford, G. Bonan, S.R. Carpenter, F.S. Chapin, M.T. Coe, G.C. Daily, H.K. Gibbs, J.H. Helkowski, T. Holloway, E.A. Howard, C.J. Kucharik, C. Monfreda, J.A. Patz, I.C. Prentice, N. Ramankutty and P.K. Snyder. 2005. Global consequences of land use. Science 309: 570-574.

Foody, G.M. 2002. Status of land cover classification accuracy assessment. Remote Sensing of Environment 80: 185-201.

Ghulam, A., Q. Qin, L. Zhu and P. Abdrahman. 2004. Satellite remote sensing of groundwater : quantitative modelling and uncertainty reduction using 6S atmospheric simulations. International Journal of Remote Sensing 25: 5509-5524.

Gu, W., R. Heikkilä and I. Hanski. 2002. Estimating the consequences of habitat fragmentation on extinction risk in dynamic landscapes. Landscape Ecology 17: 699-710.

Guindon, B., Y. Zhang and C. Dillabaugh. 2004. Landsat urban mapping based on a combined spectral-spatial methodology. Remote Sensing of Environment 92: 218-232.

Haralick, R.M. 1979. Statistical and Structural Approaches to Texture. Proceedings of the IEEE 47: 786-804.

Haralick, R.M. and K-S Fu. 1983. Pattern Recognition and Classification. *IN* J.E. Estes and G.A. Thorley (eds). Manual of Remote Sensing: Second Edition. Falls Church, Virginia. The Sheridan Press. (793- 801). 2440 p.

Janzen, D.T., A.L. Fredeen and R.D. Wheate. 2006. Radiometric corrections techniques and accuracy assessment for Landsat TM data in remote forested regions. Canadian Journal of Remote Sensing 32: 330-340.

Jensen, J. R. 2005. Introductory Digital Image Processing: A Remote Sensing Perspective. New Jersey: Pearson Prentice Hall. 526 p.

Johnson, R.D. and E.S. Kasischke. 1997. Change vector analysis: a technique for the multispectral monitoring of land cover and condition. International Journal of Remote Sensing 19: 411-426.

Laliberte, A.S., A. Rango, K.M. Havstad, J.F. Paris, R.F. Beck, R. McNeely and A.L. Gonzalez. 2004. Object-oriented image analysis for mapping shrub encroachment from 1937 to 2003 in southern New Mexico. Remote Sensing of Environment 93: 198-210.

Lillesand, T. M., R.W. Kiefer and J.W. Chipman. 2004. Remote Sensing and Image Interpretation. New York: John Wiley & Sons, Inc. 763 p.

Lindborg, R. and O. Eriksson. 2004. Historical landscape connectivity affects present plant species diversity. Ecology 85: 1840-1845.

Lira, J., A. Morales and F. Zamora. 1999. Study of sediment distribution in the area of the Panuco river plume by means of remote sensing. International Journal of Remote Sensing 18: 171-182.

Lo, C.P., D.A. Quattrochi and J.C. Luvall. 1997. Application of high-resolution thermal infrared remote sensing and GIS to assess the urban heat island effect. International Journal of Remote Sensing 182: 287-304.

Loreau, M., N. Mouquet and R.D. Holt. 2003. Meta-ecosystems: a theoretical framework for a spatial ecosystem ecology. Ecology Letters 6: 673-679.

Lu, D., P. Mausel, M. Batistella and E. Moran. 2005. Land-cover binary change detection methods for use in the moist tropical region of the Amazon: a comparative study. International Journal of Remote Sensing 26: 101-114.

Lu, D., P.Mausel, E. Brondizios and E. Moran. 2004. Change detection techniques. International Journal of Remote Sensing 12: 2365-2407.

Lunetta, R.S. and C.D. Elvidge. 1998. Remote Sensing Change Detection: Environmental Monitoring Methods and Applications. Chelsea, Michigan: Ann Arbor Press. 318 p.

Mas, J.F. 1999. Monitoring land-cover changes: a comparison of change. International Journal of Remote Sensing 20: 139-152.

Milne, L.J. and M. Milne. 1960. The Balance of Nature. New York: Alfred A. Knopf. *IN* Wu, J. and O.L. Loucks. 1995. From balance of nature to hierarchical patch dynamics: a paradigm shift. The Quarterly Review of Biology 70: 439-466.

Mitcsh W.J. and J.G. Gosselink. 2000. Wetlands. New York: John Wiley. 920 p.

National Wetlands Working Group. 1997. The Canadian Wetland Classification System, Second Edition. Eds. B.G. Warner and C.D.A. Rubec. Wetlands Research Centre, University of Waterloo, Waterloo, Ontario.

Nelson, R.F. 1983. Detecting forest canopy change due to insect activity using Landsat MSS. *IN* An assessment of several linear change detection techniques for mapping forest mortality using multitemporal Landsat TM data. Collins, J.B. and Woodcock, C.E. 1995. Remote Sensing of the Environment 56: 66-77.

Pax-Lenney, M., C.E. Woodcock, S.A. Macomber, S. Gopal and C. Song. 2001. Forest mapping with a generalized classifier and Landsat TM data. Remote Sensing of Environment 77: 241-250.

Pimm, S.L. and P. Raven. 2000. Extinction by numbers. Nature 403: 843-845.

Prenzel, B.G. and P. Treitz. 2006. Spectral and spatial filtering for enhanced thematic change analysis of remotely sensed data. International Journal of Remote Sensing 27: 835-854.

Richter, R. 1996. Atmospheric correction of satellite data with haze removal including a haze/clear transition region. Computers & Geosciences 22: 675-681.

Richter, R. 1991. Error-bounds of a fast atmospheric correction algorithm for the Landsat thematic mapper and multispectral scanner bands. Applied Optics 30: 4412-4417.

Schroeder, T.A., W.B. Cohen, C. Song, M.J. Canty and Z,Yang. 2006. Radiometric correction of multi-temporal Landsat data for characterization of early successional forest patterns in western Oregon. Remote Sensing of Environment 103: 16-26.

Singh, A. 1989. Digital change detection techniques using remotely sensed data. International Journal of Remote Sensing 10: 989-1003.

Song, C., C.E. Woodcock, K.C. Seto, M. Pax-Lenney and S.A. Macomber. 2001. Classification and change detection using Landsat TM data: When and how to correct atmospheric effects? Remote Sensing of Environment 75: 230-244.

Tilman, D., J. Fargione, B.Wolff, C. D'Antonio, A. Dobson, R. Howarth, D. Schindler, W.H. Schlesinger, D. Simberloff and D. Swackhamer. 2001. Forecasting Agriculturally Driven Global Environmental Change. Science 292: 281-284.

Thompson, I.D. 2000. Forest Vegetation of Ontario. *IN* A.H Perera, D.L. Euler and I.D. Thompson (eds). Ecology of a Managed Terrestrial Landscape: Patterns and Process of Forest Landscapes in Ontario. Vancouver; British Columbia: University of British Columbia Press. (54-73) 336 p.

Turner, M.G., R.H. Gardner and R.V. O'Neill. 2001. Landscape Ecology in Theory and Practice: Pattern and Process. New York: Springer. 401 p.

Vermote, E. F., D. Tanré, J.L. Deuzé, M. Herman and J-J. Morcrette. 1997. Second simulation of the satellite signal in the solar spectrum, 6S: an overview. IEEE Transactions on Geoscience and Remote Sensing 35: 675-686.

Virk, R. and D. King. 2007. Comparison techniques for forest change mapping using Landsat data in Karnataka, India. Geocarto International 21: 49-57.

Voogt, J.A. and T.R. Oke. 2003. Thermal remote sensing of urban climates. Remote Sensing of Environment 86: 370-384.

Wu, J. 1999. Hierarchy and scaling: extrapolating information along a scaling ladder. Canadian Journal of Remote Sensing 25: 367-380.

Wu, J. and O.L. Loucks. 1995. From balance of nature to hierarchical patch dynamics: a paradigm shift. The Quarterly Review of Biology 70: 439-466.

Yan, G., J. F. Mas, B. H. P. Maathuis, Z. Xiangmin and P. M. Van Dijk. 2006. Comparison of pixel-based and object-oriented image classification approaches - a case study in a coal fire area, Wuda, Inner Mongolia, China. International Journal of Remote Sensing 27: 4039-4055.

Yu, Q., P. Gong, N. Clinton, G. Biging, M. Kelly and D. Schirokauer. 2006. Object-based detailed vegetation classification with airborne high spatial resolution remote sensing imagery. Photogrammetric Engineering & Remote Sensing 72: 799-811.

Yuan, D. and C. Elvidge. 1998. NALC Land Cover Change Detection Pilot Study: Washington D.C. Area Experiments. Remote Sensing of Environment 66: 166-178.

Zhang, Y and B. Guindon. 2005. Using Landsat data to assess land use conversion impacts arising from urbanization: the Canadian context. From the Proceedings of the ISPRS joint conference of the 3rd International Symposium Remote Sensing and Data Fusion Over Urban Areas (URBAN 2005) and the 5th International Symposium Remote Sensing of Urban Areas (URS 2005) Tempe, AZ, USA, March 14-16 2005.

Zhao, W., M. Tamura and H. Takahashi. 2000. Atmospheric and spectral correction for estimating surface albedo from satellite data using 6S code. Remote Sensing of Environment 76: 202-212.

APPENDIX I - IMAGE DATA AND PRE-PROCESSING/ANALYSIS.

Appendix I-A contains Table I-A1 which provides information regarding the exact position and the corresponding size in lines and pixels of each Landsat image from the overall research.

Table I-A1 - Landsat TM and MSS scene positions.

Year	Path	Row	Upper Left Latitude	Upper Left Longitude	Lower Right Latitude	Lower Right Longitude	Image Lines	Image Pixels
2005	16	28	46.98	-77.62	45.04	-74.50	7276	7938
	16	29	45.57	-78.15	43.65	-75.09	7281	7946
	15	28	47.00	-76.08	45.05	-73.05	7183	7839
	15	29	45.58	-76.56	43.64	-73.59	7188	7849
1995	16	28	47.00	-77.71	45.06	-74.67	7295	7730
	16	29	45.57	-78.16	43.65	-75.19	7295	7704
	15	28	47.01	-76.10	45.05	-73.16	7206	7607
	15	29	45.59	-76.58	43.68	-73.69	7209	7629
1984	16	28	46.98	-77.56	45.06	-74.54	7222	7689
	16	29	45.55	-78.04	45.59	-75.09	7225	7694
	15	28	47.01	-76.10	45.05	-73.16	7206	7607
	15	29	45.56	-76.44	43.64	-73.56	7136	7613
1975 *	17	28	47.06	-77.44	45.03	-74.25	3801	4075
	17	29	45.38	-77.58	43.37	-74.50	3806	4075
	16	28	47.01	-76.00	44.58	-75.58	3768	4064
	16	29	45.60	-76.54	43.57	-73.47	3774	4071

(*the difference in path/row designations is due to the higher orbit of Landsat 1)

Appendix I-B contains Figures I-B1a-b, I-B2a-b and I-B3a-b which present the mosaics produced from the four Landsat scenes, the thematic maps developed from the ISODATA unsupervised classification and examples of the travels routes selected using the thematic maps derived from the ISODATA unsupervised classification.

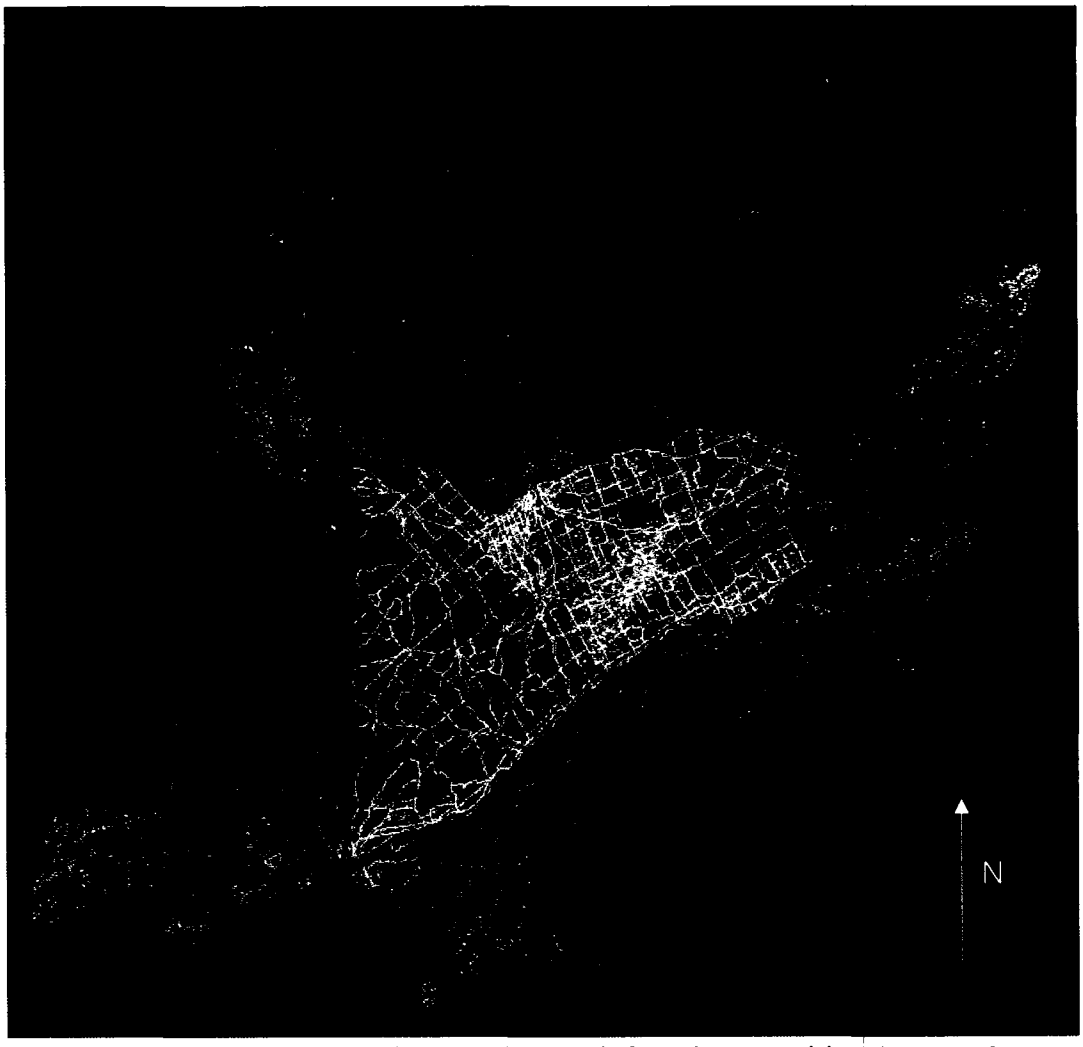

Figure I-B1a - Mosaic of 2005 scenes (colour infrared composition (NIR, red, green)).Yellow lines represent the Natural Resources of Canada road map (not co-registered).

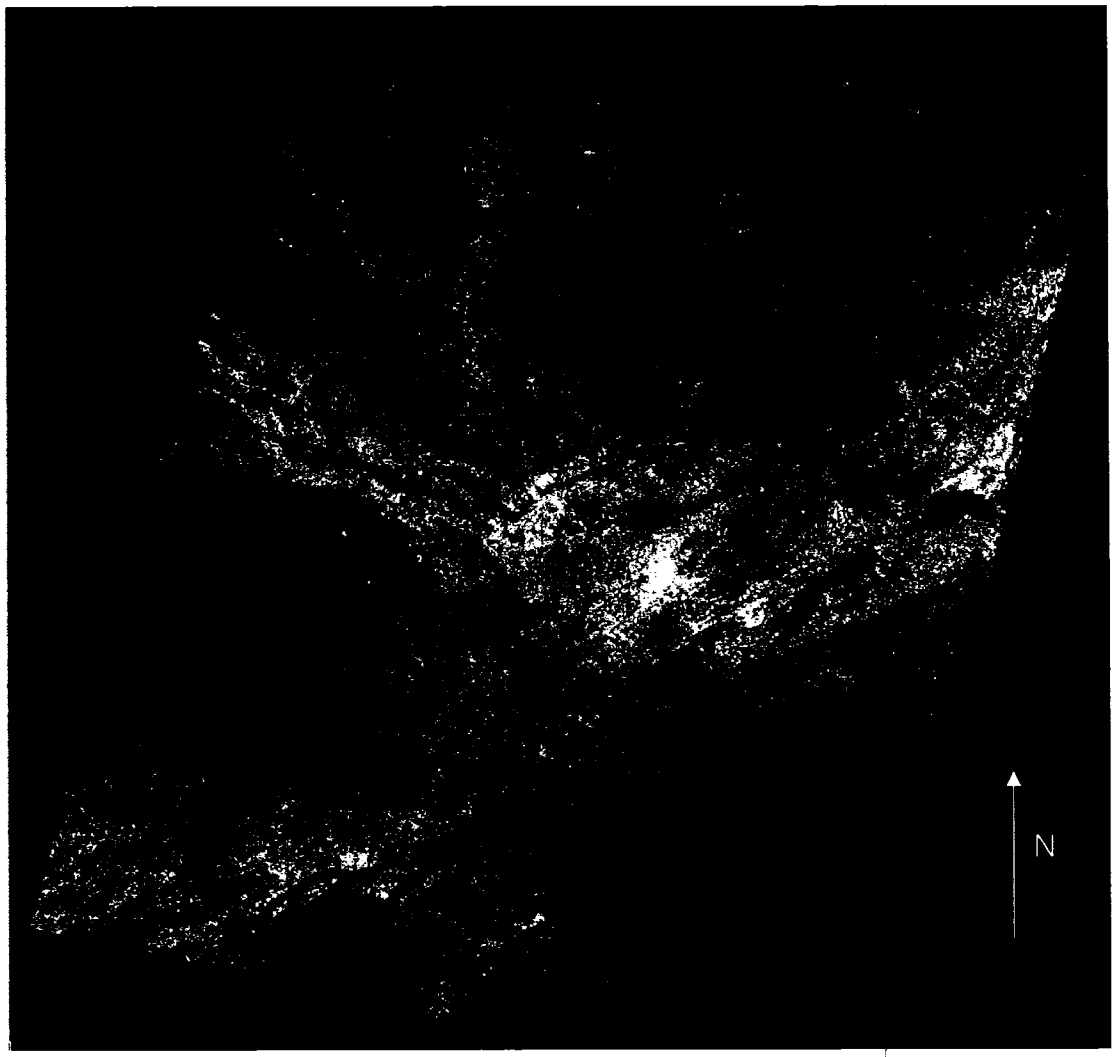

Figure I-B1b - Mosaic of 2005 scenes (true colour composition (red, green, blue)).

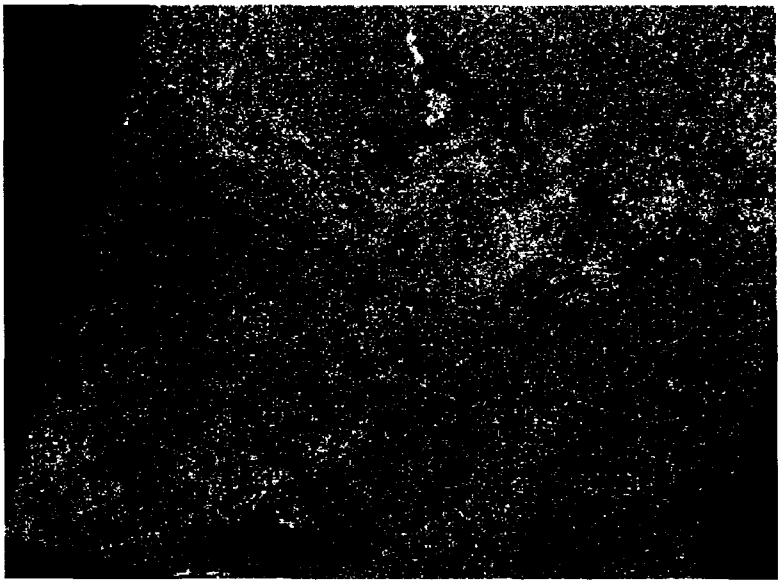

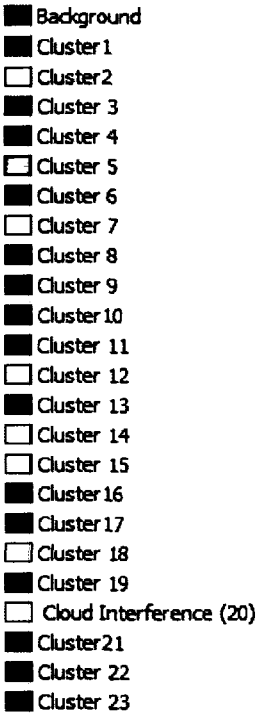

Figure I-B2a – ISODATA classification of 2005 mosaic (entire scene).

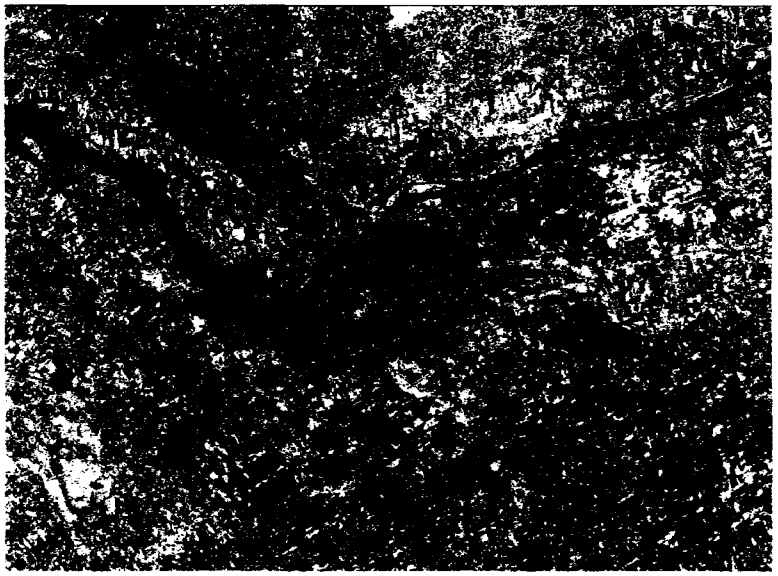

Figure I-B2b – ISODATA classification of 2005 mosaic (close-up on the Ottawa area).

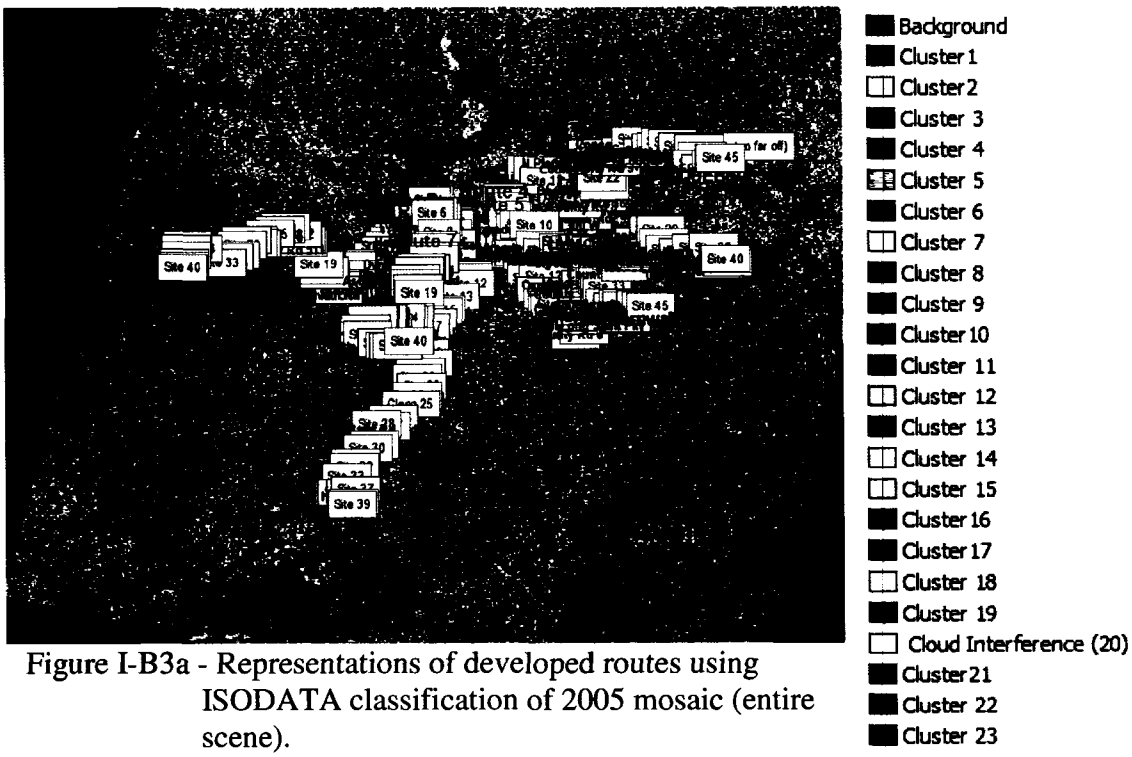

Figure I-B3a - Representations of developed routes using ISODATA classification of 2005 mosaic (entire scene).

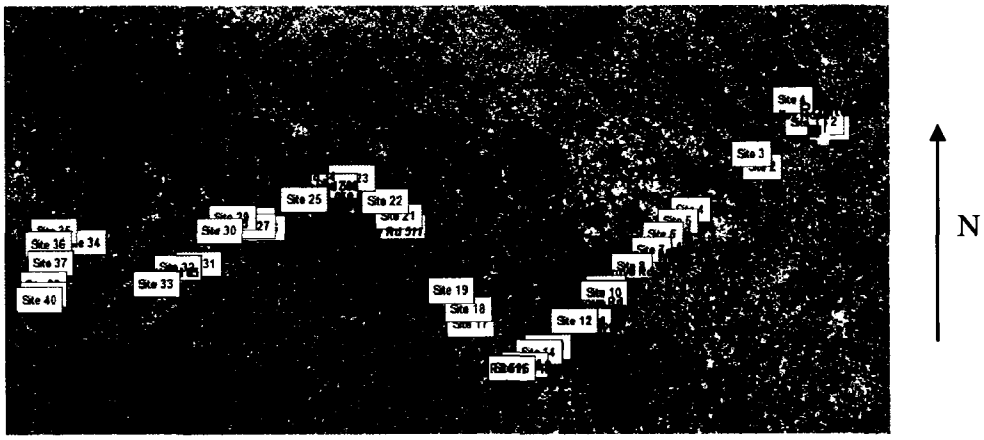

Figure I-B3b - Representation of one of the developed routes using ISODATA classification of 2005 mosaic.

Appendix I-C contains I-C1 and I-C2 which list the GCPs, CPs and individual point RMSE for the geometric registrations.

Table I-C1 – Registration of 2005 image to Natural Resources Canada Ontario road vector file: GCPs, CPs and individual point RMSE.

Point ID	RMSE	RMSE X	RMSE Y	Type	Map X	Map Y	2005 X	2005 Y
G0001	0.08	0.07	-0.04	GCP	1395.0	783.0	1395.1	783.0
G0002	0.07	0.00	0.07	GCP	428.0	4721.0	428.0	4721.1
G0003	0.07	0.06	-0.05	GCP	4968.0	1840.0	4968.1	1840.0
G0004	0.19	-0.07	0.18	GCP	3543.7	714.4	3543.7	714.6
G0005	0.17	-0.05	-0.16	GCP	2341.3	2029.3	2341.2	2029.1
C00A	0.13	0.11	-0.07	Check	1360.5	1239.5	1360.6	1239.4
C00B	0.10	0.05	0.08	Check	1610.5	2010.0	1610.6	2010.1
C00C	0.36	-0.35	0.06	Check	1072.5	3290.5	1072.1	3290.6
C00D	0.04	-0.02	-0.04	Check	2381.9	3296.7	2381.9	3296.7
C00E	0.05	0.00	-0.05	Check	1124.3	4149.2	1124.3	4149.2
C00F	0.05	0.04	0.02	Check	2885.6	368.0	2885.6	368.0
C00G	0.03	0.01	-0.03	Check	2602.1	1336.1	2602.1	1336.1
C00H	0.04	0.04	0.00	Check	4208.1	1461.6	4208.1	1461.6
C00I	0.32	-0.13	-0.30	Check	5193.5	845.5	5193.4	845.2
C00J	0.09	0.08	-0.04	Check	3472.2	2211.5	3472.3	2211. 5

Table I-C2 – Registration of 1995 image to aligned 2005 image: GCPs, CPs and individual point RMSE.

Point ID	RMSE	RMSE X	RMSE Y	Type	2005 X	2005 Y	1995 X	1995 Y
G0001	0.10	0.10	0.00	GCP	1644.0	789.0	1644.1	789.0
G0002	0.06	0.06	0.00	GCP	5251.0	1412.0	5251.1	1412.0
G0003	0.01	-0.01	0.00	GCP	1162.0	4427.0	1162.0	4427.0
G0004	0.04	-0.04	0.00	GCP	2614.0	1742.0	2614.0	1742.0
G0005	0.12	-0.12	0.00	GCP	3362.0	527.0	3361.9	527.0
C00A	0.31	-0.31	0.01	Check	1393.0	1455.0	1392.7	1455.0
C00B	0.03	0.03	0.00	Check	2658.4	921.0	2658.4	921.0
C00C	0.03	0.03	0.01	Check	2091.7	1834.0	2091.7	1834.0
C00D	0.13	-0.13	0.00	Check	4178.0	1072.0	4177.9	1072.0
C00E	0.23	-0.23	0.01	Check	5182.0	1888.0	5181.8	1888.0
C00F	0.30	0.30	0.01	Check	3657.0	1820.0	3657.3	1820.0
C00G	0.11	-0.11	0.00	Check	2294.0	1696.0	2293.9	1696.0
C00H	0.10	0.10	-0.03	Check	1162.0	2423.0	1162.1	2423.0
C00I	0.23	-0.23	0.01	Check	1941.0	3493.0	1940.8	3493.0
C00J	0.05	0.05	0.01	Check	3096.7	2489.0	3096.7	2489.0

APPENDIX II – ATMOSPHERIC CORRECTIONS.

Appendix II-A contains information about the calibration values and haze values used for the DOS atmospheric correction method. Additionally, this appendix presents the parameters used for the ATCOR2 atmospheric correction method.

Table II-A1 - 2005 calibration values for Landsat 5 TM after May 4, 2003 (Chander and Markham, 2003).

Qcal	Qcal min	Qcal max	LMAX	LMIN
1	0	254	193.000	-1.5200
2	0	254	365.000	-2.8400
3	0	254	264.000	-1.1700
4	0	254	221.000	-1.5100
5	0	254	30.200	-0.3700
6	0	162	15.303	1.2378
7	0	254	16.500	-0.1500

Table II-A2 - Haze values derived for each band for 2005 imagery.

Band	Function value (very clear atmosphere)	Starting haze value (after conversion to at-satellite radiance)	Haze value (per band, LHaze)
1* (selected as histogram band)	1.000	* 33 =	33
2	0.563		18.579
3	0.292		9.636
4	0.117		3.861
5	0.075		2.475
7	0.002		0.066

Table II-A3 - 1995 calibration values for Landsat 5 – TM March 1, 1984 to May 4, 2003 (Chander and Markham, 2003).

Qcal	Qcal min	Qcal max	LMAX	LMIN
1	0	254	152.000	-1.5200
2	0	254	296.810	-2.8400
3	0	254	204.300	-1.1700
4	0	254	206.200	-1.5100
5	0	254	27.190	-0.3700
6	0	166	15.303	1.2378
7	0	254	14.380	-0.1500

Table II-A4 - Haze values derived for each band for 1995 imagery.

Band	Function value (very clear atmosphere)	Starting haze value (after conversion to at-satellite radiance)	Haze value (per band, LHaze)
1* (selected as histogram band)	1.00		26.28000
2	0.563		14.79564
3	0.292	* 26.28 =	7.673760
4	0.117		3.074760
5	0.075		1.97100
7	0.002		0.05256

Table II-A5 - Parameters used for ATCOR2 algorithm.

Scene	Elevation (Constant)	Sensor Information			Atmospheric Information			Solar Zenith Angle	Visibility*
		Pixel	Date	Calibration File (constant)	Area	Condition	Thermal Condition		
2005_ 1529	0.2 km	30 m	Sept 6	TM_standard	Rural	Mid-latitude Summer	Mid-latitude Summer	47.49°	24.1 km
1995_ 1529	0.2 km	30 m	Aug 10	TM_standard	Rural	Mid-latitude Summer	Mid-latitude Summer	49.12°	24.1 km

*from http://www.weatheroffice.ec.gc.ca/canada_e.html

Appendix II-B contains Table II-B1 which provides the dark and light objects selected for the PIF relative correction. Tables II-B2 to II-B9 list average brightness values and Figures II-B1a-g to II-B6a-g show the regressions with equations and R^2 values for the relative calibrations performed on the DOS and ATCOR2 corrected scenes.

Table II-B1 - Pseudo-invariant features used for relative corrections.

	Easting	Northing	Feature
Dark 1	521818.2510000	5010716.1140000	Lake
Dark 2	528221.9330000	5017100.8690000	Lake
Dark 3	445136.9700000	5027035.7100000	Lake
Dark 4	433680.0980000	5037508.3460000	Lake
Dark 5	426829.6880000	4994296.8750000	Lake
Dark 6	440366.2500000	4971020.6250000	Lake
Dark 7	430268.9740000	4936238.2580000	Lake
Dark 8	434757.5360000	4961383.9640000	Lake
Dark 9	514367.5320000	4988900.4910000	Lake
Dark 10	419893.1250000	4978436.2500000	Lake
Light 1	436526.6530830	5014011.6433400	Quarry
Light 2	445767.8576210	5023932.4330700	Sandy Beach
Light 3	437190.0550000	5023769.1530000	Sandy Beach
Light 4	479563.6660000	5029148.1010000	Sand Pit
Light 5	450356.2500000	5029855.3130000	Intersection
Light 6	447894.3860000	5018269.6580000	Runway
Light 7	449865.4520000	5034347.9140000	Runway
Light 8	447949.6880000	5024266.8750000	Intersection
Light 9	446635.3080000	5027639.4090000	Parking Lot
Light 10	436789.6880000	5021806.8750000	Shopping Mall

Table II-B2 – 2005_1529 DOS reference values.

	# of Samples	Band 1	Band 2	Band 3	Band 4	Band 5	Band 6	Band 7
Dark 1	16	24.93750	29.75000	21.25000	20.87500	0.00000	34.00000	0.00000
Dark 2	6	14.00000	11.00000	12.50000	16.00000	0.00000	37.00000	0.00000
Dark 3	6	32.50000	22.50000	17.00000	18.00000	0.00000	35.00000	0.00000
Dark 4	4	27.25000	18.50000	10.75000	17.50000	0.00000	34.75000	0.00000
Dark 5	5	16.80000	17.00000	14.80000	29.40000	0.00000	37.00000	0.00000
Dark 6	6	9.50000	5.50000	8.00000	11.00000	0.00000	37.00000	0.00000
Dark 7	12	13.25000	11.41667	3.75000	6.25000	0.00000	37.00000	0.00000
Dark 8	82	10.13415	9.43902	6.45122	5.53659	0.00000	37.00000	0.00000
Dark 9	15	41.40000	34.86667	25.60000	34.80000	0.00000	33.60000	0.00000
Dark 10	4	15.75000	16.00000	9.25000	10.00000	0.00000	37.00000	0.00000
Light 1	4	130.75000	136.75000	136.25000	139.75000	20.75000	40.00000	8.25000
Light 2	4	100.00000	121.00000	139.50000	165.75000	24.50000	37.00000	8.75000
Light 3	4	108.75000	160.00000	166.25000	166.00000	29.25000	37.00000	13.50000
Light 4	9	113.66667	141.33333	155.33333	135.55556	23.44444	37.00000	9.33333
Light 5	8	107.50000	113.50000	115.37500	115.00000	13.62500	40.00000	6.00000
Light 6	6	124.00000	127.50000	117.00000	105.16667	14.00000	40.00000	6.00000
Light 7	5	97.00000	106.40000	104.60000	116.80000	18.20000	40.00000	6.00000
Light 8	4	107.75000	112.50000	112.25000	99.75000	11.75000	40.00000	6.00000
Light 9	6	120.33333	143.50000	133.33333	141.83333	22.16667	40.00000	9.50000
Light 10	6	146.33333	162.50000	173.50000	129.83333	18.50000	40.00000	7.00000

Table II-B3 – 2005_1529 ATCOR2 reference values.

	# of Samples	Band 1	Band 2	Band 3	Band 4	Band 5	Band 6	Band 7
Dark 1	16	3.43750	11.93750	7.12500	2.62500	5.93750	75.00000	4.37500
Dark 2	6	0.00000	0.00000	0.16667	0.00000	4.50000	91.00000	3.66667
Dark 3	6	5.66667	5.00000	2.66667	0.00000	3.16667	89.00000	2.83333
Dark 4	4	5.50000	5.75000	0.50000	0.00000	3.00000	86.50000	1.50000
Dark 5	5	0.00000	4.00000	2.40000	4.60000	6.80000	102.00000	2.00000
Dark 6	6	0.00000	0.00000	0.00000	0.00000	0.00000	95.33333	0.00000
Dark 7	12	0.08333	1.83333	0.00000	0.00000	0.00000	99.00000	0.33333
Dark 8	82	0.00000	1.57317	0.08537	0.00000	0.03659	96.00000	0.18293
Dark 9	15	12.86667	14.80000	9.73333	14.00000	12.33333	58.60000	9.13333
Dark 10	4	0.00000	3.25000	0.25000	0.00000	0.50000	94.00000	0.00000
Light 1	4	49.25000	56.50000	63.50000	100.25000	111.25000	132.50000	104.00000
Light 2	4	33.00000	50.00000	70.25000	123.75000	128.75000	113.00000	117.50000
Light 3	4	37.00000	74.00000	87.50000	130.00000	147.75000	117.00000	151.00000
Light 4	9	41.33333	61.11111	78.55556	92.22222	121.66667	102.00000	119.22222
Light 5	8	32.37500	40.62500	47.62500	81.37500	82.25000	129.00000	72.37500
Light 6	6	42.33333	48.50000	48.16667	70.83333	81.33333	132.66667	73.33333
Light 7	5	29.00000	39.20000	44.40000	84.00000	103.00000	125.20000	87.20000
Light 8	4	35.00000	41.25000	47.75000	65.25000	77.00000	139.50000	72.00000
Light 9	6	44.33333	62.83333	62.66667	104.83333	116.33333	124.00000	117.83333
Light 10	6	60.33333	73.66667	90.00000	91.50000	101.66667	132.00000	92.83333

Table II-B4 – *1995_1529* DOS pre-calibration values.

	# of Samples	Band 1	Band 2	Band 3	Band 4	Band 5	Band 6	Band 7
Dark 1	16	13.3125	15.0000	6.1250	6.0000	0.0000	37.0000	0.0000
Dark 2	6	9.5000	7.0000	3.1667	7.0000	0.0000	37.0000	0.0000
Dark 3	6	25.6667	20.5000	10.0000	11.0000	0.0000	37.0000	0.0000
Dark 4	4	18.7500	14.2500	5.0000	12.0000	0.0000	37.0000	0.0000
Dark 5	5	21.0000	20.4000	15.8000	42.0000	0.0000	37.0000	0.0000
Dark 6	6	18.0000	14.5000	8.5000	10.5000	0.0000	37.0000	0.0000
Dark 7	12	21.4167	16.5000	6.0000	9.7500	0.0000	37.0000	0.0000
Dark 8	82	17.8902	16.0976	8.3659	7.0610	0.0000	37.0000	0.0000
Dark 9	15	14.6000	10.6000	1.4000	5.4000	0.0000	37.0000	0.0000
Dark 10	4	20.2500	18.7500	10.2500	10.5000	0.0000	37.0000	0.0000
Light 1	4	113.2500	120.2500	107.2500	119.7500	19.7500	40.0000	7.5000
Light 2	4	82.7500	115.5000	119.5000	159.2500	23.5000	37.0000	9.0000
Light 3	4	82.0000	90.2500	84.2500	140.5000	26.5000	40.0000	9.0000
Light 4	9	86.0000	121.4444	118.4444	148.4444	28.0000	39.0000	8.6667
Light 5	8	88.2500	96.2500	83.8750	115.3750	12.6250	40.0000	3.0000
Light 6	6	78.5000	80.6667	69.1667	77.3333	8.0000	43.0000	2.0000
Light 7	5	79.0000	87.4000	79.0000	129.0000	16.6000	40.0000	6.0000
Light 8	4	89.2500	93.7500	83.2500	93.2500	12.0000	43.0000	5.0000
Light 9	6	130.8333	129.8333	112.0000	149.5000	21.1667	41.0000	7.0000
Light 10	6	102.5000	113.3333	98.0000	99.1667	10.5000	42.0000	3.3333

Table II-B5 – 1995_1529 DOS 1st calibration (new values).

	# of Samples	Band 1	Band 2	Band 3	Band 4	Band 5	Band 6	Band 7
Dark 1	16	16.37500	19.00000	13.50000	13.00000	0.00000	36.00000	0.00000
Dark 2	6	12.00000	9.16667	9.50000	14.00000	0.00000	36.00000	0.00000
Dark 3	6	31.00000	26.33333	18.66667	18.00000	0.00000	36.00000	0.00000
Dark 4	4	22.75000	18.00000	12.00000	19.00000	0.00000	36.00000	0.00000
Dark 5	5	25.00000	26.20000	26.40000	48.20000	0.00000	36.00000	0.00000
Dark 6	6	21.83333	18.33333	16.66667	17.50000	0.00000	36.00000	0.00000
Dark 7	12	25.58333	21.00000	13.33333	16.75000	0.00000	36.00000	0.00000
Dark 8	82	21.68293	20.46341	16.48780	14.06098	0.00000	36.00000	0.00000
Dark 9	15	17.73333	13.60000	7.06667	12.40000	0.00000	36.00000	0.00000
Dark 10	4	24.25000	24.00000	19.00000	17.50000	0.00000	36.00000	0.00000
Light 1	4	135.00000	148.50000	147.75000	125.00000	20.00000	38.00000	9.00000
Light 2	4	98.75000	142.75000	164.00000	164.25000	24.00000	36.00000	10.75000
Light 3	4	98.00000	111.50000	117.00000	145.50000	27.25000	38.00000	10.50000
Light 4	9	102.55556	149.88889	162.55556	153.44444	29.00000	37.33333	10.33333
Light 5	8	105.37500	118.87500	116.87500	121.12500	12.62500	38.00000	3.25000
Light 6	6	93.66667	99.50000	97.33333	83.33333	8.00000	40.00000	2.00000
Light 7	5	94.20000	108.00000	110.60000	134.40000	16.60000	38.00000	7.00000
Light 8	4	106.75000	115.75000	116.25000	99.25000	12.00000	40.00000	5.75000
Light 9	6	147.83333	150.33333	147.66667	154.00000	21.50000	38.66667	8.33333
Light 10	6	122.50000	140.00000	135.66667	104.83333	10.50000	39.33333	3.66667

Table II-B6 – 1995_1529 DOS 2nd calibration (Final values).

	# of Samples	Band 1	Band 2	Band 3	Band 4	Band 5	Band 6	Band 7
Dark 1	16	16.37500	19.00000	13.50000	13.00000	0.00000	36.00000	0.00000
Dark 2	6	12.00000	9.16667	9.50000	14.00000	0.00000	36.00000	0.00000
Dark 3	6	31.00000	26.33333	18.66667	18.00000	0.00000	36.00000	0.00000
Dark 4	4	22.75000	18.00000	12.00000	19.00000	0.00000	36.00000	0.00000
Dark 5	5	25.00000	26.20000	26.40000	48.20000	0.00000	36.00000	0.00000
Dark 6	6	21.83333	18.33333	16.66667	17.50000	0.00000	36.00000	0.00000
Dark 7	12	25.58333	21.00000	13.33333	16.75000	0.00000	36.00000	0.00000
Dark 8	82	21.68293	20.46341	16.48780	14.06098	0.00000	36.00000	0.00000
Dark 9	15	17.73333	13.60000	7.06667	12.40000	0.00000	36.00000	0.00000
Dark 10	4	24.25000	24.00000	19.00000	17.50000	0.00000	36.00000	0.00000
Light 1	4	135.00000	148.50000	147.75000	125.00000	20.00000	38.00000	9.00000
Light 2	4	98.75000	142.75000	164.00000	164.25000	24.00000	36.00000	10.75000
Light 3	4	98.00000	111.50000	117.00000	145.50000	27.25000	38.00000	10.50000
Light 4	9	102.55556	149.88889	162.55556	153.44444	29.00000	37.33333	10.33333
Light 5	8	105.37500	118.87500	116.87500	121.12500	12.62500	38.00000	3.25000
Light 6	6	93.66667	99.50000	97.33333	83.33333	8.00000	40.00000	2.00000
Light 7	5	94.20000	108.00000	110.60000	134.40000	16.60000	38.00000	7.00000
Light 8	4	106.75000	115.75000	116.25000	99.25000	12.00000	40.00000	5.75000
Light 9	6	147.83333	150.33333	147.66667	154.00000	21.50000	38.66667	8.33333
Light 10	6	122.50000	140.00000	135.66667	104.83333	10.50000	39.33333	3.66667

Table II-B7 – 1995_1529 ATCOR2 pre-calibration values.

	# of Samples	Band 1	Band 2	Band 3	Band 4	Band 5	Band 6	Band 7
Dark 1	16	0.00000	9.00000	5.87500	0.00000	0.12500	109.62500	0.43750
Dark 2	6	0.00000	0.33333	0.50000	0.00000	0.00000	111.00000	0.33333
Dark 3	6	0.00000	3.83333	3.83333	0.00000	0.00000	113.00000	0.00000
Dark 4	4	0.00000	6.50000	4.00000	0.00000	2.25000	104.00000	0.75000
Dark 5	5	0.00000	6.60000	9.80000	18.60000	11.40000	110.00000	6.20000
Dark 6	6	0.00000	3.00000	4.33333	0.00000	1.16667	108.00000	0.00000
Dark 7	12	0.00000	8.00000	4.66667	0.50000	0.41667	110.00000	0.75000
Dark 8	82	0.00000	10.06098	8.31707	1.37805	0.15854	107.62195	0.31707
Dark 9	15	0.00000	5.60000	2.20000	0.00000	0.00000	102.40000	0.40000
Dark 10	4	0.00000	8.75000	7.25000	0.00000	0.25000	110.00000	0.00000
Light 1	4	41.00000	61.00000	74.75000	92.25000	118.00000	134.75000	120.50000
Light 2	4	24.00000	64.25000	89.25000	125.50000	133.50000	126.50000	139.75000
Light 3	4	19.25000	43.00000	60.25000	115.50000	145.00000	140.00000	132.00000
Light 4	9	25.77778	64.11111	86.66667	113.44444	149.55556	130.00000	134.33333
Light 5	8	24.12500	44.75000	55.50000	89.12500	82.75000	151.00000	72.50000
Light 6	6	17.66667	34.16667	44.00000	54.66667	63.83333	161.00000	62.33333
Light 7	5	20.00000	40.80000	54.40000	102.20000	100.20000	147.00000	95.20000
Light 8	4	26.00000	43.75000	57.50000	69.50000	84.25000	164.00000	84.50000
Light 9	6	64.33333	71.66667	80.50000	120.50000	120.83333	159.33333	103.16667
Light 10	6	34.83333	56.83333	68.50000	74.83333	74.83333	166.66667	70.50000

Table II-B8 – 1995_1529 ATCOR2 1st calibration (new values).

	# of Samples	Band 1	Band 2	Band 3	Band 4	Band 5	Band 6	Band 7
Dark 1	16	58.25000	19.00000	11.43750	9.12500	8.81250	108.00000	4.81250
Dark 2	6	56.00000	16.33333	10.33333	10.33333	8.83333	108.33333	5.00000
Dark 3	6	64.16667	20.83333	13.50000	11.66667	9.33333	109.00000	5.33333
Dark 4	4	61.00000	18.75000	11.00000	12.00000	11.00000	107.00000	6.00000
Dark 5	5	62.60000	20.80000	14.60000	22.40000	18.20000	108.00000	8.80000
Dark 6	6	60.66667	18.83333	12.66667	11.50000	10.16667	108.00000	4.83333
Dark 7	12	62.50000	19.50000	11.33333	11.25000	9.25000	108.00000	5.33333
Dark 8	82	60.62195	19.36585	12.65854	10.32927	8.78049	108.00000	4.89024
Dark 9	15	58.66667	17.53333	9.53333	8.80000	8.60000	106.20000	5.06667
Dark 10	4	62.00000	20.25000	13.25000	11.50000	9.25000	108.00000	5.25000
Light 1	4	110.25000	47.50000	49.25000	52.00000	86.00000	116.50000	57.75000
Light 2	4	94.50000	46.25000	53.75000	66.00000	96.00000	114.25000	65.50000
Light 3	4	94.00000	39.25000	40.75000	59.00000	102.25000	118.50000	62.00000
Light 4	9	96.33333	47.66667	53.33333	62.22222	106.88889	115.00000	63.55556
Light 5	8	97.50000	40.87500	40.37500	49.87500	63.50000	122.00000	37.50000
Light 6	6	92.33333	36.66667	34.83333	35.83333	51.50000	126.00000	33.00000
Light 7	5	92.80000	38.40000	38.20000	55.20000	74.40000	120.40000	46.40000
Light 8	4	98.00000	40.00000	40.25000	41.75000	64.50000	127.00000	42.00000
Light 9	6	125.66667	50.83333	51.00000	63.00000	87.83333	125.00000	49.66667
Light 10	6	104.50000	45.33333	46.00000	43.66667	58.00000	127.66667	36.33333

Table II-B9 – 1995_1529 ATCOR2 2nd calibration (final values).

	# of Samples	Band 1	Band 2	Band 3	Band 4	Band 5	Band 6	Band 7
Dark 1	16	1.37500	5.00000	1.81250	0.00000	3.56250	90.00000	1.62500
Dark 2	6	0.16667	0.50000	0.50000	0.66667	3.50000	90.66667	2.00000
Dark 3	6	6.50000	8.66667	5.16667	3.33333	4.33333	92.00000	2.66667
Dark 4	4	4.00000	4.50000	1.00000	4.00000	6.25000	87.00000	4.00000
Dark 5	5	5.60000	8.60000	7.20000	26.40000	16.40000	90.00000	10.60000
Dark 6	6	3.66667	4.66667	3.83333	3.00000	5.33333	90.00000	1.66667
Dark 7	12	5.33333	6.00000	1.66667	2.50000	4.16667	90.00000	2.66667
Dark 8	82	3.62195	5.73171	3.78049	0.70732	3.50000	90.00000	1.78049
Dark 9	15	1.66667	2.06667	0.06667	0.00000	3.26667	85.40000	2.13333
Dark 10	4	5.00000	7.50000	4.75000	3.00000	4.25000	90.00000	2.50000
Light 1	4	47.00000	62.00000	71.00000	90.00000	114.50000	110.75000	117.25000
Light 2	4	33.50000	59.50000	79.00000	120.50000	129.00000	105.50000	134.25000
Light 3	4	33.00000	45.50000	55.50000	105.25000	137.75000	116.00000	126.50000
Light 4	9	35.11111	62.33333	78.33333	112.11111	144.33333	107.00000	129.88889
Light 5	8	36.12500	48.75000	54.62500	85.50000	82.00000	125.00000	72.87500
Light 6	6	31.66667	40.33333	44.50000	55.16667	64.50000	135.00000	63.33333
Light 7	5	32.00000	43.80000	50.80000	97.00000	97.80000	120.60000	92.40000
Light 8	4	36.25000	47.00000	54.25000	68.00000	83.50000	138.00000	82.75000
Light 9	6	61.00000	68.66667	74.00000	113.83333	117.16667	132.66667	99.66667
Light 10	6	42.00000	57.66667	64.83333	72.33333	74.16667	139.00000	70.33333

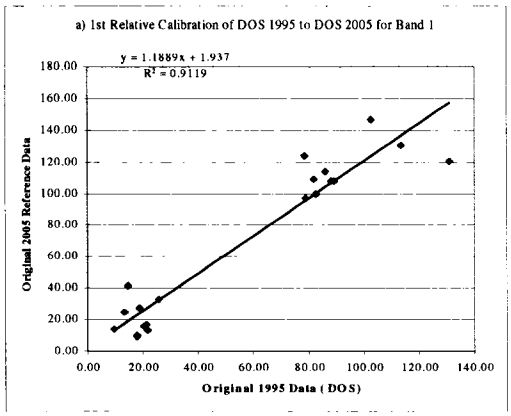

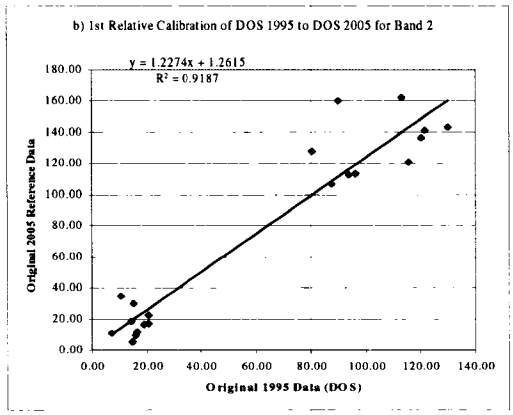

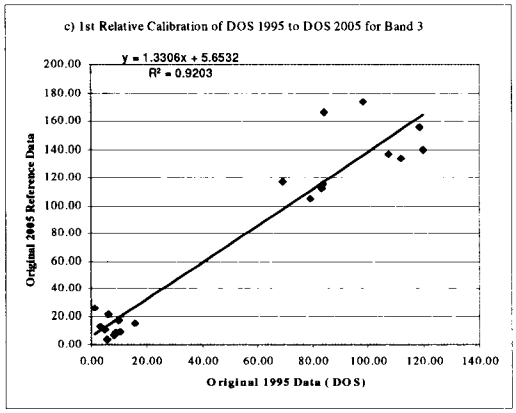

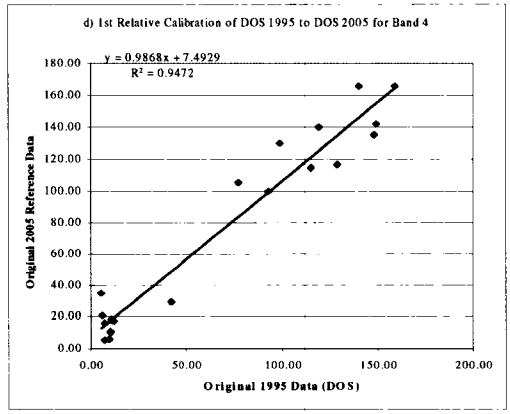

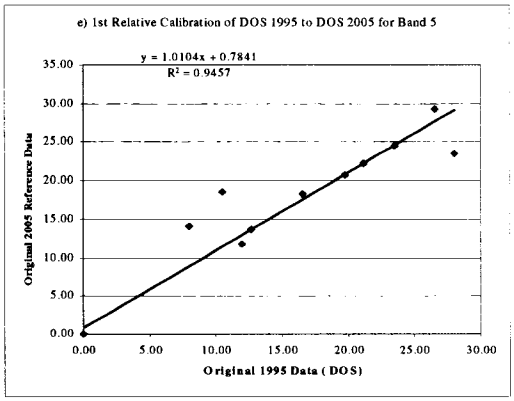

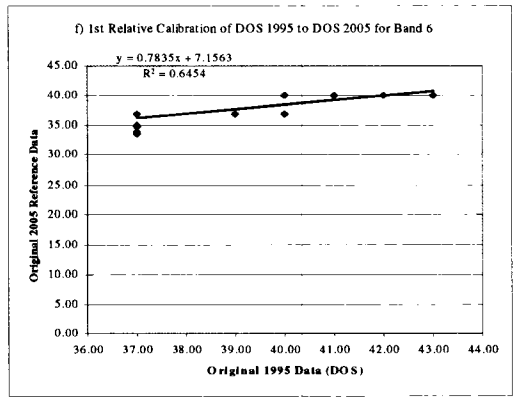

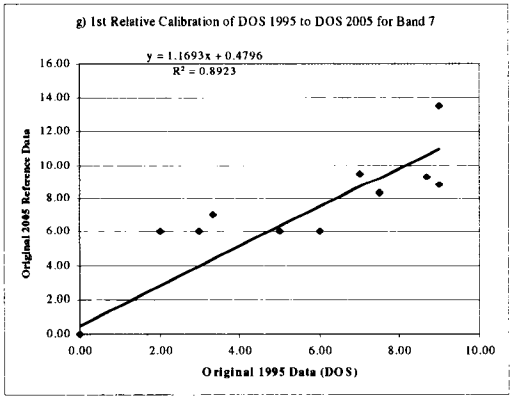

Figures II-B1a-g – Graphs of DOS corrected scenes relative calibration (1st regression).

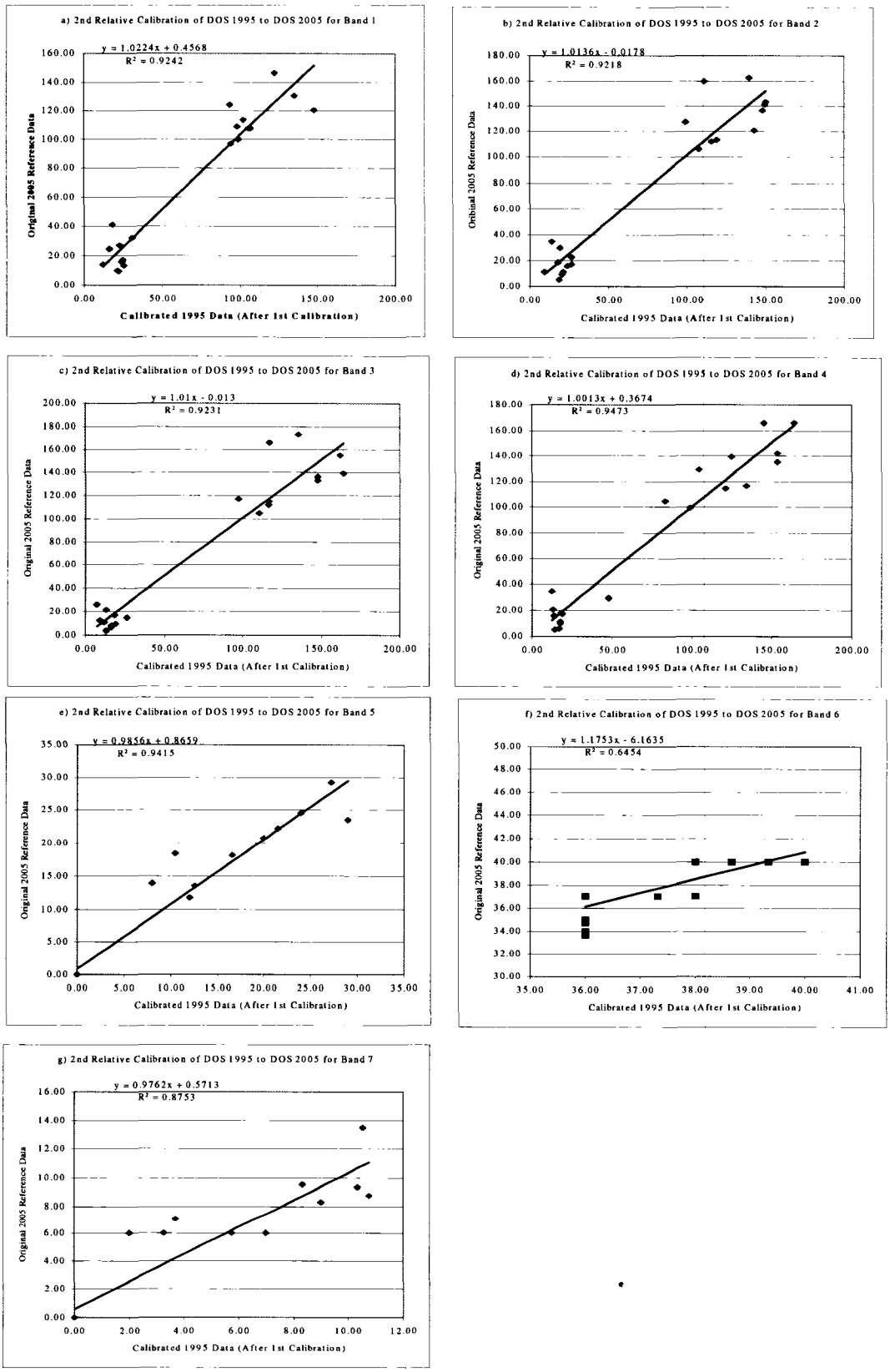

Figures II-B2a-g – Graphs of DOS corrected scenes relative calibration (2nd regression).

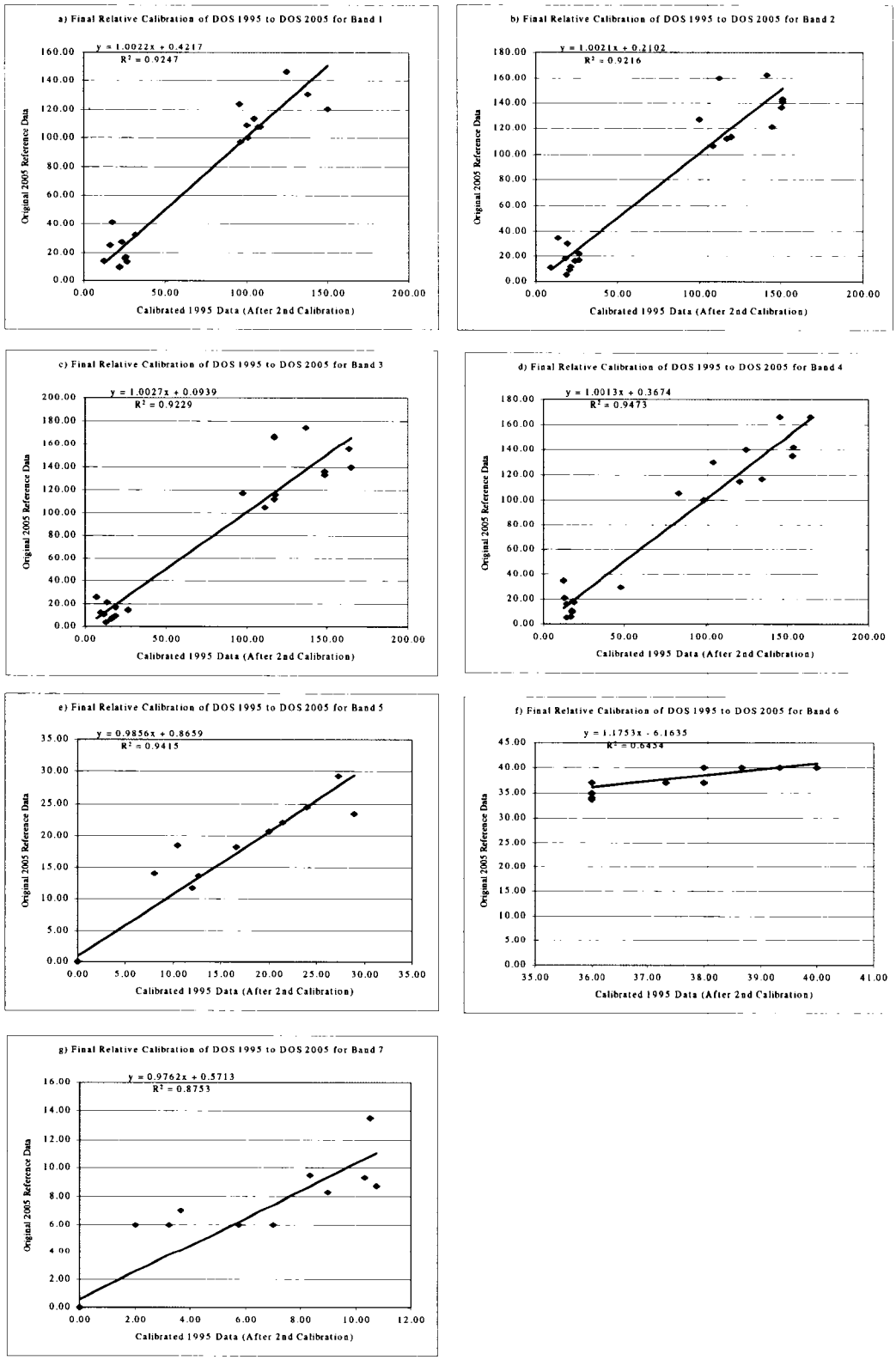

Figures II-B3a-g – Graphs of DOS corrected scenes relative calibration (final regression).

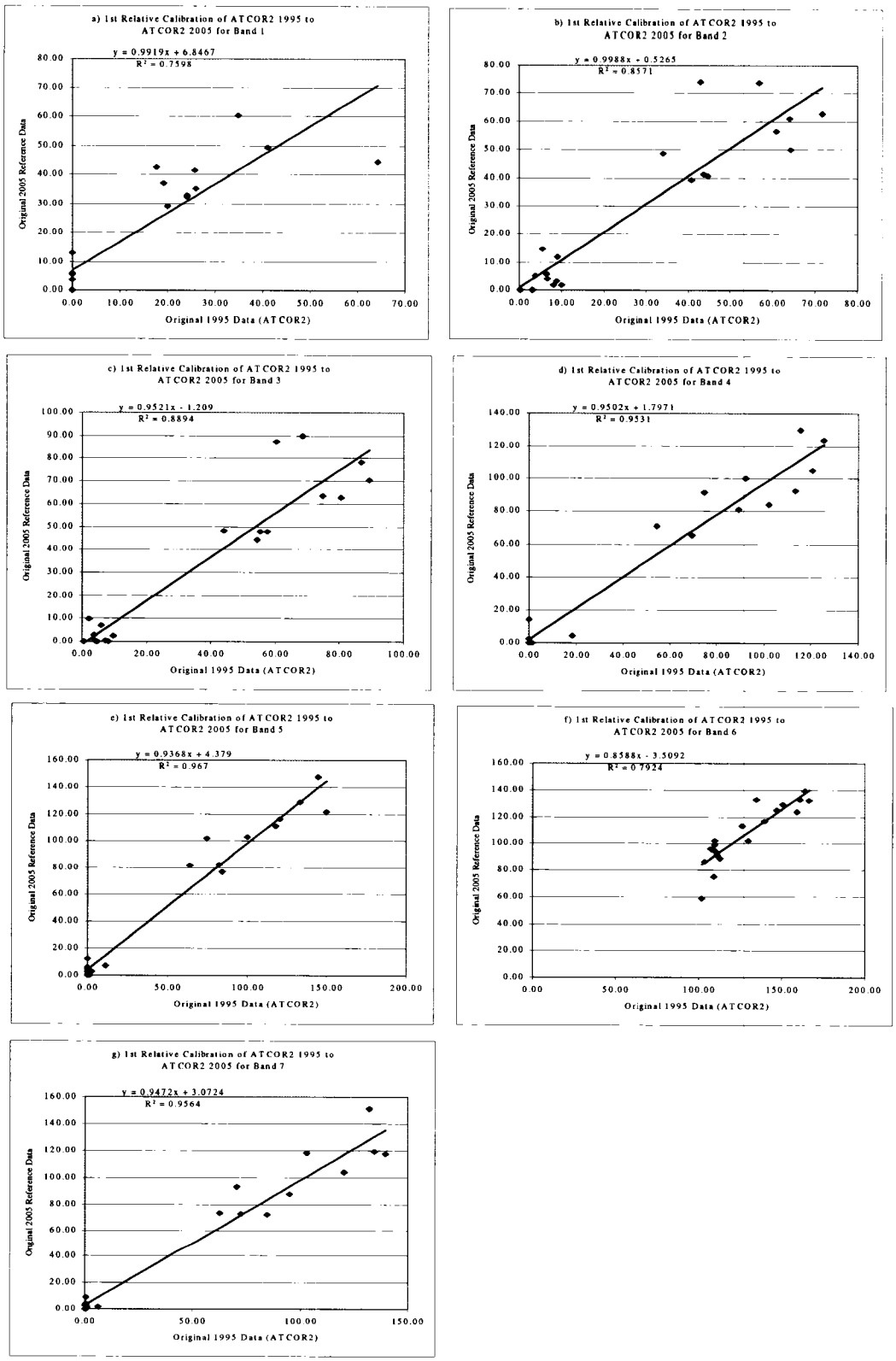

Figures II-B4a-g – Graphs of ATCOR2 corrected scenes relative calibration (1st regression).

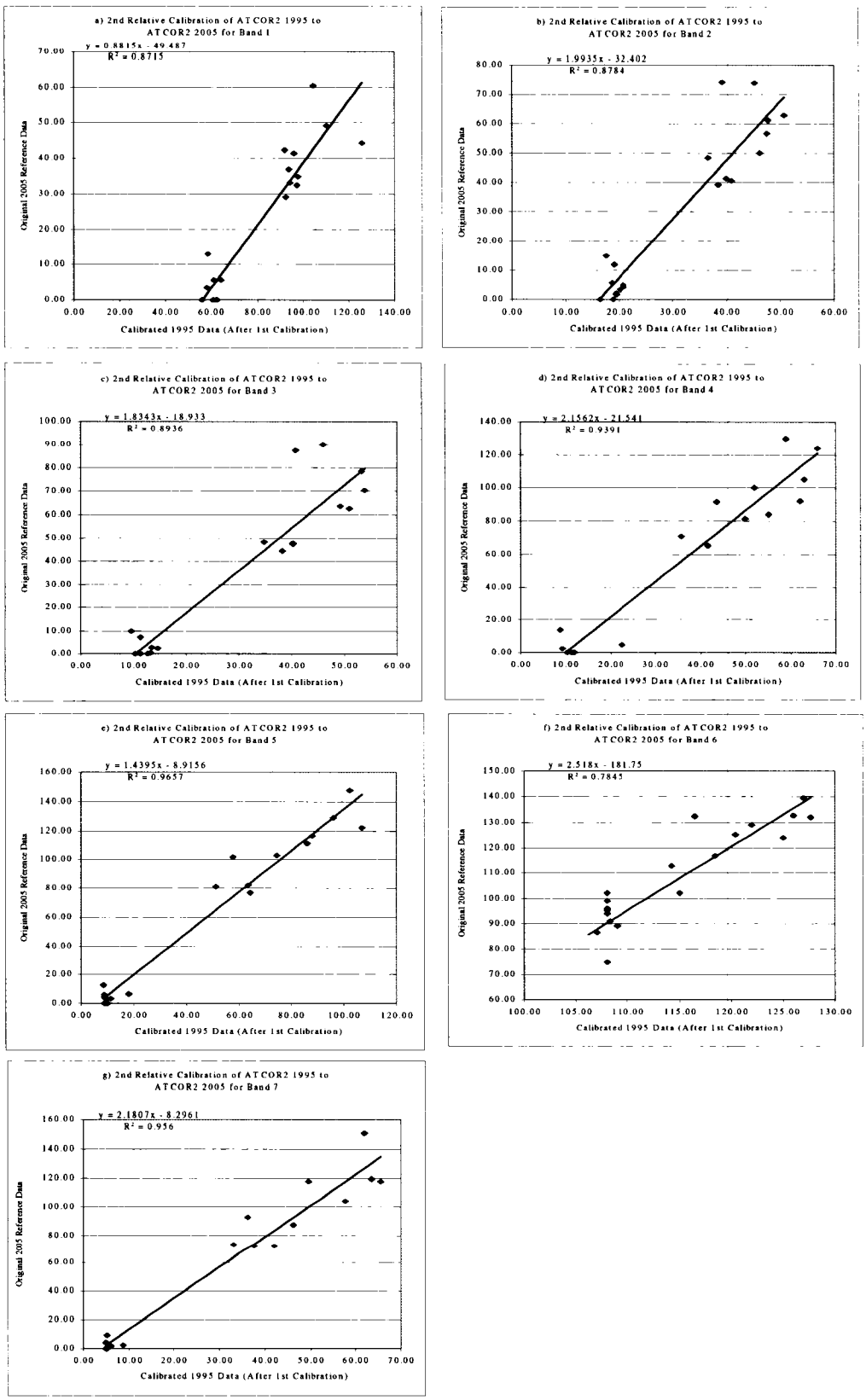

Figures II-B5a-g – Graphs of ATCOR2 corrected scenes relative calibration (2nd regression).

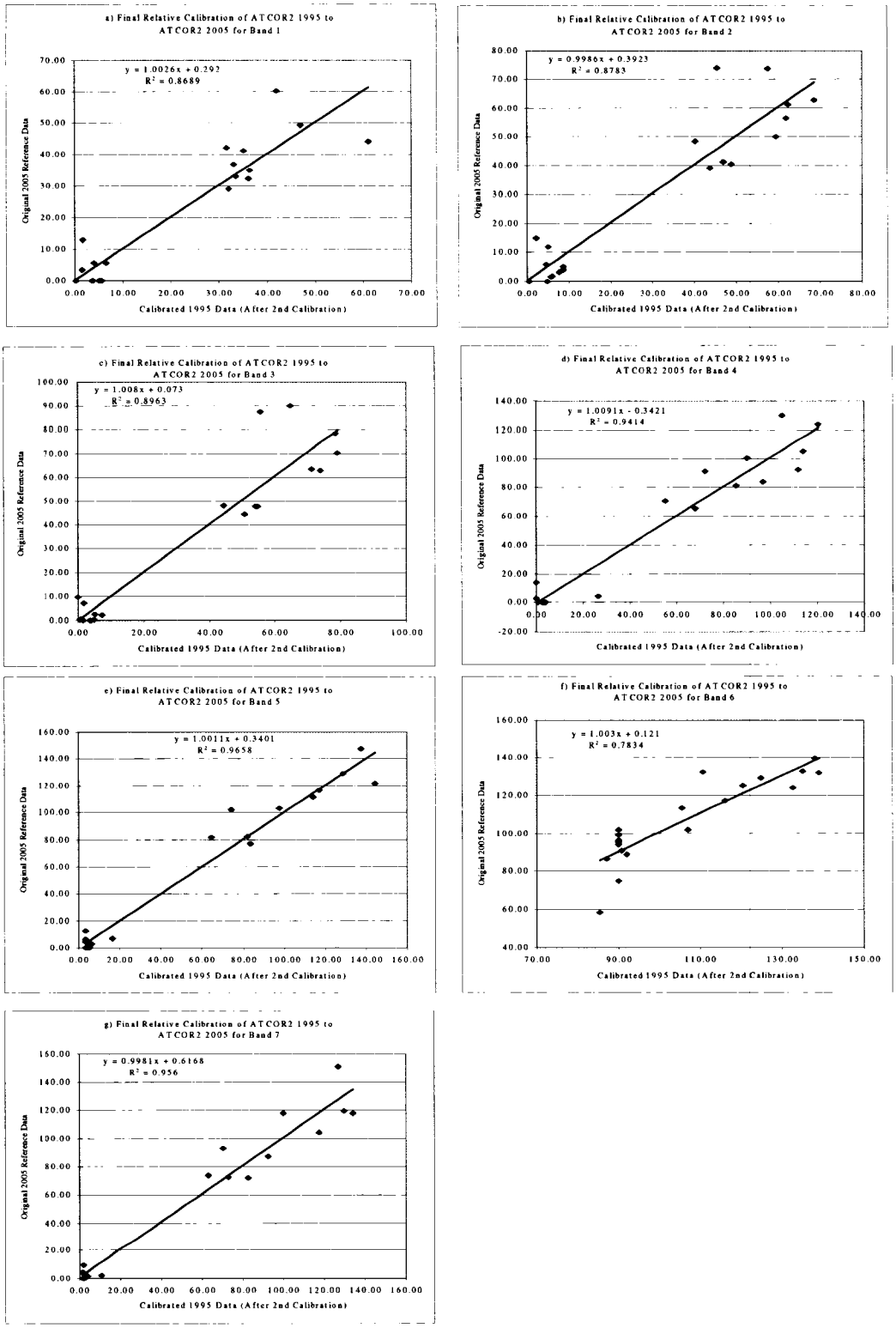

Figures II-B6a-g – Graphs of ATCOR2 corrected scenes relative calibration (final regression).

Appendix II-C presents tables of the assessments of the atmospheric corrections applied to 2005_1529 and 1995_1529. Based upon these results it was decided to only continue processing with the 2005_1529 DOS (scaled) and the 1995_1529 DOS (scaled, not relatively calibrated to 2005_1529).

Table II-C1a – Thematic map accuracy statistics for 2005_1529 with no atmospheric correction.

Overall Accuracy:	73.0%		
Overall Kappa:	0.66		
Class	Producer's Accuracy	User's Accuracy	Kappa Statistic
High Density Urban	76.2%	64.0%	0.60
Bare Rock	66.7%	50.0%	0.49
Coniferous	80.0%	66.7%	0.65
Deciduous / Mixed	48.3%	73.7%	0.70
Low Density Urban	82.6%	54.3%	0.49
Water	54.6%	100.0%	1.00
Wetlands	50.0%	55.6%	0.53
Agricultural Field 2	58.6%	81.0%	0.78
Agricultural Field 1	88.9%	83.7%	0.74
Bare Field	60.0%	75.0%	0.74

Table II-C1b - Thematic map accuracy statistics for 2005_1529 with ATCOR2 correction.

Overall Accuracy:	73.9%		
Overall Kappa:	0.67		
Class	Producer's Accuracy	User's Accuracy	Kappa Statistic
High Density Urban	76.2%	61.5%	0.58
Bare Rock	66.7%	100.0%	1.00
Coniferous	60.0%	66.7%	0.65
Deciduous / Mixed	48.2%	63.6%	0.58
Low Density Urban	73.9%	51.5%	0.46
Water	72.7%	100.0%	1.00
Wetlands	60.0%	75.0%	0.74
Agricultural Field 2	62.1%	90.0%	0.89
Agricultural Field 1	90.1%	83.0%	0.73
Bare Field	80.0%	80.0%	0.80

Table II-C1c - Thematic map accuracy statistics for 2005_1529 with DOS (scaled) correction.

Overall Accuracy:	75.7%		
Overall Kappa:	0.70		
Class Name:	Producer's Accuracy:	User's Accuracy	Kappa Statistic:
High Density Urban	76.2%	69.6%	0.66
Bare Rock	66.7%	66.7%	0.66
Coniferous	80.0%	66.7%	0.65
Deciduous / Mixed	62.1%	78.3%	0.75
Low Density Urban	87.0%	54.1%	0.49
Water	45.5%	100.0%	1.00
Wetlands	70.0%	50.0%	0.48
Agricultural Field 2	65.5%	82.6%	0.80
Agricultural Field 1	85.2%	90.8%	0.86
Bare Field	80.0%	80.0%	0.80

Table II-C2a - Thematic map accuracy statistics for 1995_1529 with DOS (scaled) correction then relatively (PIF) corrected.

Overall Accuracy:	76.1%		
Overall Kappa:	0.69		
Class	Producer's Accuracy	User's Accuracy	Kappa Statistic:
High Density Urban	55.0%	73.3%	0.70
Bare Rock	0.0%	0.0%	0.00
Coniferous	66.7%	75.0%	0.74
Deciduous / Mixed	100.0%	71.0%	0.67
Low Density Urban	68.2%	65.2%	0.61
Water	77.8%	100.0%	1.00
Wetlands	57.1%	50.0%	0.48
Agricultural Field 2	55.0%	52.4%	0.47
Agricultural Field 1	90.1%	88.0%	0.80
Bare Field	25.0%	100.0%	1.00

Table II-C2b - Thematic map accuracy statistics for 1995_1529 with DOS (scaled) correction and with no relative correction.

Overall Accuracy:	79.2%		
Overall Kappa:	0.73		
Class Name:	Producer's Accuracy:	User's Accuracy	Kappa Statistic:
High Density Urban	75.0%	78.9%	0.77
Bare Rock	100.0%	75.0%	0.75
Coniferous	66.7%	66.7%	0.65
Deciduous / Mixed	95.5%	72.4%	0.69
Low Density Urban	86.4%	61.3%	0.56
Water	77.8%	100.0%	1.00
Wetlands	42.9%	50.0%	0.48
Agricultural Field 2	50.0%	90.9%	0.90
Agricultural Field 1	87.7%	89.9%	0.83
Bare Field	25.0%	50.0%	0.49

Table II-C2c – Thematic map accuracy statistics for 1995_1529 with ATCOR2 correction and with a relative (PIF) correction.

Overall Accuracy:	77.7%		
Overall Kappa:	0.72		
Class Name:	Producer's Accuracy:	User's Accuracy	Kappa Statistic:
High Density Urban	55.0%	84.6%	0.83
Bare Rock	33.3%	33.3%	0.81
Coniferous	55.6%	100.0%	1.00
Deciduous / Mixed	90.9%	87.0%	0.85
Low Density Urban	81.8%	75.0%	0.72
Water	77.8%	92.9%	1.00
Wetlands	85.7%	35.3%	0.33
Agricultural Field 2	45.0%	50.0%	0.44
Agricultural Field 1	92.6%	88.2%	0.80
Bare Field	25.0%	50.0%	0.49

Table II-C2d – Thematic map accuracy statistics for 1995_1529 with ATCOR2 correction and without a relative (PIF) correction.

Overall Accuracy:	73.6%		
Overall Kappa:	0.66		
Class Name:	Producer's Accuracy:	User's Accuracy	Kappa Statistic:
High Density Urban	80.0%	61.5%	0.57
Bare Rock	100.0%	37.5%	0.37
Coniferous	55.6%	100.0%	1.00
Deciduous / Mixed	45.5%	90.9%	0.90
Low Density Urban	45.5%	47.6%	0.41
Water	77.8%	100.0%	1.00
Wetlands	14.3%	14.3%	0.11
Agricultural Field 2	80.0%	66.7%	0.63
Agricultural Field 1	95.0%	87.5%	0.79
Bare Field	0.0%	0.0%	0.00

APPENDIX III - LAND USE/LAND COVER CLASSIFICATIONS AND TEMPORAL ANALYSIS.

Appendix III-A presents the initial 30 classes observed in the field (Table III-A1a), the initial 20 classes (Table III-A1b) used for MLC training and shows examples of training polygons (Figures III-A1a-d) for those selected 20 classes. Additionally, this appendix presents the signature separability statistics for the 10 final classes (presented Tables III-A1c, III-A2a-b).

Table III-A1a – List and sample description of the initial 30 classes observed in the field.*

	Observed Class	Examples of Descriptions from the field
1	Shrubby Field	2m shrubs (80% deciduous/20% coniferous); grasses; Hydro easement; low grasses shrubs of 1 - 2 m; shrubs of 2 to 4 metres; tall grasses; daylilies
2	Wild Field	Field; wild grasses; random trees; weeds; wildflowers, herbs; no shrubs; taller grasses
3	Cultivated Field (Crop)	Yellow hay, leafy greens, corn field, cereal field, potatoes,
4	Cultivated Field (Pasture)	German Sheppard kennel, pasture grazing cows, grasses, no weeds; generally greener
5	Cultivated Field (Soccer Field)	Soccer fields
6	Cultivated Field (Golf)	Golf courses
7	Cultivated Field (Mowed Grass)	Mowed lawns; mowed grasses in parks – Lees & Queensway
8	Bare Field	Dirt fields, some vegetation bits, plowed,
9	Water (Lake/pond)	Lakes and ponds
10	Water (River)	Rivers - part of St. Lawrence; lots of floating vegetation; surrounded by emergent vegetation
11	Coniferous Open	100% Pine Plantation (growing apart; understory present)
12	Coniferous Closed	100% Pine Plantation (closely growing together; understory not present)
13	Deciduous closed	100% deciduous; dense canopy; maples, poplars, birches; similar height canopy
14	Deciduous open	100% deciduous; dense understory; birches and poplars; poplar/birch with rocky outcrops; open canopy; scrubby understory
15	Mixed closed	Pine and poplar; saplings, 60%coniferous; 40% deciduous; short cedars (saplings along edge; dense canopy; cedar/pine/poplar/ mixed; dense understory with cedar/pine saplings; dense birch/poplar/pine forest;

16	Mixed open	20% Coniferous/80% Deciduous; wet ground; cedars; dead standing trees; open mixed; on a rock outcroppings; pines/deciduous; dense understory 80% coniferous; 20% Deciduous; pines and poplars in canopy with fairly open canopy and dense understory consisting of sumac seedlings and rock outcrops;
17	Urban Rural	Avonmore; rural; houses; with small roads; treed and grasses; going into Brockville; houses with shingled roofs; larger yards mowed grasses with trees hedges and fences; road going down the middle
18	Urban Commercial	Paved lots with large factory buildings; commercial and industrial area Brockville; South Keys Shopping Mall; parking lots; big box stores;
19	Urban Dense Commercial	Downtown Gananoque, O'Connor Street (downtown Ottawa)
20	Urban Dense Residential	Tree-lined streets; asphalt; multiple roofs of different colours; sidewalks streets and houses – Greenfield Ave.
21	Urban Suburb Trees	Tree-lined streets; no sidewalks; short houses; multi-coloured roofs (Walkley)
22	Urban Suburb Not Treed	Very dense residential; new without any backyards or trees; roofs of black red or grey only; (St. Laurent); No trees no yards; uniform brown roofs;
23	Urban Parking Lot	(Eagleson P&R); lots of cars; grey/black asphalt
24	Urban School	Urban West Carleton High School; paved with asphalt and concrete; flat roofs; surrounded by fields of grass; P. Aubrey Moodie Public school; school with surrounding fields;
25	Sand	beach; Moonies Bay beach; long beach alongside the river; with some trees scattered throughout; sand pit; very white
26	Rock	loose; quarry of aggregates; crushed white rock; industrial rock stuff; Omya; pits; Leonard Quarry; rocks and gravels; Gemmills aggregates
27	Dirt	Bare; dirt; construction area, Peat Farm
28	Wetlands with dead/dying trees (Swamp)	cattails with dead standing trees; big open centre area; lots of shrubs; Long Swamp outside of Perth

29	Wetlands without dead/dying trees (Marsh)	floating vegetation (lilies); open water; weird shrubs; cattails; water flowers; little grass islands and open water; grasses; drier; with cattails
30	Wetlands bog	Mer Bleue Bog, Alfred Bog

*Excel file listing all sites with individual site descriptions and photos is available from the author (ldrobert@connect.carleton.ca) upon request.

Table III-A1b – List of initial 20 combined classes used for classification training showing how the field observed classes (from Table III-A1a) were merged into these classes.

	Initial Classes	Observed Classes (from Table III-A1a)
1	High Density Urban (more coverage of impervious surfaces)	18. Urban Commercial; 19. Urban Dense Commercial; 22. Urban Suburb Not Treed; 23. Urban Parking Lot
2	Low Density Urban (less coverage of impervious surfaces – more vegetation).	17. Urban Rural; 20. Urban Dense Residential; 21. Urban Suburb Trees; 24. Urban Schools
3	Coniferous	11. Coniferous Open; 12 Coniferous Closed
4	Deciduous Open	13. Deciduous Open
5	Deciduous Closed	14. Deciduous Closed
6	Mixed Forest Open	15. Mixed Open
7	Mixed Forest Closed	16. Mixed Closed
8	Water Deep	9. Water (Lake/pond)
9	Water Shallow	10. Water (River)
10	Wetlands Swamp	28. Wetlands with dead/dying trees
11	Wetlands Marsh	29. Wetland with no dead/dying trees; 30. Wetlands Bog
12	Vegetated Field 1	3. Cultivated Field (Crop) – tall leafy green crops (corn)
13	Vegetated Field 2	3. Cultivated Field (Crop) – short leafy green crops (potatoes)
14	Vegetated Field 3	3. Cultivated Field (Crop) – yellow crops (hay; cereals)
15	Wild Field	1. Shrubby Field; 2. Wild Field
16	Short Grass	4. Cultivated Field (Pasture); 5. Cultivated Field (Soccer); 6. Cultivated Field (Golf); 7. Cultivated Field (Mowed Grass)
17	Harvested Field (Soil mixed with dead vegetation)	8. Bare Field
18	Bare Field (Soil)	27. Dirt
19	Bare Sand	25. Sand
20	Bare Rock	26. Rock

Table III-A1c - List of 10 final combined classes used for both classification methods showing how the 20 initial classes (from Table III-A1b) were merged into these classes.

	Final 10 Classes	20 Initial Classes (from Table III-A1b)
1	High Density Urban	1. High Density Urban
2	Low Density Urban	2. Low Density Urban
3	Coniferous	3. Coniferous
4	Deciduous/Mixed	4. Deciduous Open; 5. Deciduous Closed; 6. Mixed Open; 7. Mixed Closed
5	Bare Rock	19. Bare Rock; 20. Bare Sand
6	Bare Field	17. Harvested Field; 18. Bare Field
7	Water	8. Water Deep; 9. Water Shallow
8	Wetlands	10. Wetlands Swamp; 11. Wetlands Marsh
9	Agricultural Field 1	12. Vegetated Field 1; 13. Vegetated Field 2; Split out 16. - 4. Cultivated Field (Pasture); 5. Cultivated Field (Soccer); 6. Cultivated Field (Golf); Split out 15. - 1. Shrubby Field In general this class had greener, taller vegetation (although the short grasses of the soccer, golf, pastures merged into this class);
10	Agricultural Field 2	14. Vegetated Field 3; split out 16. - Cultivated Field (mowed Grass); Split out of 15 - 2. Wild Field In general this class crops were shorter and yellowier (although some of the hay crops were taller and some of the wild fields had taller yellow grasses).

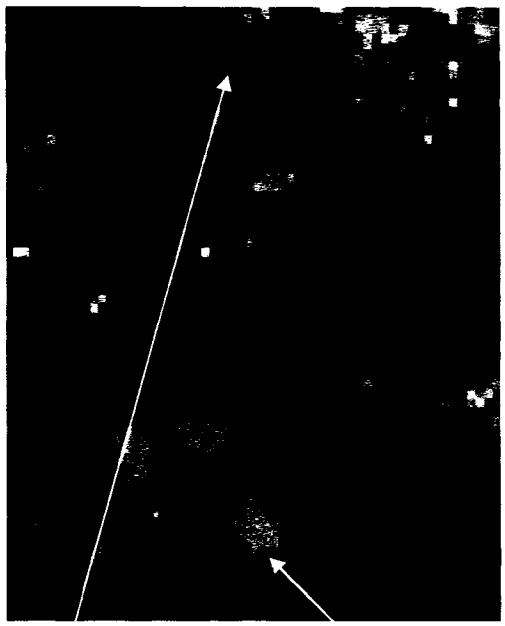

a) High density urban & low density urban (445333.58E 5030051.10N & 445143.19E 5028861.19N)

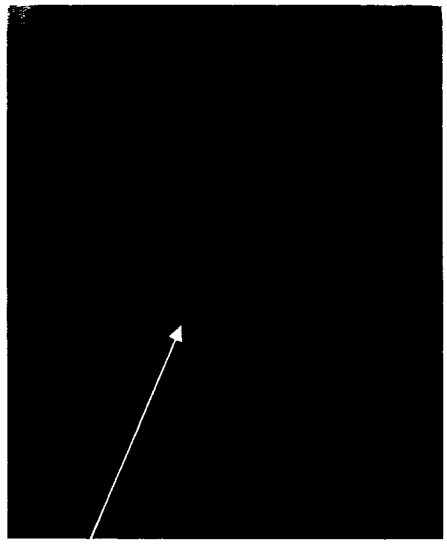

b) Coniferous (480459.385 E 5025542.896 N)

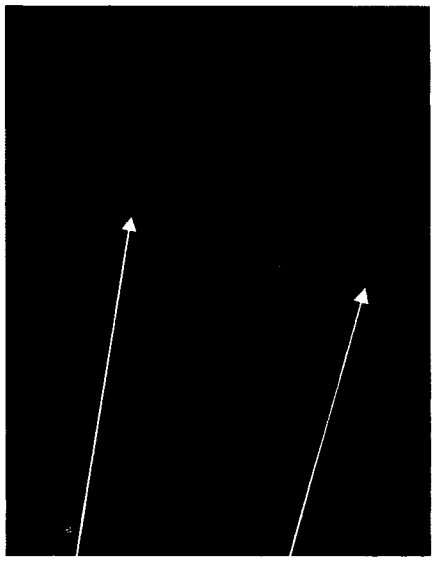

c) Deep water & wetlands marsh (424135.490E 5028589.536N & 432287.997E 5028691.872N)

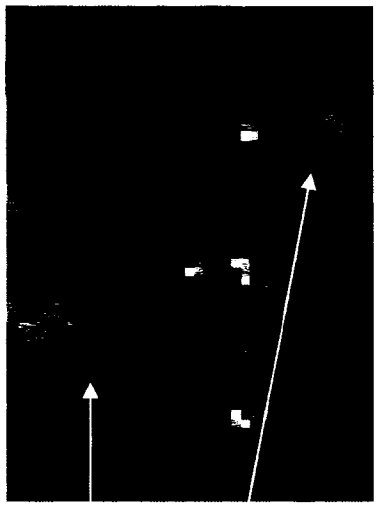

d) Agricultural field 1 & agricultural field 2 (402881.850E 4947533.051N & 402124.545E 4946888.074N

Figure III-A1a-d – Examples of training samples for a select number of classes.

Table III-A2a - 2005 signature separability (MLC, DOS scaled, no texture).

Separability Measure = Bhattacharrya Distance
Since the signatures were extended to 1995 the separabilities were the same as 2005.

Average Separability:	1.936272
Minimum Separability:	1.553918
Maximum Separability	2.000000
Signature pair with minimum separability:	High Density Urban and Bare Rock

	High Density Urban	Bare Rock	Coniferous	Deciduous / Mixed	Low Density Urban	Water	Wetlands	Agricultural Field 2	Agricultural Field 1
Bare Rock	1.553918								
Coniferous	1.999439	2.000000							
Deciduous/ Mixed	1.999068	2.000000	**1.569940**						
Low Density Urban	1.612983	1.969377	1.905436	1.922366					
Water	1.999889	2.000000	2.000000	2.000000	2.000000				
Wetlands	1.987485	1.999979	1.927389	1.960108	~~1.759722~~	1.999979			
Agricultural Field 2	1.718641	1.945569	1.998904	1.992592	1.923539	2.000000	1.936167		
Agricultural Field 1	1.989990	1.999845	1.953189	1.650259	1.849443	2.000000	1.855106	1.885615	
Bare Field	1.900871	1.915794	2.000000	2.000000	1.994841	2.000000	2.000000	1.817589	1.999930

Table III-A2b - 2005 signature separability (DOS scaled, with homogeneity on bands 2, 3, and 4).

Separability Measure = Bhattacharrya Distance
Since the signatures were extended to 1995 the separabilities were the same as 2005.

Average Separability:	1.956319
Minimum Separability:	1.588219
Maximum Separability	2.000000
Signature pair with minimum separability:	Coniferous and Deciduous/ Mixed

	High Density Urban	Bare Rock	Coniferous	Deciduous / Mixed	Low Density Urban	Water	Wetlands	Agricultural Field 2	Agricultural Field 1
Bare Rock	1.760986								
Coniferous	1.999794	2.000000							
Deciduous / Mixed	1.999712	2.000000	**1.588219**						
Low Density Urban	1.691365	1.989630	1.937881	1.951904					
Water	2.000000	2.000000	2.000000	2.000000	2.000000				
Wetlands	1.995804	1.999988	1.935469	1.964423	1.874261	2.000000			
Agricultural Field 2	1.803930	1.966897	1.999046	1.994217	1.950336	2.000000	1.947468		
Agricultural Field 1	1.995347	1.999923	1.964065	1.750661	1.933248	2.000000	1.876069	1.918577	
Bare Field	1.964680	1.946145	2.000000	2.000000	1.999331	2.000000	2.000000	1.898187	1.999978

With the addition of the texture measure the separability improved; especially with those pairs that had the worst seperability without texture (see highlighted pairs for examples (e.g. green highlight on deciduous/mixed and vegetated field)).

Appendix III-B contains the signatures of each training class for the MLC method (Table III-B1a) and for the object-based method (Table III-B1b).

Table III-B1a –Signatures for 10 classes from the 2005 maximum likelihood classification.

	Mean Band 1	Mean Band 2	Mean Band 3	Mean Band 4	Mean Band 5	Mean Band 6	Mean Band 7	Homogeneity Band 2	Homogeneity Band 3	Homogeneity Band 4
High Density Urban	89.711	40.624	45.889	49.973	69.893	225.128	41.295	0.326	0.301	0.253
Low Density Urban	71.522	30.040	29.720	61.116	58.301	215.677	26.845	0.150	0.104	0.085
Coniferous	57.072	22.328	18.194	63.495	39.772	196.288	13.324	0.449	0.381	0.173
Deciduous / Mixed	57.114	22.818	18.056	81.096	61.171	200.918	18.818	0.369	0.402	0.094
Water	58.475	20.544	15.984	13.180	9.981	188.128	5.310	0.471	0.417	0.723
Wetlands	61.658	25.775	25.167	62.852	59.903	206.641	22.497	0.365	0.314	0.166
Agricultura l Field 1	63.890	28.553	25.524	91.752	81.898	204.874	28.282	0.392	0.301	0.223
10 Field 2	68.667	31.536	36.694	56.413	87.339	209.275	43.474	0.425	0.354	0.246
Bare Field	82.743	39.914	50.665	59.330	111.264	221.411	67.118	0.648	0.795	0.300
Bare Rock	99.804	50.428	62.442	62.283	100.572	221.355	61.268	0.846	0.808	0.085

Table III-B1b - Signatures for 10 classes from the 2005 object-based classification.

	Mean Band 1	Mean Band 2	Mean Band 3	Mean Band 4	Mean Band 5	Mean Band 6	Mean Band 7	StDev Band 1	StDev Band 2	StDev Band 3	StDev Band 4	StDev Band 5	StDev Band 6	StDev Band 7
High Density Urban	78.1-159.3	33.8-75.2	36.0-94.9	41.2-91.0	57.2-107.4	211.8-231.4	34.7-63.5	4.8-27.2	2.5-18.5	3.8-19.2	4.5-12.4	5.9-18.4	1.4-6.8	3.9-12.4
Low Density Urban	67.7-83.0	28.2-37.6	27.3-39.9	47.0-73.4	51.2-70.9	193.4-223.3	22.8-35.7	3.4-13.8	1.7-7.1	2.3-8.8	4.8-13.5	3.7-9.6	0.8-6.3	2.3-7.0
Coniferous	54.8-61.3	20.6-24.4	16.7-20.6	54.8-75.3	30.6-56.2	189.0-205.6	9.9-18.9	1.1-3.4	0.4-2.1	0.4-2.3	3.1-7.9	2.6-9.6	0.8-5.7	1.2-3.9
Deciduous/ Mixed	54.8-60.5	21.6-24.4	16.7-20.6	71.4-87.0	54.2-70.9	194.1-212.2	15.9-23.8	1.1-3.0	0.4-2.1	0.8-3.5	5.2-10.7	4.1-9.6	0.9-4.1	1.9-5.0
Water	50.0-71.7	15.0-31.9	10.0-30.2	7.0-23.6	4.0-19.7	170.9-199.3	2.0-10.9	1.1-2.2	0.4-2.5	0.4-2.3	0.3-6.2	0.7-4.8	0.5-2.6	0.8-1.9
Wetlands	57.2-71.7	23.5-30.1	19.6-27.3	50.9-83.1	34.5-72.9	171.6-214.8	12.9-29.8	1.1-3.4	0.4-2.1	0.8-3.5	2.4-9.0	2.2-9.6	0.4-3.8	1.2-6.2
Agricultural Field 1	58.8-65.3	25.4-29.1	18.6-24.4	93.9-124.2	67.0-83.7	192.7-211.1	20.9-31.8	1.1 - 2.2	0.4 - 1.7	0.8 - 2.7	3.1-12.1	2.2-5.9	1.3-3.2	1.2-5.4
Agricultural Field 2	59.6-70.9	25.4-33.8	22.5-37.9	49.0-105.6	73.9-112.3	192.3-222.9	23.8-48.6	1.1-5.6	0.8-3.4	1.2-5.0	3.8-12.1	2.9-12.9	1.4-4.5	1.9-7.0
Bare Field	73.3-87.8	35.7-45.1	43.7-53.4	56.8-69.5	90.6-119.2	198.2-228.8	50.6-78.4	2.2-4.8	1.3-3.4	1.9-6.5	1.7-7.6	4.1-12.5	1.5-6.1	3.9-10.9
Bare Rock	81.4-109.5	37.6-58.3	40.8-74.6	38.2-75.3	52.2-130.0	214.8-224.7	31.8-79.4	5.2-16.8	3.4-10.9	4.6-16.1	3.1-11.7	7.0-17.7	1.0-4.4	4.7-12.8

Appendix III-C contains examples of each land cover type (photographs) that comprise each class and an example of the corresponding thematic class from the 2005_1529 thematic map. Additionally, this appendix presents photographs of the land covers that make up each class.

Legend for thematic map examples.

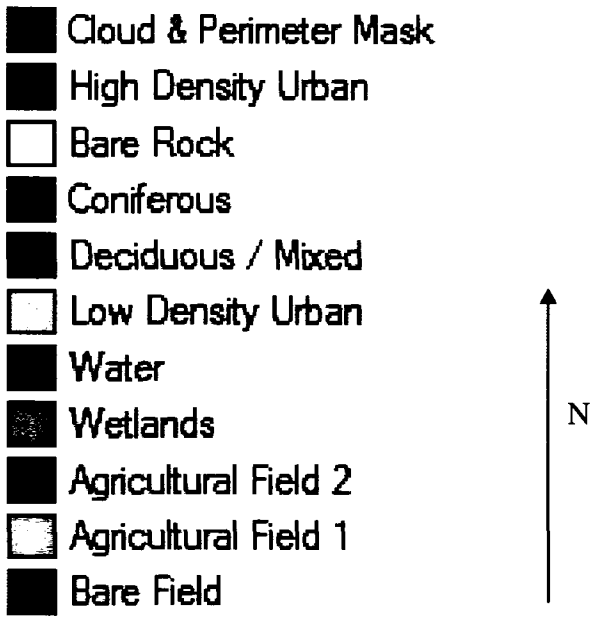

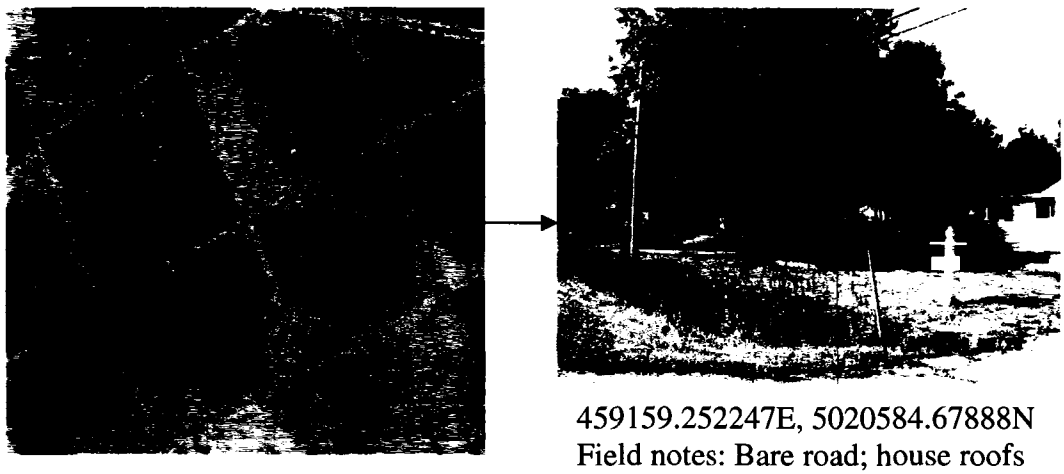

459159.252247E, 5020584.67888N
Field notes: Bare road; house roofs black and white; with grasses; asphalt; both deciduous and coniferous trees.

Figure III-C1a - Low Density Urban example.

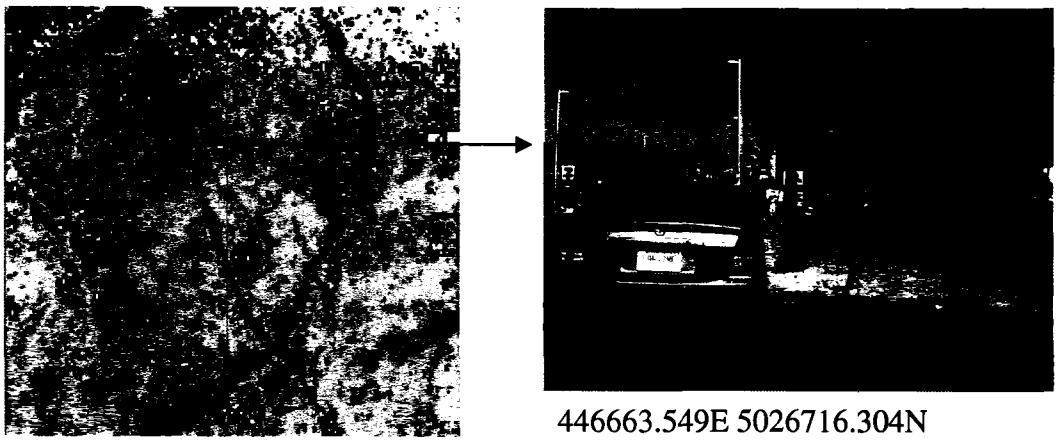

446663.549E 5026716.304N
Field notes: Very few trees; commercial buildings; streets; sidewalks.

Figure III-C1b - High Density Urban example.

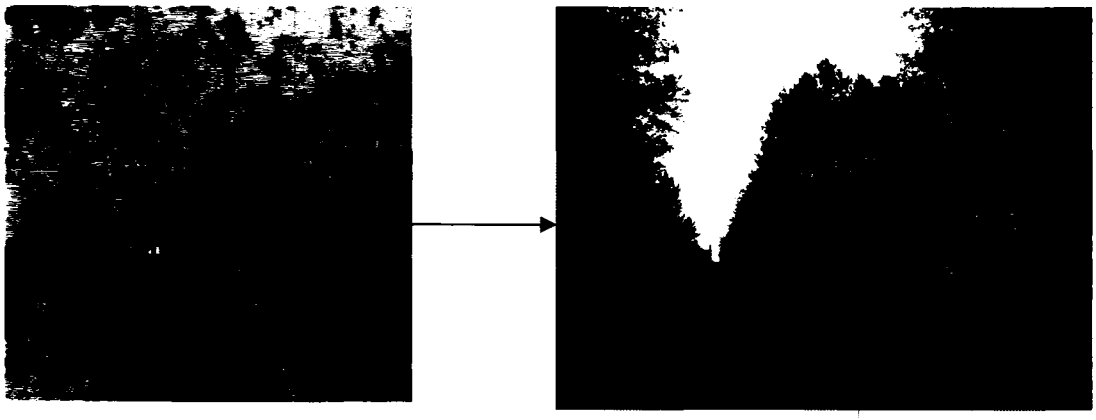

Figure III-C1c - Coniferous example.

480408.153159E, 5026063.93678N
Field notes: forest; 100% coniferous; pine plantation open.

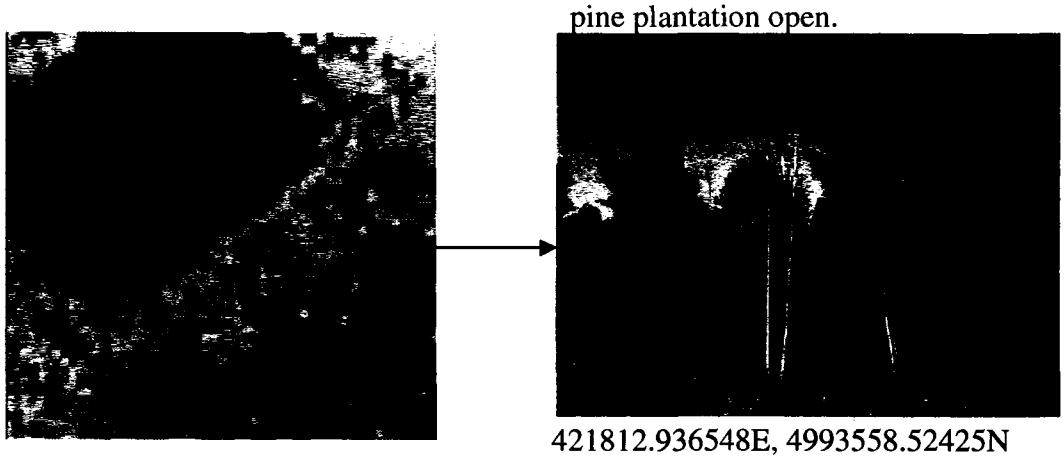

421812.936548E, 4993558.52425N
Field notes: 100% deciduous; Poplar/birch forest with open canopy; dense under storey with maple saplings; bushes.

Figure III-C1d - Deciduous/Mixed example.

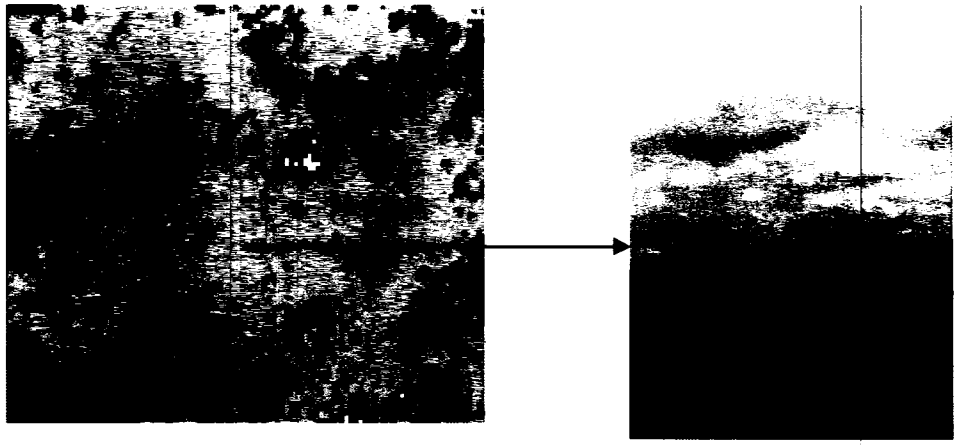

405199.489097E, 4928629.03578N
Field notes: field; agriculture; leafy greens.

Figure III-C1e - Agricultural Field 1 example.

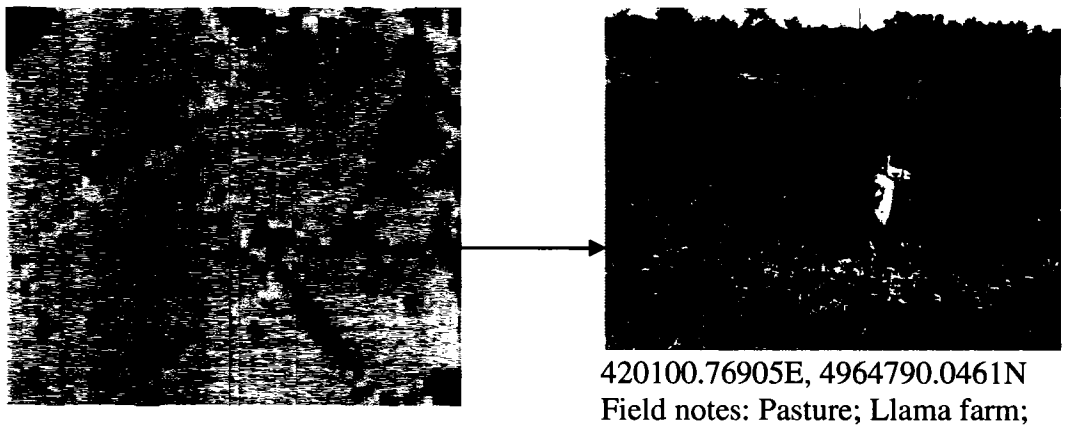

420100.76905E, 4964790.0461N
Field notes: Pasture; Llama farm; yellowier field, bare patches.

Figure III-C1f - Agricultural Field 2 example.

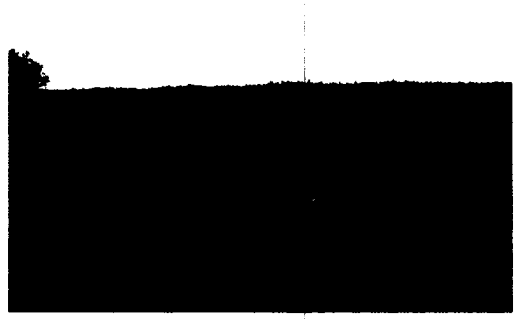

Example of bare field (only visual, most samples were selected upon visual inspection of scene – Peat farm.

Figure III-C1g - Bare Field example.

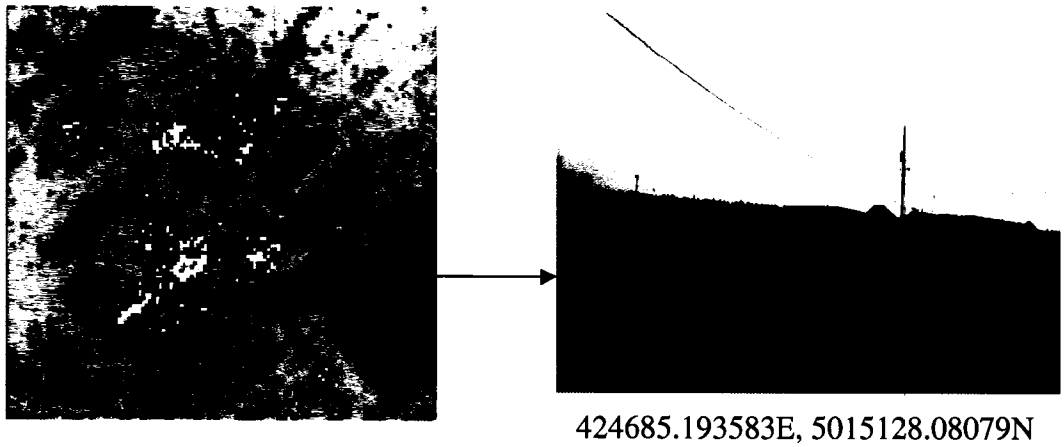

424685.193583E, 5015128.08079N
Field notes: Bare, loose rock; Karson Aggregate Gravel Pit/Quarry.

Figure III-C1h - Bare Rock example.

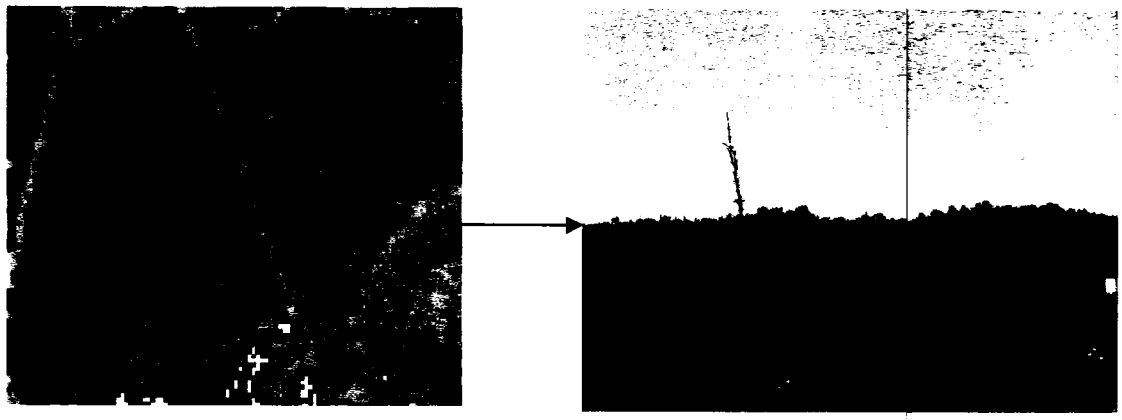

436495.13873E, 5014515.22471N
Field notes: Wetland; cattails with dead standing trees; big open centre area.

Figure III-C1i - Wetland example.

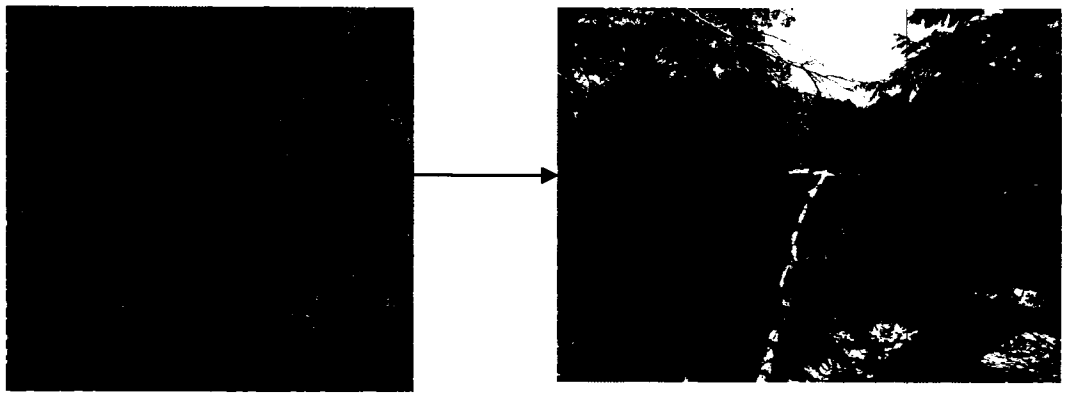

431914.962299E, 5041755.49511N
Field notes: Meech Lake.

Figure III-C1j - Water example.

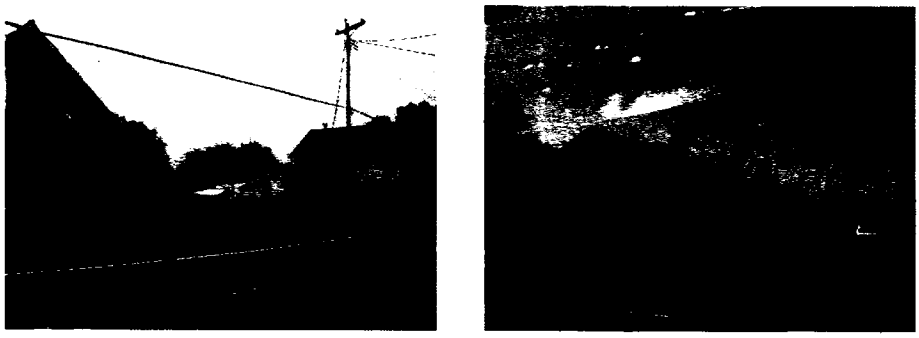

Figure III-C2a – Examples of cover included in Low Density Urban.

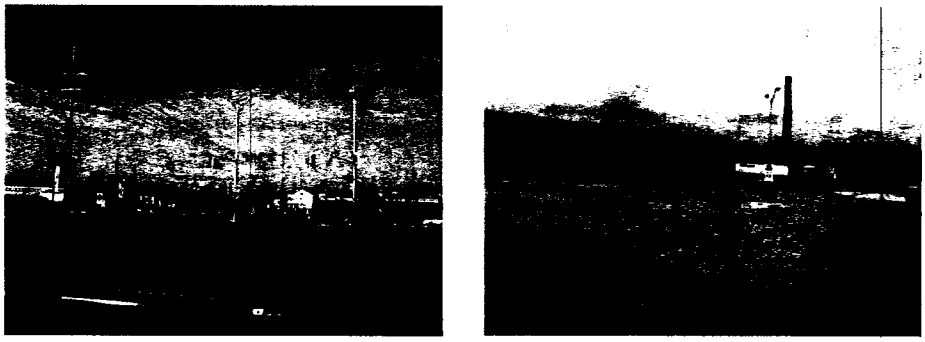

Figure III-C2b – Examples of cover included in High Density Urban.

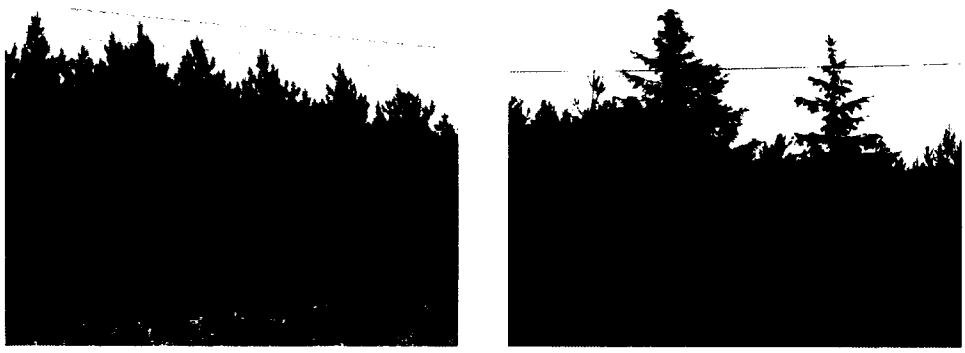

Figure III-C2c – Examples of cover included in Coniferous.

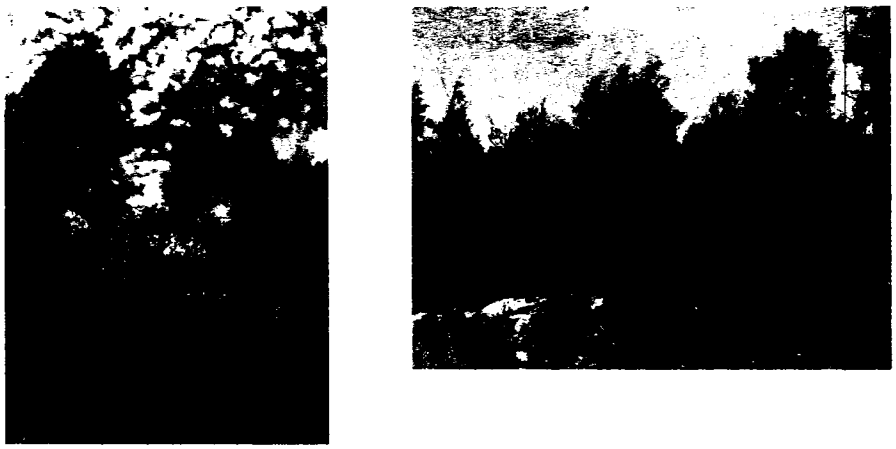

Figure III-C2d – Examples of cover included under Deciduous/Mixed.

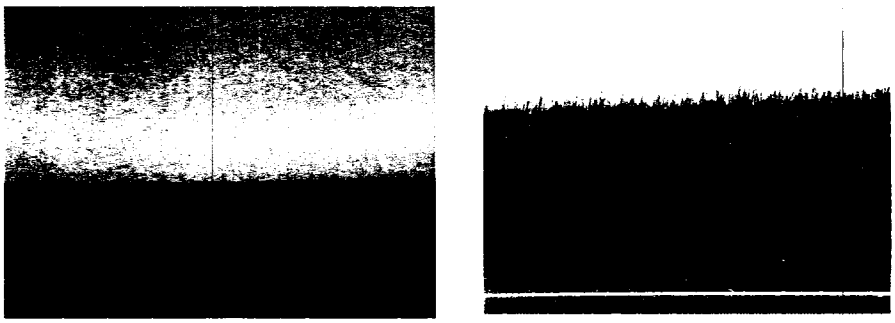

Short Leafy Tall Leafy (Corn)

Figure III-C2e – Examples of land included under Agricultural Field 1.

Pasture Mowed Hay Cereal

Figure III-C2f – Examples of cover included under Agricultural Field 2.

Black Gravel Grey Gravel White Gravel

Figure III-C2g – Examples of cover included under Bare Rock.

Figure III-C2h – Examples of cover included under Wetlands.

Figure III-C2i – Examples of cover included under Water.

Appendix III-D presents the differenced scenes (Figure III-D1) used to develop a change map over which the reference sites (collected in the field in 2006) were projected. This was used to develop validation sites for 1995.

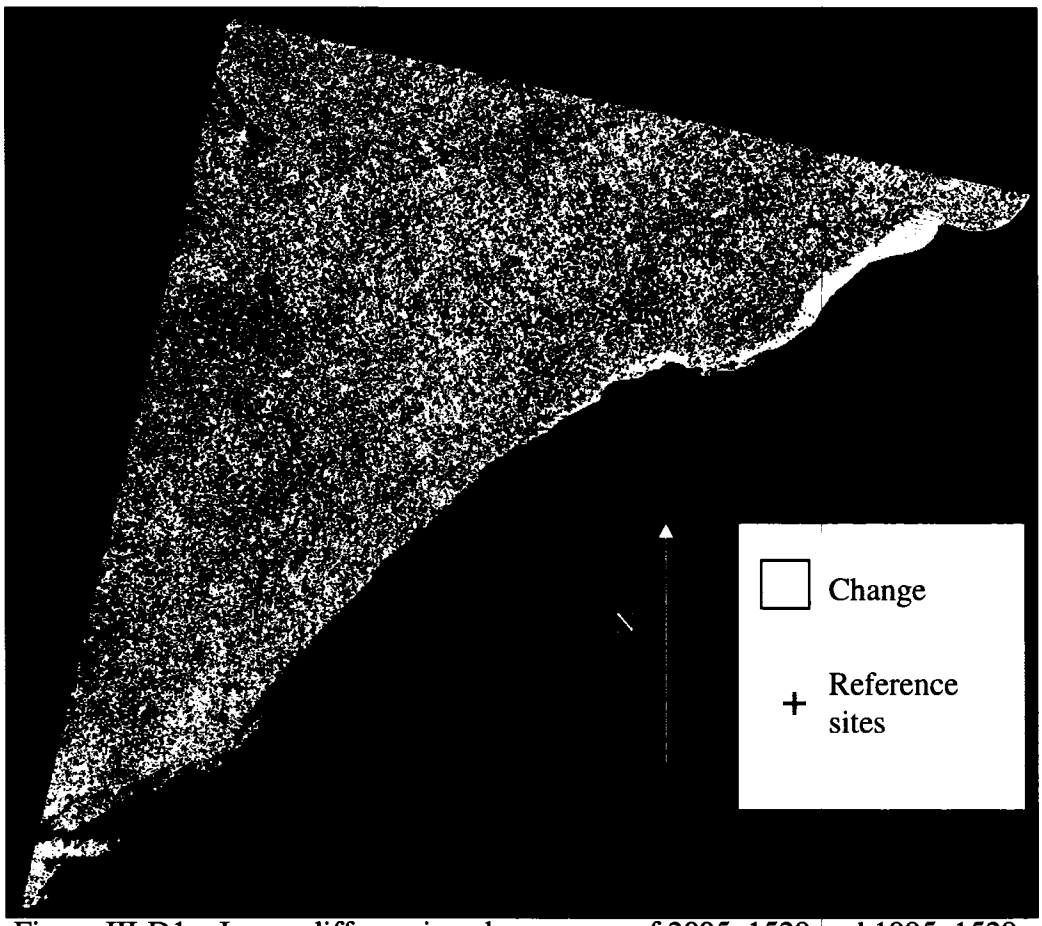

Figure III-D1 – Image differencing change map of 2005_1529 and 1995_1529. Areas in white represent change. Blue crosses are reference sites from 2006.